

# Biochemical exploration of EDS1 family members and their interaction with helper-NLRs



Inaugural-Dissertation

zur  
Erlangung des Doktorgrades  
der Mathematisch-Naturwissenschaftlichen Fakultät  
der Universität zu Köln

vorgelegt von

**Huanhuan Sun**

aus Henan, China

Köln, März 2023



Die vorliegende Arbeit wurde am Max-Planck-Institut für Pflanzenzüchtungsforschung in Köln, Arbeitsgruppe Prof. Dr. Jijie Chai und Arbeitsgruppe Prof. Dr. Jane Parker durchgeführt.

The work described in this thesis was conducted under the supervision of Prof. Dr. Jijie Chai and Prof. Dr. Jane Parker at the Max Planck Institute for Plant Breeding Research.

Berichterstatter: Prof. Dr. Jijie Chai

Prof. Dr. Karsten Niefind

Prüfungsvorsitzender: Prof. Dr. Alga Zuccaro

Tag der Disputation: 17.01.2023



MAX-PLANCK-GESELLSCHAFT



# ABSTRACT

EDS1 family members are important immune hubs which influence many aspects of plant defense. In Arabidopsis, there are three EDS1 proteins: EDS1, SAG101, and PAD4. In unchallenged plants EDS1 is forming heterodimers with SAG101 and PAD4, respectively, and both heterodimers are important for TNL-mediated immune responses. NRG1s and ADR1s are two groups of NLRs, which are integrated with  $CC_R$  domains in the N-terminus instead of TIR or CC domains in canonical NLRs. Unlike sensor NLRs, they function downstream of EDS1 family members in effector-triggered immunity and are therefore referred to as helper NLRs. Recently, research shows that two EDS1 family heterodimers are exclusively responsible for two parallel immune branches downstream of TIR-NLR receptors. Typically, upon effector recognition, E-S heterodimers activate downstream NRG1s to trigger the HR response. In contrast, E-P heterodimers activate ADR1s to induce resistance. However, how the signals are transmitted from upstream TNL activation to downstream EDS1 family members and further down to helper-NLRs and eventually elicit the ETI response was still a mystery.

In this study, I applied multiple biochemical techniques to investigate the activation mechanism of EDS1 family members and their interaction with helper-NLRs. PAD4 was first purified and tested as a heterodimer together with EDS1 *in vitro*. A chimera chi2 formed of N-terminal PAD4 and C-terminal SAG101 was used to mimic the active form of SAG101. However, chi2 was not able to activate helper-NLRs under the tested conditions. Given the indispensable role of TNL NADase products in ETI response, we reconstituted the TNL resistosome together with EDS1 family members and helper-NLRs in insect cells, and surprisingly, we captured the interaction of the E-S complex with NRG1A, and the interaction of the E-P complex with ADR1\_L1. Furthermore, these results were confirmed by pull-down assays, in which TIR/TNL NADase products were incubated with EDS1, SAG101, and NRG1A, respectively after incubation with EDS1, PAD4, and ADR1\_L1. However, in the absence of TIR/TNL NADase products, the interactions could not be induced. This suggests, perhaps the most important finding of this study, that activation of helper-NLRs is controlled by the products of TNL NADases that are captured and delivered to helper-NLRs by the EDS1 family of heterodimers.



# ZUSAMMENFASSUNG

Mitglieder der EDS1-Proteinfamilie sind wichtige Drehscheiben des Immunsystems, die viele Aspekte der Pflanzenabwehr beeinflussen. In *Arabidopsis* gibt es drei EDS1-Proteine: EDS1, SAG101 und PAD4. In ungeschädigten Pflanzen bildet EDS1 Heterodimere mit SAG101 bzw. PAD4, und diese sind wichtig für TNL-vermittelte Immunreaktionen. NRG1 und ADR1 sind zwei Gruppen von NLRs, die mit C<sub>R</sub>-Domänen im N-Terminus anstelle von TIR- oder CC-Domänen in kanonischen NLRs integriert sind. Im Gegensatz zu den Sensor-NLRs sind sie den Mitgliedern der EDS1-Familie bei der durch den Effektor ausgelösten Immunität nachgeschaltet und werden daher als Helfer-NLRs bezeichnet. Neueste Forschung hat gezeigt, dass zwei Heterodimere der EDS1-Familie spezifisch für zwei parallele Immunantworten ausgelöst von TIR-NLR-Rezeptoren verantwortlich sind. Normalerweise aktivieren E-S-Heterodimere bei der Erkennung von Effektoren nachgeschaltete NRG1s, um die HR-Reaktion anzuschalten. Im Gegensatz dazu aktivieren E-P-Heterodimere ADR1s, um Resistenz zu induzieren. Wie jedoch die Signale von der stromaufwärts gelegenen TNL-Aktivierung zu den stromabwärts gelegenen Mitgliedern der EDS1-Familie und weiter zu den Helfer-NLRs übertragen werden und schließlich die ETI-Reaktion auslösen, war bisher ein völlig unklar.

In dieser Studie habe ich verschiedene biochemische Methoden angewandt, um den Aktivierungsmechanismus von Mitgliedern der EDS1-Familie und ihre Interaktion mit Helfer-NLRs zu untersuchen. Zunächst wurde PAD4 gereinigt und als Heterodimer zusammen mit EDS1 *in vitro* getestet. Eine Chimäre chi2, die aus N-terminalem PAD4 und C-terminalem SAG101 besteht, wurde verwendet, um die aktive Form von SAG101 nachzuahmen. Allerdings war chi2 unter den getesteten Bedingungen nicht in der Lage, Helfer-NLRs zu aktivieren. Angesichts der unverzichtbaren Rolle der TNL-NADase-Produkte bei der ETI-Antwort haben wir das TNL-Resistosom zusammen mit Mitgliedern der EDS1-Familie und Helfer-NLRs in Insektenzellen rekonstituiert, und überraschenderweise konnten wir die Interaktion des E-S-Komplexes mit NRG1A und die Interaktion des E-P-Komplexes mit ADR1\_L1 nachweisen. Diese Ergebnisse wurden durch Pull-Down-Assays bestätigt, bei denen TIR/TNL-NADase-Produkte mit EDS1, SAG101 und NRG1A, beziehungsweise EDS1, PAD4 und ADR1\_L1 inkubiert wurden. In Abwesenheit von TIR/TNL-NADase-Produkten konnten die Wechselwirkungen jedoch nicht ausgelöst werden. Dies deutet auf die vielleicht wichtigste Erkenntnis dieser Studie hin, dass die

Aktivierung der Helfer-NLRs durch die TNL-NADase-Produkte gesteuert wird, die von Heterodimeren der EDS1-Familie eingefangen und an die Helfer-NLRs weitergeleitet werden.



# TABLE OF CONTENTS

Abstract .....	I
Zusammenfassung.....	III
Table of contents.....	V
1 Introduction.....	1
1.1 Plant immunity.....	1
1.1.1 Activation of plant NLRs .....	2
1.1.2 Recognition of effectors by NLR receptors .....	2
1.1.3 Structure-guided activation of NLRs .....	3
1.1.3.1 Activation of CNLs .....	3
1.1.3.2 Activation of TNLs .....	4
1.2 EDS1 functions as an immune node in ETI immune responses .....	5
1.2.1 Function of EDS1 heterodimers in Arabidopsis .....	5
1.2.2 Structural analysis of EDS1 family heterodimers .....	6
1.3 How do helper-NLRs help?.....	7
1.4 TNL-mediated ETI requires EDS1 family members and helper-NLRs.....	8
1.4.1 Association of TIR domain and TNLs .....	8
1.4.2 NADase activity of plant TIR domains .....	9
1.4.3 The products of TIR domain enzymatic activity .....	10
2 Aims of this study .....	12
3 Materials and Methods.....	13
3.1 Molecular cloning.....	13
3.1.1 PCR cloning.....	13
3.1.2 DNA gel electrophoresis.....	16
3.1.3 PCR products clean up.....	16
3.1.4 Restriction digestion of DNA and empty vectors .....	17
3.1.5 Plasmid construction.....	17
3.1.6 Plasmids construction and transformation.....	20
3.2 Protein expression and purification .....	21
3.2.1 Recombinant protein expressing in <i>E. coli</i> .....	21
3.2.2 Recombinant protein expression in insect cell .....	23
3.2.3 Expression and purification of PreScission protease .....	24

3.2.4	Affinity purification .....	25
3.2.5	Size exclusion chromatography (SEC, gel filtration) of target proteins .....	25
3.2.6	Negative staining.....	25
3.3	Pull-down assay.....	26
4	Results .....	27
4.1	Structural alignment of NRG1A model with ZAR1 .....	27
4.2	Expression, purification, and characterization of helper-NLRs.....	28
4.2.1	Optimizing the expression of helper-NLRs in <i>E. coli</i> .....	28
4.2.2	Optimizing the expression of helper-NLRs in insect cells .....	29
4.2.3	Optimizing the purification of helper-NLRs .....	30
4.2.4	Expression, purification and characterization of NRG1A in insect cells .....	30
4.2.5	Expression, purification, and characterization of ADR1_L1 in insect cells .....	32
4.3	Expression and purification of EDS1 family heterodimers .....	33
4.3.1	Expression and purification of EDS1-PAD4 in insect cells.....	33
4.3.2	Crystallization of the EDS1-PAD4 heterodimer.....	36
4.4	Pull-down assay analyzing the interaction of helper-NLRs and EDS1 family heterodimers <i>in vitro</i> .....	37
4.5	Can EDS1-chi2 escape the control of upstream signals? .....	38
4.5.1	Auto-immune PAD4-SAG101 chimera .....	38
4.5.2	Expression and purification of chi2.....	39
4.5.3	Interaction assay of EDS1-chi2 and helper-NLRs .....	41
4.6	Reconstitution of EDS1 family members and helper-NLR association <i>in vitro</i> .....	43
4.6.1	Co-expression and/or co-purification of TIR proteins with EDS1 heterodimers and helper NLRs.....	43
4.6.2	Role of TIR products in inducing the interaction of NRG1A and the EDS1-SAG101 heterodimer .....	45
4.7	TIR NADase products mediate SAG101 cleavage <i>in vitro</i> .....	47
5	Discussion .....	51
5.1	Protein interaction studies <i>in vitro</i> .....	51
5.2	Studying the interaction of EDS1 heterodimers and helper-NLRs using a reconstitution system ..	52
5.3	Structural comparison of inactive and active EDS1 family heterodimers .....	54
5.4	Why does auto-immune EDS1-chi2 not robustly interact with NRG1A?.....	57
5.5	Small molecule binding promotes the interaction of EDS1 family heterodimers with helper-NLRs.....	59

5.6	Function of helper-NLRs.....	60
5.7	The biological relevance of SAG101 cleavage <i>in planta</i> .....	61
5.8	Outlook.....	62
6	References.....	63
	List of abbreviations.....	69
	Acknowledgements.....	73
	Erklärung zur Dissertation.....	74
	Curriculum vitae.....	75



# 1 Introduction

Like animals, plants have developed a variety of special tissues and biochemical mechanisms to cope with harsh environments and biological attacks. Proteins that detect malicious microbial invaders either outside or inside plant cells and communicate their presence to intracellular defense components are important weapons in plant disease resistance strategies.

## 1.1 Plant immunity

The members of one group of extracellular protein receptors are called pattern recognition receptors (PRRs). PRRs sense small molecules that are secreted into the shared environment by pathogens (pathogen-associated molecular patterns, PAMPs) and also debris of cell damage or death (damage-associated molecular patterns, DAMPs). Ligand recognition of PRRs triggers a series of immune responses, namely, pattern-triggered immunity (PTI), which includes the expression of defense genes, reactive oxygen species (ROS) production, and activation of mitogen-activated protein kinase (MAPK) cascades.

To suppress the PTI response and aid infection, host-adapted pathogens deliver effectors into plant cells (Jones and Dangl, 2006; Teper et al., 2014). Whereas PAMPs and DAMPs are conserved groups of small molecules, effectors are diverse molecules ranging from nucleotide acids to peptides. Effectors are capable of dampening plant resistance and altering plant physiology to accommodate infection (Dou and Zhou, 2012). On the other hand, plants have evolved resistance proteins (R proteins) to fight back. In this way, the second layer of the immune response is activated, namely, effector-triggered immunity (ETI). There are two typical ETI immune responses in the model plant *Arabidopsis thaliana*: a local hypersensitive response (HR) to constrain the growth of pathogens by triggering cell death and resistance to strengthen immunity (Jones et al., 2016).

Given the importance of plant protection and crop improvement, research on plant immunity has developed rapidly over the last two decades. However, questions about the activation of receptors, and how signals are transmitted downstream to trigger multiple immune responses, remain to be addressed.

### 1.1.1 Activation of plant NLRs

Many R proteins are typical intracellular multi-domain receptors (NLRs) with high similarity to animal receptors involved in immunity and apoptosis. In plants, there are three types of NLRs distinguished by their N-terminal domains: the coiled-coil (CC) domain NLRs (CNLs), the Toll/interleukin-1 receptor (TIR) domain NLRs (TNLs) and the resistance to powdery mildew 8-like (RPW8) coiled-coil (CC<sub>R</sub>) domain NLRs (RNLs). Functionally, CC, TIR, and CC<sub>R</sub> found at N-termini are signaling domains, the central nucleotide-binding oligomerization domain (NOD) exhibits regulatory and oligomerization properties, and the leucine-rich repeat (LRR) domain in the C-terminus is for ligand binding and auto-inhibition (Jones et al., 2016).

### 1.1.2 Recognition of effectors by NLR receptors

Most CNLs and TNLs are specific receptors that recognize pathogen effectors. The mechanism of effector recognition was first proposed to function as a “gene-for-gene” mechanism in 1942 (Flor, 1971; Keen, 1990). In this model, the avirulent genes from pathogens (effectors) and the resistance genes of hosts (NLR receptors) are considered as a pair and sense each other by direct binding. Some mechanisms of effector and receptor recognition are explained by this model. For example, in Flax (*Linum usitatissimum*), flax rust fungus AvrL567 molecules are recognized by the plant’s L5, L6, and L7 R proteins, respectively. Yeast two-hybrid assays indicate that this recognition is based on the amino-acid-specific R-Avr protein interaction. The recognition shows a high genetic diversity at corresponding R and Avr gene loci, which is shaped by plant-pathogen coevolution (Dodds et al., 2006). Similarly, the *polymorphic barley mildew A* (MLA) locus encodes CC-containing allelic immune receptors that specifically recognize effectors of the pathogenic powdery mildew fungus, *Blumeria graminis f. sp. hordei* (*Bgh*), and trigger allele-specific cell death. Recognition of the effector AVRA1 by barley MLA1 is maintained in transgenic Arabidopsis, indicating a high possibility of direct binding between MLA1 and AVRA1 (Lu et al., 2016).

However, decades of research on effector recognition mechanisms have revealed that NLRs perceive effectors also indirectly. For example, in Arabidopsis, the RIN4 protein forms a complex with the CNLs RPM1 and RPS2 and functions as a biochemical guard. Phosphorylation of RIN4 induced by association with AvrRpm1 or AvrB triggers the activation of RPM1, whereas degradation of RIN4 protein by AvrRpt2 activates RPS2 (Mackey et al., 2003; Lee et al., 2004).

Another indirect recognition model is called the “decoy” model, exemplified by the HOPZ-ACTIVATED RESISTANCE 1 (ZAR1) receptor. ZAR1 is not the direct effector target but recognizes modifications of additional non-NLR host proteins that are modified by pathogen effectors, and in this way, activates the immune response (Wang et al., 2015). Some NLRs also form a pair, in which association of two NLRs traps the NLRs in an inactive state. Generally, one NLR functions as the sensor and the other one acts as an executor upon effector recognition, as in the case of RRS1/RPS4, and RGA4/RGA5 (Cesari et al., 2014; Le Roux et al., 2015).

These diverse recognition models reflect the sophisticated immune system and conserved recognition mechanisms in plants. Even though effector-receptor interactions have been studied in many systems, little is known about the structural basis of these interactions. In particular, questions such as which structural domain of the receptor binds to the corresponding effector, what is the conformational change upon activation, and which part induces the downstream response, remain unresolved.

### 1.1.3 Structure-guided activation of NLRs

The N receptor in tobacco is a TNL receptor and recognizes the helicase domain of the TMV replicase. Using transient expression followed by immunoprecipitation, Mestre et al. provided the first evidence of ligand-induced N protein oligomerization upon effector perception (Mestre and Baulcombe, 2006). After many years of intense efforts, the mechanism of how NLRs are activated and oligomerize into a large protein complex has recently been elucidated.

#### 1.1.3.1 Activation of CNLs

Using a recombinant expression system and cryo-electron microscopy techniques, Wang et al. unraveled the mechanism of the effector-triggered ZAR1-mediated immune response at the structural level (Wang et al., 2019a; Wang et al., 2019b). This includes the inactive state ZAR1-RKS1 complex, intermediate ZAR1-RKS1-PBL2<sup>UMP</sup> after perception of the effector, and active protoplast membrane-associated pentamer formed by the intermediate ZAR1-RKS1-PBL2<sup>UMP</sup> complex. In summary, there are four steps involved in the activation of the ZAR1 resistosome: (1) A preformed ZAR1-RKS1 heterodimer is present in unchallenged Arabidopsis and is stabilized by ADP binding to the NBD pocket. ZAR1<sup>CC</sup> appears to be kept in an inactive state via contacts with ZAR1<sup>LRR</sup>, ZAR1<sup>HD1</sup>, and ZAR1<sup>WHD</sup>. (2) The AvrAC effector is delivered into plant cells during

infection and then uridylylates PBL2, thus leading to interaction of PBL2<sup>UMP</sup> with RKS1. Formation of a ZAR1-RKS1- PBL2<sup>UMP</sup> complex then drives conformational change in multiple ZAR1 domains, resulting in replacement of ADP with ATP. (3) ATP binding triggers the self-association of the ZAR1-RKS1- PBL2<sup>UMP</sup> complex, which involves the interaction of the CC domain, NB domain (NBD), helical domain1(HD1), winged-helix domain (WHD), and LRR domain of ZAR1. (4) Pentamerization promotes projection of the  $\alpha$ 1 helix out of the CC domain, which results in formation of a pore-like structure together with the four neighboring  $\alpha$ 1 helices.

The pore-like structure allows the ZAR1 resistosome to associate with the plasma membrane. Through electrophysiological recordings, Bi et al. found that the ZAR1 resistosome forms cation-selective Ca<sup>2+</sup>-permeable channels. Mutation of the pore-lining residue Glu11 abolished the current *in vitro* as well as cell death in plant cells, which again confirmed the importance of ion channels for ZAR1-mediated cell death. Altogether, they demonstrated that ZAR1, as a sensor NLR, upon activation, acts as a cell death executor in the plant immune response through generating a novel Ca<sup>2+</sup>-permeable cation channel (Bi et al., 2021).

### 1.1.3.2 Activation of TNLs

TNLs have evolved a different activation mechanism to that of CNLs. In two recent breakthroughs, researchers uncovered the cryo-EM resistosome structures of the TNLs RPP1 (Recognition of *Peronospora parasitica* 1) and ROQ1 (recognition of XopQ 1). In both cases, effectors are recognized directly by the LRR domain and PL (post-LRR) domain, (also called C-terminal jelly roll and Ig-like domain, C-JID domain). Despite the lack of structures of inactive TNLs, the structures of the RPP1 and Roq1 resistosomes suggest similar dynamic conformational changes upon activation. Recognition of the pathogen effector triggers the release of the NB-ARC domain, which is blocked by the LRR structural domain and then facilitates a conformational switch to the ATP-bound state. The arrangement of TNLs into a tetramer brings the TIR domains into close contact, resulting in two distinct interfaces. Unlike ZAR1, which acts as an ion channel upon activation, TNL assembles into a tetramer that activates a catalytic center on one of the interfaces (Ma et al., 2020; Martin et al., 2020). It was shown that both the RPP1 and ROQ1 resistosome act as holoenzymes that hydrolyze NAD<sup>+</sup> (nicotinamide adenine dinucleotide). Importantly, mutation in the catalytic center abolishes TNL-mediated cell death upon effector recognition. However, it remains a mystery how NADase activity is linked to ETI-mediated cell death and resistance.



## 1.2 EDS1 functions as an immune node in ETI immune responses

EDS1 (Enhanced Disease Susceptibility 1) was first reported by researchers who identified several instances of RPP gene-specific resistance using mutational ecotypes of *Arabidopsis* (Parker et al., 1996). The high susceptibility of *eds1* mutants suggested that EDS1 is critical for the resistance to certain *Peronospora. parasitica* isolates in *Arabidopsis*. Further inspection of EDS1 function demonstrated that EDS1 is involved in basal immunity, TNL-mediated immune responses, and occasionally some CNL-mediated immunity (Aarts et al., 1998).

### 1.2.1 Function of EDS1 heterodimers in *Arabidopsis*

*In vivo* data shows that EDS1 and PAD4 (Phytoalexin Deficient 4) associate into a heterodimer both in unchallenged plants and in pathogen-infected plants (Jirage et al., 1999; Feys et al., 2001). The function of the EDS1-PAD4 hub in basal immunity and TNL-mediated immunity against pathogens is partially dependent on SA. Although EDS1 and PAD4 are both essential for all the instances of TNL-mediated resistance, EDS1 seems to be more critical because loss of function of EDS1 abolishes PAD4-independent TNL-triggered cell death (Zhou et al., 1998; Jirage et al., 1999; Feys et al., 2001; Cui et al., 2017). This implies that there might be another branch involving EDS1 that regulates TNL-mediated cell death.

In 2005, SAG101 (Senescence Associated Gene 101) was identified as an additional interactor of EDS1 (Feys et al., 2005). EDS1<sup>L262P</sup>, which is capable of interacting with SAG101, but not PAD4, maintains TNL-mediated resistance and cell death but not basal resistance (Rietz et al., 2011). Analysis of TNL CHS3 (Chilling Sensitive 3)-related immune factors shows that the *pad4* mutant could only mildly suppress the auto-immune phenotype of a gain-of-function CHS3 mutant. In contrast, a *chs3* autoimmune mutant showed full dependency on SAG101 and EDS1 (Xu et al., 2015). These data suggest that EDS1-SAG101 heterodimers and EDS1-PAD4 heterodimers function distinctly in the TNL-mediated ETI response in *Arabidopsis*. The engagement of EDS1 family members in TNL-mediated immune responses identifies these proteins as a key node connecting effector recognition by receptors and ETI immune responses.

## 1.2.2 Structural analysis of EDS1 family heterodimers

EDS1, PAD4, and SAG101 all belong to the EDS1 family of proteins and have high similarity in their N-terminus lipase-like domains and C-terminus EDS1-PAD4 defined (EP) domains despite lacking the catalytic triad at the N-terminal of SAG101. Wagner et al. solved the crystal structure of EDS1-SAG101 and demonstrated the structural importance of the EDS1-SAG101 heterodimer and EDS1-PAD4 heterodimer for TNL-mediated resistance (Wagner et al., 2013). In the N-terminal lipase-like domains of EDS1 and SAG101, one  $\alpha$ -helix domain precisely inserted into a pocket in the N-terminus of SAG101. Maintained by hydrophobic force, this stable interaction is a critical trigger for EDS1 and SAG101 heterodimerization (Wagner et al., 2013; Voss et al., 2019). Abolishment of the interface by mutation markedly compromises resistance against host-adapted pathogens (Wagner et al., 2013). This indicates that the association of EDS1 and SAG101 is indispensable for the ETI response.

The EDS1-SAG101 heterodimer structure exhibits two interesting features. (1) On one side of the complex,  $\alpha$ -helices from both EDS1 and SAG101, which bridge the N-terminus and C-terminus, form a platform which might be an interface for interaction with other proteins through helix-helix packing. (2) On the other side of the EP domain interface, interaction of EDS1 and SAG101 results in formation of a cavity, which is  $\sim 1.2$  nm in length. The cavity might enable the EDS1-SAG101 heterodimer to bind a small molecule ligand and function in a yet uncovered branch of ETI (Wagner et al., 2013).

EDS1<sup>R493</sup> is located on the surface of the cavity in the EDS1-SAG101 heterodimer and EDS1-PAD4 heterodimer model together with several other positively charged residues, such as lysine and histidine. The amino acids (AAs) at these positions are highly conserved across seed plants. Deepak showed that mutation of those AAs to alanine (from a positively charged AA to a hydrophobic AA), especially mutation of EDS1<sup>R493</sup> to alanine, completely suppressed resistance mediated by some TNLs. This implies that the positively charged surface-electrical activity of the cavity is key to the functioning of EDS1 family heterodimers. EDS1<sup>F419</sup> and EDS1<sup>H476</sup> are two additional amino acids located on the surface of the cavity. In contrast to mutation of EDS1<sup>R493A</sup>, which compromised resistance, results showed that single mutation of EDS1<sup>F419</sup> and EDS1<sup>H476</sup> abolished TNL-mediated cell death (Bhandari et al., 2019; Lapin et al., 2019). As noted in

Arabidopsis, resistance and cell death are the two main EDS-dependent outputs of ETI-mediated immunity, indicating that the different amino acids define two distinct functions of EDS1.

### 1.3 How do helper-NLRs help?

In contrast to sensor NLRs, a small group of plant NLRs participate in signaling networks downstream of sensor NLRs and are thus considered as “helper” NLRs (Bonardi et al., 2011). N Required Gene1 (NRG1) and Accelerated Disease Resistance1 (ADR1) NLRs are two sequence-related groups of helper-NLRs. There are two functional NRG1s (NRG1A and NRG1B) and three functional ADR1s (ADR1, ADR1\_L1, AND ADR1\_L2) in Arabidopsis (Wu et al., 2019).

NRG1 was first identified in *N. benthamiana*, and researchers found that the protein plays a critical role in resistance following recognition of the tobacco mosaic virus effector P50 by the TNL N receptor (Peart et al., 2005). In the last decade, an increasing number of studies have demonstrated the indispensable role of NRG1s in TNL-mediated immune responses, for example for ROQ1 and RPP1. However, for defense responses mediated by CNLs, NRG1s mostly play neither a role in cell death nor in resistance (Qi et al., 2018; Castel et al., 2019; Wu et al., 2019; Saile et al., 2020).

The MHD motif is one of the important features of plant NLRs. Mutation of the MHD motif causes constitutive activation of NLRs and leads to autoimmunity. To test the function of the MHD motif in NRG1s, the NRG1A<sup>D485V</sup> mutant was generated. Data shows that expression of NRG1A<sup>D485V</sup> in a NRG1 mutant background triggers an auto-active phenotype. More importantly, this phenotype is not dependent on EDS1. Further investigation in Arabidopsis suggests that the EDS1-dependent TNL-mediated immune response requires the presence of NRG1 (Qi et al., 2018; Castel et al., 2019; Lapin et al., 2019; Wu et al., 2019). Altogether, this indicates that NRG1s function downstream of EDS1 in the ETI response.

Lapin et al. showed that upon avrRps4 effector perception, leaves functionally deficient in PAD4 still exhibited robust cell death, identical to the phenotype observed in *adr1* triple mutant plants and WT plants; however, compared to WT plants, resistance to Pst avrRps4 was compromised in these plants. In contrast to *pad4* and *adr1* triple mutant plants, *sag101* and *nrg1a/nrg1b* mutant plants remained fully resistant as did WT plants, but the cell death phenotype was abolished upon avrRps4 recognition. In addition, the *eds1* mutant abolishes both cell death and resistance. Thus,

they claimed that in Arabidopsis, upon effector recognition, there are two branches downstream of EDS1, one in which EDS1 interacts with SAG101 and signals to NRG1s, a pathway that is used more for host cell death in ETI responses, and a second one in which EDS1 interacts with PAD4 to activate downstream ADR1s for resistance (Lapin et al., 2019; Wu et al., 2019).

In addition to the function of ADR1s in TNL-mediated immune responses, recent data suggest that ADR1s are also critical for some CNL-mediated immune responses. For example, ADR1s are required for the hypersensitive response at an early stage of infection (10 hpi) after CNL RPS2 activation by *Pst DC3000* AvrPphB (Saile et al., 2020). PTI and ETI have traditionally been considered as two independent defense pathways. However, a growing body of evidence suggests that some components resemble joint nodes between PTI and ETI. For example, EDS1, PAD4, and ADR1s are required for defense after perception of the LRR-RP ligand nlp20, and it is likely that ADR1s act through interactions with receptor complexes (Pruitt et al., 2021; Tian et al., 2021). Although NRG1s is structurally very close to ADR1s, there's no clear evidence showing that NRG1s play a role in this pathway. This implies that these two groups of helper-NLRs employ different defense mechanisms against pathogen infections (**Fig. 1**).

## **1.4 TNL-mediated ETI requires EDS1 family members and helper-NLRs**

### **1.4.1 Association of TIR domain and TNLs**

Self-association of TIR domains has been shown to be important for the function of TIR proteins. Crystal structures of several TIR domains display a global fold with four-strand  $\beta$ -sheets surrounded by several  $\alpha$ -helices ( $\alpha$ A- $\alpha$ E) (Swiderski et al., 2009). Although structures of different TIR domains are highly conserved, self-association generates different interfaces. For instance, the crystal structure of L6<sup>TIR</sup> forms an interface (DE interface), which consists of the  $\alpha$ D and  $\alpha$ E helix from the two TIR units (Bernoux et al., 2011). Besides the DE interface, the SNC1<sup>TIR</sup> crystal structure also forms an AE interface. This interface is formed when the  $\alpha$ A and  $\alpha$ E interact with the counterpart of TIR. Mutation of both interfaces disrupted the self-association and cell death (Zhang et al., 2017). This is probably because of the disorder of the amino acid interactions on the interface, and, consequently, the TIR domain remains as an inactive monomer.

The cryo-EM structures of the ROQ1 resistosome and RPP1 resistosome elucidated how TNLs are assembled into tetramers upon the recognition of specific effectors. After direct recognition of their specific effectors, RPP1 and ROQ1 both formed tetramers, which very likely assembled asymmetrically with two symmetrically assembled receptor-effector homodimers (Ma et al., 2020; Martin et al., 2020). The symmetric homodimer creates an AE interface, which was shown to be important for the self-association of TIR domains. The asymmetric assembly of two homodimers generates two identical interfaces in the tetramer. This interface stabilizes the BB-loop, which is located near the catalytic center. Evidence showed that the highly conserved catalytic center in TNLs plays a critical role in EDS1- and NRG1-dependent cell death (Ma et al., 2020; Martin et al., 2020).

However, the lack of inactive TNL structures and NAD<sup>+</sup> binding structures mean that the mechanisms of self-association and of the enzymatic reaction remain unclear. By analyzing RUN1TIR- $\Delta$ AE- and RUN1TIR-RPV1-like structures, Burdett et al. showed that the AE interface is critical for bringing about conformational changes that cause the BB loop (connecting the  $\beta$ B strand and the  $\alpha$ B helix) to move away to open the catalytic center and bind NAD<sup>+</sup>. Mutation of proximal residues revealed that the intact DE surface is essential for NADase activity (Burdett et al., 2021). Taken together, these data suggest a dynamic link between TIR self-association and NADase activity. The discovery of TIR catalytic activity upon TNL activation raises the prospect that TIR domain catalytic products might be involved in downstream EDS1 signaling.

#### **1.4.2 NADase activity of plant TIR domains**

Besides canonical TNLs, some TIR proteins only contain the TIR domain (termed TO), some contain the TIR domain and NBD domain (named TN), and some are named TX because they have a TIR domain and an unidentified domain X. TIR proteins can induce EDS1-dependent cell death without an effector trigger (Nandety et al., 2013). Consistent with this, over-expression of the TIR domain of some TNL proteins in plants is sufficient to induce cell death without infection (Swiderski et al., 2009; Bernoux et al., 2011; Zhang et al., 2017). However, the mechanism of TNL-mediated EDS1-dependent resistance and cell death was for a long time unclear.

Research on animal and bacterial TIR proteins showed that the TIR domain can function as an enzyme and cleave NAD<sup>+</sup> to nicotinamide, ADP-ribose, and cyclic-ADPR. A conserved amino

acid glutamic acid is responsible for executing the catalysis in the active center. The depletion of NAD<sup>+</sup> is important for axon destruction and neuronal cell death upon injury in animals and phage resistance in bacteria (Essuman et al., 2018; Horsefield et al., 2019; Ofir et al., 2021).

To determine whether plant TIRs have NADase activity like SARM1 (sterile alpha and TIR motif containing 1) and bacterial TIR proteins, Wan et al. analyzed the TIR-only protein RBA1 and the TIR domains of two plant TNLs, RPS4 and RPP1<sup>NdA</sup>. In addition, they also tested the TIR-only protein BdTIR from a monocot plant, *Brachypodium distachyon*. Unlike dicotyledons, monocots do not have full-length TNLs proteins; therefore, the function of TIR proteins in monocotyledonous species is of great interest. All these four TIRs could induce EDS1-dependent cell death upon transient expression in *Nicotiana* species. In addition, mutation of the conserved glutamic acid abolished both NADase activity and cell death in plants (Wan et al., 2019). Consistent with these data, some other TIR domains from TNLs, like RPS4 and SNC1, also show NADase activity, which is dependent on the conserved glutamic acid (Swiderski et al., 2009; Duxbury et al., 2020). This implies that NADase activity is a common feature of TIR proteins across the plant kingdom, which is dependent on the glutamic acid in the active center.

### 1.4.3 The products of TIR domain enzymatic activity

Using NAD<sup>+</sup> as a substrate, TIR domains produce a group of small molecules. In contrast to SARM1 TIR, but similar to bacterial TIRs, plant TIR proteins produce an additional small molecule, which refers to a variant cADPR (v-cADPR), which has the same molecular size as cADPR, but with a different retention time on the HPLC-MS (High performance liquid chromatography-mass spectrometry) profile (Essuman et al., 2018; Horsefield et al., 2019; Wan et al., 2019). The variant c-ADPR also accumulates in plants upon TNL activation but not activation of CNL. However, expression of SARM1<sup>TIR</sup> and TIRAbTIR fails to trigger cell death in plants, although they both have a higher NADase activity and produce cADPR and/or v-cADPR. As plant TIR is able to trigger cell death, these data imply that NADase is necessary but not sufficient for cell death in plants (Duxbury et al., 2020). This indicates that plant TIR proteins may produce some unique signals to bridge TNLs and ETI immune responses (**Fig. 1**). Thus, here the question is: how does the EDS1 family link upstream TNLs and downstream helper-NLRs?

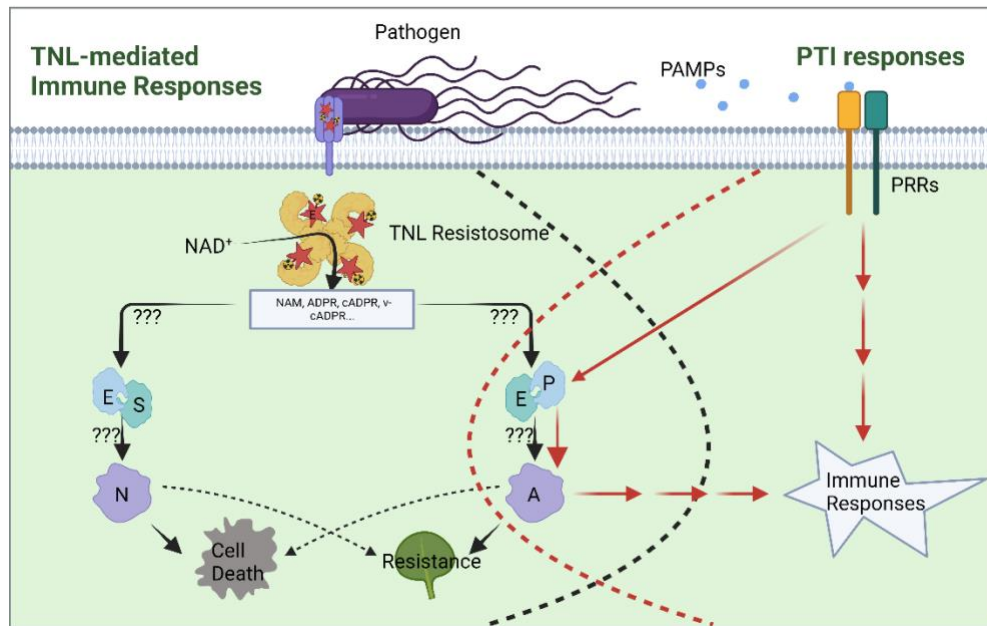


**Figure 1 Schematic representation of TNL-mediated immune responses and crosstalk with PTI in Arabidopsis.** After recognition of effectors by TNLs, self-associated TNLs catalyze  $\text{NAD}^+$  and deliver products such as v-cADPR, ADPR, and NAM to downstream EDS1 family members via an unknown mechanism. Activated EDS1 family members transmit signals to helper-NLRs, which trigger ETI responses (Horsefield et al., 2019; Wan et al., 2019). Following effector sensing by TNLs, two branches arise downstream of EDS1. In one branch, the EDS1-PAD4 complex acts together with ADR1s and is primarily responsible for plant resistance. In the other branch, the EDS1-SAG101 complex acts with NRG1s and triggers cell death (Lapin et al., 2019; Sun et al., 2021). EDS1, PAD4, and ADR1s are also involved in some PTI responses (Pruitt et al., 2021)

## 2 Aims of this study

The expression and purification of NRG1s and ADR1s as well as of PAD4 have yet to be reported, thus constituting a serious barrier to their biochemical study. In my project, I first attempted to express and purify helper NLRs and EDS1 family members from the model plant *Arabidopsis thaliana* in recombinant expression systems. Then, experiments were designed to test the hypothesis that EDS1 complexes act as a molecular bridge between sensor TNL receptors and helper NLRs.

We developed a few questions which guided us through the study:

- 1) Do helper-NLRs self-activate in the *in vitro* recombinant system?
- 2) Do EDS1 family members interact with helper-NLRs *in vitro*?
- 3) How do EDS1 family members activate helper-NLRs?
- 4) How do activated TNLs or TIR proteins influence EDS1 family member activation of helper-NLRs?

I aimed to uncover the answers to these questions in order to understand the mechanisms of TNL-mediated cell death and resistance.



### 3 Materials and Methods

#### 3.1 Molecular cloning

##### 3.1.1 PCR cloning

All target genes were cloned using Q5 High Fidelity DNA Polymerase (NEB) according to manufacturers' instructions with gene-specific primers (**Table 3.1, 3.2, and 3.3**). A typical reaction setup and the thermocycling conditions are described in **Table 3.1** and **Table 3.2**, respectively:

**Table 3.1 PCR reaction mixture.**

Components	Volume ( $\mu$ l)
5 $\times$ Q5 Reaction Buffer	10
10 $\mu$ M Forward Primer	1
10 $\mu$ M Reverse Primer	1
10 mM dNTPs	2
Template DNA	1-10 ng
Q5 High-Fidelity DNA Polymerase	0.5
ddH <sub>2</sub> O	to 50 $\mu$ l

**Table 3.2 PCR reaction conditions.**

Steps	Temperature	Duration
Pre-denaturation	98°C	30 seconds
Denaturation	98°C	15 seconds
Annealing	50-72°C	15 seconds
Elongation	72°C	~15 seconds/kb

25-35 cycles

Final elongation	72°C	5 minutes
Hold	4-10°C	--

Oligonucleotides were purchased from Sigma-Aldrich or Invitrogen. Lyophilized primers were resuspended in bidistilled water to a final concentration of 100 µM. Working solutions were diluted to 10 µM. All the primers are stored at -20°C and freshly thawed before use.

**Table 3.3 Primers used in this study.**

No.	Name	5'-3' sequence
SH_23	NRG1A_F	GAAATTGGATCCATGAACGATTGGGCTAGTTTGGG
SH_24	NRG1A_R	GAAATTCTCGAGTTAAAACATTTGAAGCAAGTTCAG
SH_25	NRG1B_F	GAAATTGGATCCATGGTCGTGGTCGATTGGCTTGG
SH_26	NRG1B_R	GAAATTCTCGAGTTAAAACGTTAGAAGCAACTTC
SH_27	ADR1_F	GAAATTGGATCCATGGCTTCGTTTCATAGATCTTTTC
SH_28	ADR1_R	GAAATTCTCGAGCTAATCGTCAAGCCAATCCACG
SH_29	ADR1-L1_F	GAAATTGGATCCATGGCCATCACCGATTTTTTCG
SH_30	ADR1-L1_R	GAAATTCTCGAGTTATTCGTCAAGCCAGTCTAGG
SH_31	ADR1-L2_F	GAAATTGGATCCATGGCAGATATAATCGGCGGGC
SH_32	ADR1-L2_R	GAAATTCTCGAGCTAATCGTCGAGCCAATCCCTG
SH_44	NRG1_F	CTGGAAGTTCTGTTTCAGGGGCCCATGAACGATTGGGCTA GTTTGGG
SH_45	NRG1_R	ACCGGTACGCGTAGAATCGAGACCTTAAAACATTTGAAG CAAGTTCAG
SH_50	ADR1-L1_F	CTGGAAGTTCTGTTTCAGGGGCCCATGGCCATCACCGATT TTTTTCG
SH_51	ADR1-L1_R	ACCGGTACGCGTAGAATCGAGACCTTATTCGTCAAGCCA GTCTAGG

<b>SH_52</b>	ADR1-L2_F	CTGGAAGTTCTGTTTCAGGGGCCCATGGCAGATATAATCG GCGGCG
<b>SH_53</b>	ADR1-L2_R	ACCGGTACGCGTAGAATCGAGACCCTAATCGTCGAGCCA ATCCCTG
<b>SH_77</b>	NRG1B_F	GAAATTGGATCCATGGTGGTGGTGGATTG
<b>SH_78</b>	NRG1B_R	GAAATTCTCGAGTTAGAAGGTCAACAGCAGC
<b>SH_79</b>	NRG1A_F	GAAATTGGATCCATGAACGACTGGGCTTC
<b>SH_80</b>	NRG1A_R	GAAATTCTCGAGTTAGAACATCTGCAGCAGG
<b>SH_90</b>	NRG1B_F	GAAATTGGATCCATGCTGGGTCTGTGGCTGGTG
<b>SH_91</b>	NRG1A <sup>Δ10</sup> _F	GAAATTGGATCCATGTCCATCGGAGAGGCTGTGTTC
<b>SH_94</b>	EDS1_R	GAAATTCTCGAGTTAGGTATCTGTTATTTTCATCCATC
<b>SH_127</b>	SAG101_F	GAAATTGGATCCATGGAGTCTTCTTCTTCACTAAAAGG
<b>SH_128</b>	SAG101_R	GAAATTGTCGACTTATTGTGACTTACCATAACTCTCGTAC
<b>SH_131</b>	EDS1_F	GAAATTAGATCTATGGCGTTTGAAGCTCTTAC
<b>SH_132</b>	PAD4_F	GAAGTTCTGTTTCAGGGGCCCTGATGGACGATTGTCGAT TCGAGAC
<b>SH_133</b>	PAD4_R	CGTTGGCCGTTTACCCGTGAGTAGCTAAGTCTCCATTGCG TCACTCTC
<b>SH_167</b>	PAD4_F	GAAATTGGATCCATGGACGATTGTCGATTTCGAG
<b>SH_168</b>	SAG101_R	GAAATTCTCGAGTTATTGTGACTTACCATAACTCTC
<b>SH_171</b>	EDS1_R	GAAATTCTCGAGGGTATCTGTTATTTTCATCCATCATATAG
<b>SH_172</b>	PAD4_F	GTTCTGTTTCAGGGGCCCTGGGATCCATGGACGATTGTC GATTCGAGAC
<b>SH_179</b>	ADR1-L1_F	GAAATTGGATCCATGGCCATCACCGAT
<b>SH_180</b>	ADR1-L1_R	GAAATTCTCGAGTTCGTCAAGCCAGTCTAG
<b>SH_183</b>	ADR1-L1 <sup>Δ10</sup> _F	GAAATTGGATCCACGGAGCTCCTGAAGCAG

<b>SH_184</b>	ADR1-L1 <sup>Δ30</sup> _F	GAAATTGGATCCAACACCGCCAAACAACCTCCTC
<b>SH_191</b>	PAD4_R	CCCTGAAACAGAACTTCCAGAGTCTCCATTGCGTCACTCT C
<b>SH_198</b>	PAD4_F	TACCGTCCCACCATCGGGCGCGGATCCATGGACGATTGTC GATTCGAGAC

### 3.1.2 DNA gel electrophoresis

To purify the DNA fragments, PCR products were separated using DNA gel electrophoresis (**Table 3.4**).

**Table 3.4 DNA gel electrophoresis.**

<b>Buffer name</b>	<b>Buffer components</b>
50×TAE running buffer	2 M Tris base, 1 M Acetic acid, 50 mM EDTA, pH 8.5
6×loading buffer	40 % (w/v) Sucrose, 0.5 M EDTA, 0.2 % (w/v) Bromophenol blue
DNA molecular weight marker (600 μl)	100 μl 6×loading buffer, 100 μl 1 kb Plus DNA Ladder (NEB)

### 3.1.3 PCR products clean up

After DNA gel electrophoresis, target bands were cut and collected in 1.5 ml Eppendorf tubes, and the PCR products were cleaned up using PCR clean up and gel extraction kit (MACHERY-NAGEL).

### 3.1.4 Restriction digestion of DNA and empty vectors

DNA fragments and empty vectors carrying specific restriction endonuclease digestion sites were incubated with enzymes and buffers for the appropriated time according to the manufacturers' instructions and then separated by DNA gel electrophoresis. Target DNA fragments and target vectors must each have the same digestion sites, respectively. The most commonly used enzymes in this study are listed in **Table 3.5**, and the digestion mixture is described in **Table 3.6**.

**Table 3.5 restriction endonuclease used in this study.**

Name	Supplier
BamHI	NEB
XhoI	NEB
BglIII	NEB
SalI	NEB
EcoRI	NEB
HindIII	NEB

**Table 3.6 Enzyme digestion mixture.**

Components	Volume ( $\mu$ l)
DNA	1-5 $\mu$ g
10 $\times$ Digestion buffer	5 $\mu$ l
Restriction Enzyme A	1 $\mu$ l
Restriction Enzyme B	1 $\mu$ l
ddH <sub>2</sub> O	to 50 $\mu$ l

### 3.1.5 Plasmid construction

Digested DNA fragments were cloned into specific plasmids either by T4 ligase or Gibson assembling kit (**Table 3.7 and 3.8**).

**Table 3.7 T4 ligation mixture.**

<b>Components</b>	<b>Volume (<math>\mu</math>l)</b>
10 $\times$ T4 DNA Ligase Buffer	1-5 $\mu$ g
Digested Vector	~100 ng
Digested DNA fragment	2-3-fold molar of vector
T4 DNA ligase	1 $\mu$ l
ddH <sub>2</sub> O	to 20 $\mu$ l

**Table 3.8 Gibson assembly mixture.**

<b>Components</b>	<b>Volume (<math>\mu</math>l)</b>
Vector	~100 ng
Digested DNA fragment	2-3-fold molar of vector
Gibson assembly master mix	10 $\mu$ l
ddH <sub>2</sub> O	to 20 $\mu$ l

**Table 3.9 Plasmids generated in this study.**

<b>No.</b>	<b>Gene</b>	<b>Vector</b>	<b>Strain</b>	<b>N-terminus Deletion</b>	<b>Tag</b>	<b>Sequence origin</b>	<b>Primers</b>
<b>H19</b>	NRG1A	pFastbac1	DH10	--	N-Sumo-6 $\times$ His	Native	SH_23, SH_24
<b>H20</b>	NRG1B	pFastbac1	DH10	--	N-Sumo-6 $\times$ His	Native	SH_25, SH_26
<b>H21</b>	ADR1	pFastbac1	DH10	--	N-Sumo-6 $\times$ His	Native	SH_27, SH_28

<b>H22</b>	ADR1-L1	pFastbac1	DH10	--	N-Sumo-6×His	Native	SH_29, SH_30
<b>H23</b>	ADR1-L2	pFastbac1	DH10	--	N-Sumo-6×His	Native	SH_31, SH_32
<b>H25</b>	NRG1A	pBAD1	top10	--	N-Sumo-6×His	Native	SH_44, SH_45
<b>H26</b>	ADR1-L1	pBAD1	top10	--	N-Sumo-6×His	Native	SH_50, SH_51
<b>H27</b>	ADR1-L2	pBAD1	top10	--	N-Sumo-6×His	Native	SH_52, SH_53
<b>H42</b>	NRG1B	pFastbac1	DH10	--	N-Sumo-6×His	Optimized	SH_77, SH_78
<b>H43</b>	NRG1B	pFastbac1	DH10	10 AA	N-Sumo-6×His	Optimized	SH_78, SH_90
<b>H44</b>	NRG1A	pFastbac1	DH10	--	N-Sumo-6×His	Optimized	SH_79, SH_80
<b>H45</b>	NRG1A	pFastbac1	DH10	10 AA	N-Sumo-6×His	Optimized	SH_91, SH_80
<b>H54</b>	PAD4	pFastbac1	DH10	--	N-Sumo-6×His	Native	SH_132, SH_133
<b>H57</b>	EDS1	pFastbac1	DH10	--	N-Sumo-6×His	Native	SH_131, SH_94
<b>H58</b>	SAG101	pFastbac1	DH10	--	N-Sumo-6×His	Native	SH_127, SH_128
<b>H67</b>	chi1	pFastbac1	DH10	--	N-Sumo-6×His	(Lapin et al. , 2019)	SH_167, SH_168
<b>H68</b>	chi2	pFastbac1	DH10	--	N-Sumo-6×His	(Lapin et al. , 2019)	SH_167, SH_168

<b>H73</b>	ADR1-L1	pFastbac1	DH10	10 AA	N-Sumo-6×His-C-strep	Optimized	SH_183, SH_180
<b>H83</b>	EDS1	pFastbac1	DH10	--	C-Strep	Native	SH_131, SH_171
<b>H98</b>	chi2	pFastbac1	DH10	--	C-Strep	Native	SH_167, SH_168
<b>H99</b>	PAD4	pFastbac1	DH10	--	C-Strep	Native	SH_172, SH_133
<b>H100</b>	SAG101	pFastbac1	DH10	--	C-Strep	Native	SH_191, SH_198
<b>H101</b>	EDS1	pFastbac1	DH10	--	no tag	Native	SH_131, SH_94
<b>H102</b>	NRG1A	pFastbac1	DH10	--	N - GST	Optimized	SH_79, SH_80
<b>H103</b>	NRG1A	pFastbac1	DH10	10 AA	N - GST	Optimized	SH_91, SH_80
<b>H104</b>	ADR1-L1	pFastbac1	DH10	--	N - GST	Optimized	SH_179, SH_180
<b>H111</b>	ADR1-L1	pFastbac1	DH10	10 AA	N - GST	Optimized	SH_183, SH_180
<b>H112</b>	ADR1-L1	pFastbac1	DH10	10 AA	N - GST	Optimized	SH_184, SH_180

### 3.1.6 Plasmids construction and transformation

Plasmids were generated and transformed into different strains to express target proteins (**Table 3.9, 3.10 and 3.11**). EDS1 and SAG101 were also purified both from insect cells and from *E. coli*.



Plasmids for expressing EDS1-no tag and SAG101-N-6×His were generally provided by the Jane Parker group and the Niefind group (Wagner et al., 2013).

**Table 3.10 Competent cells and insect cell strains.**

Name	Supplier	Genotype
<i>E. coli</i> BL21(DE3)	Invitrogen	F <sup>-</sup> <i>ompT hsdS</i> (r <sub>B</sub> <sup>-</sup> m <sub>B</sub> <sup>-</sup> ) <i>gal dcm</i> (DE3)
<i>E. coli</i> DH5α	Invitrogen	F <sup>-</sup> <i>endA1 glnV44 thi-1 recA1 relA1 gyrA96 deoR nupG purB20 Φ80dlacZΔM15Δ(lacZYA-argF)U169</i> , <i>hsdR17</i> (r <sub>K</sub> <sup>-</sup> m <sub>K</sub> <sup>+</sup> ), λ <sup>-</sup>
<i>E. coli</i> DH10Bac	Thermo Fisher	F <sup>-</sup> <i>mcrA Δ(mrr-hsdRMS-mcrBC) Φ80lacZΔM15 ΔlacX74 recA1 endA1 araD139 Δ(ara, leu)7697 galU galK λ<sup>-</sup> rpsL nupG/pMON14272/pMON7124</i>
<i>E. coli</i> Top10	Thermo Fisher	<i>mcrA, Δ(mrr-hsdRMS-mcrBC), Phi80lacZ(del)M15, ΔlacX74, deoR, recA1, araD139, Δ(ara-leu)7697, galU, galK, rpsL(SmR), endA1, nupG</i>
Insect cell <i>sf21</i>	Thermo Fisher	--

**Table 3.11 Empty vectors used in this study.**

Name	Supplier	Resistance
pFastbac1	Invitrogen	Ampicillin
pBAD	Invitrogen	Kanamycin

## 3.2 Protein expression and purification

### 3.2.1 Recombinant protein expressing in *E. coli*

To express and purify NRG1s, ADR1s in *E. coli*, plasmids H25, H26 and H27 (**Table 3.9**) were transformed into the Top10 strain, which encodes a tandem histidine amino acid at the N-terminus

of the target protein. The transformation mixtures were then spread on LB plates containing 50 µg/ml kanamycin and incubated for 12-16 h at 37°C. To test the expression levels of each protein, three single colonies were picked from each plate and were shaken in LB medium overnight at 37°C in 15 ml tubes. One milliliter of each culture was taken and induced with 0.2 mM arabinose and shaken at 37°C for 4 hours. To identify the expression of target proteins, controls were induced with ddH<sub>2</sub>O. In the next step, all samples were centrifuged at 13,000×g for 1 minute. The pellet was then resuspended with 30 µl of wash buffer and 1 µl of each sample was taken, boiled at 95°C for 10 minutes together with SDS loading buffer and then applied to the protein gel electrophoresis. The successfully expressed samples were then cultured in a big scale at 37°C and the temperature was reduced to 18°C once the concentration reached an OD<sub>600</sub> of ~0.8. All cultures were then induced with 0.2 mM arabinose after cooling to 18°C and cultured overnight in a shaker.

The expression and purification of EDS1 and SAG101 in *E. coli* were performed following the methods described in Wagner et al. (Wagner et al., 2013).

**Table 3.12 Protein extraction and purification buffer.**

<b>Buffer name</b>	<b>Buffer components</b>
Plant protein extraction buffer	20 mM PIPES-KOH pH 7, 150 mM NaCl, 10 mM MgCl <sub>2</sub> , 10% Glycerol, 5 mM DTT, 1% Triton-X-100, 1% Protease Inhibitor, fill up with ddH <sub>2</sub> O
His-tag resuspend/wash buffer	150 mM NaCl, 25 mM Tris-HCl pH 8.0, 15 mM Imidazole pH 8.0
GST/Strep-tag resuspend/Wash buffer	150 mM NaCl, 25 mM Tris-HCl pH 8.0
His-tag elution buffer	150 mM NaCl, 25 mM Tris-HCl pH 8.0, 250 mM Imidazole pH 8.0
GST-tag elution buffer	150 mM NaCl, 25 mM Tris-HCl pH 8.0, 60 mM Reduced Glutathion

**Table 3.13 Protein gel electrophoresis.**

<b>Buffer name</b>	<b>Buffer components</b>
10×TGS running buffer	0.25 M Tris base, 1.9 M Glycine, 35 mM SDS
6×SDS loading buffer	60 mM Tris pH 6.8, 12 % (w/v) SDS, 600 mM DTT, 47 % (v/v) Glycerol, 0.6 % (w/v) Bromophenol blue
Coomassie Brilliant Blue Staining buffer	25 % (v/v) Isopropanol, 10 % (v/v) Acetic acid, 0.04 % (w/v) Coomassie Brilliant Blue G-250
Destaining buffer	10 % (v/v) Ethanol, 2 % (v/v) Orthophosphoric acid

### 3.2.2 Recombinant protein expression in insect cell

Target genes were cloned into commercially available vector pFASTBAC1 for expression in insect cells. Plasmids were first transformed into competent cells DH10 and incubated on LB plates containing 50 µg/ml kanamycin, 50 µg/ml gentamicin, and 25 µg/ml tetracycline for ~48 hours at 37°C. 110 µl X-gal and 70 µl IPTG were also added to these agar plates (100 mm) to distinguish positive colonies (white) and negative colonies (blue). The white colonies were picked and cultured for bacmid purification.

The transfection of bacmids to *Sf21* insect cells was performed as described in the manufacturers' instructions which includes the preparation of P0 and P1 viral stocks.

Preparing the P0 viral stock:

- 1) Mix Cellfectin II well before use, and dilute 8 µl in 100 µl Gibco sf-900 Medium. Then mix 8 µl purified bacmids with 100 µl medium as well. Combine these two mixtures and incubate at room temperature for up to 30 minutes.
- 2) Plate  $8 \times 10^5$  *Sf21* cells which has the cell density in range of  $1.5-2.5 \times 10^6$  cells/ml per well. Allow cells to attach the well wall for 15 minutes at room temperature under the hood. Then remove the medium and add two ml Gibco sf-900 Medium to each well.

- 3) Add 800  $\mu$ l medium to the mixture generated in step 1, and apply the mixtures to each well prepared in step 2. Then incubate the cells at 28°C for six hours.
- 4) Remove the medium in each well and replace with new medium which contains 1 $\times$  Gibco Penicillin-Streptomycin (10.000 U/ml). Then incubate the culture at 28°C for 4-5 days. As control, instead of bacmid, ddH<sub>2</sub>O was added so that the cell density and cell size can be observed and compared in this process.

Preparing the P1 viral stock:

- 5) Once the transfected cells (from step 4) demonstrate signs of late stage infection (e.g., cell size increasing, detachment), collect the medium containing the virus from each well (~two ml) and transfer to sterile 15 ml snap-cap tubes. Centrifuge the tubes at 500 $\times$ g for five minutes to remove cells and large debris.
- 6) Transfer the clarified supernatant to fresh 15 ml snap-cap tubes (P1 viral stock). Store at 4°C, protected from light.

Once the P1 viral stock was obtained, it was amplified by infecting healthy cells. The supernatant was used for further experiments, such as protein expression.

### 3.2.3 Expression and purification of PreScission protease

The PreScission protease was constructed in pGex6p-1-N-GST and then transformed into BL21. For expression, 500 ml of medium was inoculated with 10 ml of starter culture and incubated at 37°C in the shaker until it reached an OD<sub>600</sub> of ~0.8. The incubator was then cooled to 18°C and cells were induced by adding IPTG at a final concentration of 0.4 mM. These cultures were incubated and shaken overnight at 18°C, and 180 rpm.

For purification, resuspension/wash buffer and elution buffer for GST-tagged proteins were used. Gel filtration was performed using Superdex 200 as it forms a dimer with a size of about 90 KDa, generally peaking at 13 ml. Buffers were 10 mM TRIS pH 8.0 and 100 mM NaCl. Collect all target protein, dilute to a concentration of 3 mg/ml, make 100  $\mu$ l aliquots, freeze in liquid nitrogen and store at -80°C. In general, a yield of around 5-10 mg/L of PreScission protease can be achieved. Buffer information is listed in **Table 3.12**.

### 3.2.4 Affinity purification

After infection, culture and induction, cell cultures were harvested and centrifuged for 15 minutes at 3500×g, 4°C. All proteins investigated in this study are intracellular proteins; therefore, the cell pellet was collected and the supernatant was discarded after centrifugation. To purify target protein, the pellet was resuspended with resuspending buffer and lysed by ultrasonication for 10 minutes at 60% output for *E. coli* cells and 45% for insect cells. Cell debris was then spun down for 2 hours at 20000×g, 4°C. Next, clear lysate was loaded to manually packed affinity columns according to manufacturers' instructions. To increase the binding effect, the lysate was reloaded to the column after one round through. After all the lysate went through the column twice, the column was washed with three volumes washing buffer. Finally, the target protein was eluted with elution buffer for at least three resin-volume and the protein product was visualized by SDS-PAGE gel (**Table 3.13**). Buffer information is listed in **Table 3.12**.

### 3.2.5 Size exclusion chromatography (SEC, gel filtration) of target proteins

To prepare samples for gel filtration, the eluted samples from affinity purification were first concentrated to an appropriate volume which is not bigger than the loading loop on the gel filtration. The samples were then applied to a prepacked and equilibrated column and eluted according to their molecular weights. In this study, HiLoad 26/600 Superdex 200 pg column (Cytiva) was used for the protein size range from 50 KDa to 200 KDa and Superose 6 Increase 10/300 GL glass columns (Cytiva) from 200 KDa to 1000 KDa.

### 3.2.6 Negative staining

To briefly observe the homogeneity and/or the status of the target proteins, samples were prepared for transmission electron microscope (Hitachi H-7650 TEM). In general, a concentration of ~1.0 mg/ml protein was first applied to the EM grid and then the concentration was optimized according to the TEM observations. The preparation of sample grid is described as follows:

- 1) Glow discharging of grids: Place slide with grids on top (carbon side up) in vacuum chamber with automatic timer, and pull vacuum and glow discharge.

- 2) Pipette drops of 2% uranyl acetate UrAc (8  $\mu$ l each) onto Parafilm. Have one piece of filter paper ready to absorb excessive stain and wash buffer from grids away during staining.
- 3) Hold a grid in clamping forceps. Pipette 5  $\mu$ l of protein solution onto grid. After 55 seconds, blot off protein solution onto filter paper, touch to UrAc drop and slightly move around for 8 seconds, then incubate for 50 seconds, and finally blot off UrAc (take care to blot out liquid trapped in forceps).
- 4) Allow grids to dry for a few minutes, then place in grid box (note positions/IDs in lab book). Grids can be visualized immediately, and are usually stable for months or years.

### 3.3 Pull-down assay

To analyze the interactions of EDS1 family members and helper-NLRs *in vitro*, N-terminal GST-tagged NRG1A and ADR1\_L1 were expressed, respectively. EDS1 family proteins, which are tagged either with twin-strep or not tagged, were either prepared beforehand or co-expressed with helper-NLRs. The pull-down assay is described as follows:

- 1) Allow the cell lysate supernatant from NRG1A and ADR1\_L1 flow through GST-affinity column and then wash with three column-volume using GST wash buffer.
- 2) Resuspend the resins with 5 ml wash buffer, take 20  $\mu$ l resin and mix with 5  $\mu$ l SDS loading buffer, and then boil the samples at 95°C for 10 minutes. Visualize protein expression level and EDS1 family proteins with SDS-PAGE gel. Continue the pull-down assay only when reasonable amount of proteins was achieved.
- 3) Split the resins evenly to new empty column. For each new column, add sufficient amount of EDS1 family heterodimers and incubate at 4°C overnight. For control, add same volume of wash buffer.
- 4) After incubation, collect and label the buffers during the flow-through. Wash the columns with three column-volume and resuspend the resins with two resin-volume using wash buffer. In the step one to four, keep proteins always on ice so that protein degradation can be maximal avoid.
- 5) Take 30  $\mu$ l of well-resuspend resin solutions and mix with 10  $\mu$ l SDS loading buffer and then boil the samples at 95°C for 10 minutes. Visualize proteins with SDS-PAGE gel.

For the co-expression pull down assay, experiments were performed without step 3.

## 4 Results

### 4.1 Structural alignment of NRG1A model with ZAR1

The structure of the ZAR1 (CC-NLR) resistosome has shed light on the oligomerization of the CC domain and thus constitutes an excellent model for plant NLRs (Wang et al., 2019a; Wang et al., 2019b). Since there was no structural information about helper-NLRs available, in order to biochemically analyze the function of helper-NLRs, I used the I-TASSER (Iterative Threading Assembly Refinement) on-line platform from the Yang Zhang Lab to predict the structure of Arabidopsis NRG1A (Yang et al., 2015).

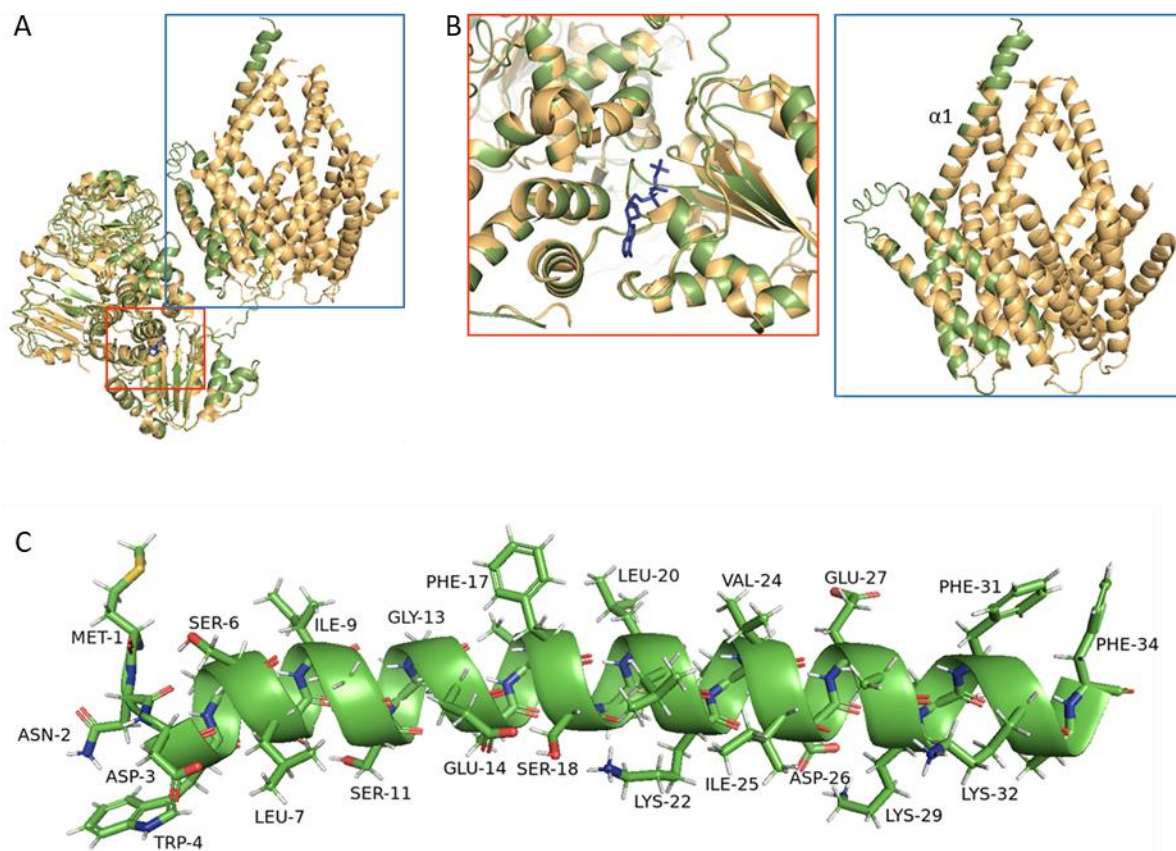


**Figure 4.1 Structural alignment of NRG1A model and active ZAR1.** (A) Cartoon showing the overall structural alignment of the NRG1A model and active ZAR1. Gold color refers to the structure of active ZAR1, green refers to the model of NRG1A. The CC domain and ATP binding regions are highlighted with blue and red open frames, respectively. (B) Detailed structural alignment of the CC domain (blue frame) and the ATP (blue sticks) binding region (red frame). (C) Amino acid labeling on the two sides of the  $\alpha 1$  helix in the NRG1A model.

The model of NRG1A aligns very closely with that of active ZAR1 including the ATP binding site (**Fig. 4.1A and B**). Although the N-terminus of NRG1A features a HeLo domain, the  $\alpha 2$ ,  $\alpha 3$ , and  $\alpha 4$  helical bundles stack together as in ZAR1 (**Fig. 4.1A and B**). Notably, the  $\alpha 1$  helix of NRG1A is significantly longer than that of ZAR1, but the rest of the helix still matches perfectly with ZAR1 (**Fig. 4.1A and B**). This indicates that the biological function and biochemical structure of activated NRG1A might be very similar to those of ZAR1.

The  $\alpha 1$  helix of ZAR1 forms a pore and anchors to the membrane (Wang et al., 2019a; Wang et al., 2019b). This pore regulates calcium influx and thus triggers cell death to constrain the growth of pathogens (Bi et al., 2021). The function of the  $\alpha 1$  helix of ZAR1 is favored by its amphipathic amino acids. One side of this amphipathic helix interacts with the hydrophobic membrane and on the other side, hydrophilic amino acids allow ions to shuttle through.

In Arabidopsis, NRG1A is critical for TNL-mediated cell death upon effector recognition (Qi et al., 2018; Castel et al., 2019; Lapin et al., 2019; Sun et al., 2021). My hypothesis was that NRG1A can also form a pore on the membrane and induce cell death by functioning as an ion channel. To investigate this, I analyzed the amino acid features of the NRG1A  $\alpha 1$  helix. This analysis shows that on one side of the  $\alpha 1$  helix, there is a high ratio of amino acids with hydrophobic side chains, like valine, leucine, isoleucine, and phenylalanine (**Fig. 4.1C**). Importantly, this side is projecting outside of the funnel in the alignment of model NRG1A and active ZAR1. On the other side of the  $\alpha 1$  helix, most of the amino acids have polar side chains or electrically charged side chains, like serine, glutamic acid, lysine, and aspartic acid (**Fig. 4.1C**). This side aligns with the ion channel side of the ZAR1  $\alpha 1$  helix. Given that the  $\alpha 1$  helix from NRG1A is amphipathic, this strongly suggested that NRG1A might associate with the membrane and form an ion channel.

## **4.2 Expression, purification, and characterization of helper-NLRs**

### **4.2.1 Optimizing the expression of helper-NLRs in *E. coli***

Although recent technological progress in both crystallography and cryo-electron microscopy has greatly reduced the amount of protein required, preparation of milligram amounts and high purity are still necessary for experiments *in vitro*. As NLRs, AtNRG1s and AtADR1s are relatively large proteins (monomer ~92 KDa) and have never been successfully purified either in *E. coli* or in insect



cells. In my project, I first took advantage of the pBAD expression system, which allows tightly controlled, titratable expression of proteins through the regulation of specific carbon sources such as glucose, glycerol, and arabinose (Guzman et al., 1995). pBAD is ideal for expressing toxic proteins and optimizing protein solubility in *E. coli*. Taking the native nucleotide acid sequences, NRG1A, ADR1\_L1 and ADR1\_L2 were successfully cloned into the pBAD vector and expressed in the *E. coli* TOP strain. NRG1A and ADR1\_L2 could not be purified, and ADR1\_L1 was purified but with high contamination of nucleotide acids, as evidenced by the high absorbance of 260 nm in size exclusion chromatography (SEC, also called gel filtration, Bio-Rad). The failure to purify NRG1A and ADR1\_L2 does not mean that the proteins were not expressed in *E. coli*, because significant amounts of target proteins from culture lysate was visualized on the SDS-PAGE gel. However, the prokaryotic expression system seems to not support the appropriate folding of plant NLRs to produce soluble proteins.

#### 4.2.2 Optimizing the expression of helper-NLRs in insect cells

Contamination of DNA from cell wall lysis seems to be a common problem with recombinant protein expression in prokaryotic systems. To avoid unnecessary contamination and to optimize the expression and purification of helper NLRs, I utilized the Bac-to-Bac baculovirus expression system for protein expression by transfection into insect cells.

First, codon-optimized sequences of NRG1A, NRG1B, ADR1, ADR1\_L1, and ADR1\_L2 were cloned into the pFASTBAC1 vector. The pFASTBAC1 vector was fused with N-terminal Sumo (to increase the protein solubility, ~18 kDa) and a six-histidine tandem affinity tag. As the N-terminus  $\alpha$ -helix of helper-NLRs may insert into membranes and interfere with the integrity of cell membranes, I also prepared a construct with the N-terminal 10 amino acids deleted from the *NRG1A* gene sequence. After expression and His-affinity purification (using Ni Sepharose 6 Fast Flow resin), protein samples were collected and visualized on an SDS-PAGE gel using Coomassie brilliant blue staining. Expression levels of NRG1A and ADR1\_L1 were the highest of all the homologs in the family. Expression of the codon-optimized sequence in insect cells strongly increased the proportion of soluble NRG1A compared to expression in the *E. coli* system and insect cell system using native amino acid sequences (**Fig. 4.2**). In addition, the N-terminal deletion of NRG1A markedly improved the intensity of the target band on SDS-PAGE gel (**Fig. 4.2**). Considering that deletion of several N-terminal amino acids didn't influence the overall structure

and ligand binding of ZAR1 (Wang et al., 2019a; Wang et al., 2019b), and the high similarity between the  $\alpha 1$  helices of NRG1A and ZAR1, I performed all the following experiments using the helper-NLRs from which the 10 N-terminal amino acids were deleted in an attempt to increase expression levels and prevent toxicity and degradation in insect cells.

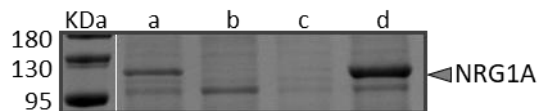


**Figure 4.2 Optimization of NRG1A expression.** NRG1A was expressed in either *E. coli* or in insect cells, then purified using Ni Sepharose 6 Fast Flow resin (His tag affinity resin, Cytiva). Eluted proteins were separated by SDS-PAGE gel and then detected by Coomassie brilliant blue staining. a. Full-length codon-optimized NRG1A was purified from insect cells. b. Full-length native NRG1A cannot be purified from insect cells. c. NRG1A with native sequence cannot be purified from *E. coli*. d. N-terminal 10-amino-acid deleted, codon-optimized NRG1A was purified from insect cells.

### 4.2.3 Optimizing the purification of helper-NLRs

Glycerol is a common co-solvent in buffers for protein purification because it can preferentially interact with hydrophobic surface regions and, thus, favor amphiphilic interactions (Vagenende et al., 2009). Buffers containing 5% to 20% glycerol can increase protein stabilization and solubility. Glycerol also prevents aggregates and reduces unspecific bands during the purification. In my study, inclusion of 5% glycerol in the resuspension buffer and wash buffer significantly improved the purity of NRG1A and was therefore considered as an essential component of the purification buffers.

### 4.2.4 Expression, purification and characterization of NRG1A in insect cells

To obtain milligram amounts of NRG1A for biochemical studies, cell culture was prepared on a large scale and infected with virus carrying NRG1A.

Significant amounts of NRG1A was prepared in two steps: (1) proteins were purified using affinity column and (2) eluted proteins were then concentrated and loaded for gel filtration. On the gel filtration, NRG1A generated two distinct peaks using Superose 6 Increase 10/300 GL glass columns (Cytiva) (**Fig. 4.3A**). Calibration of Superose increase 6 using the SEC high-molecular-weight kit indicated that the first one is ~700 kDa, very likely a higher-order structure of NRG1A and the second one is ~100 kDa, which matches the size of monomeric NRG1A (**Fig. 4.3A**). Protein

samples from different fractions were separated by SDS-PAGE gel and then detected by Coomassie brilliant blue staining. The result showed a high purity of NRG1A. The intensity of the bands on the gel followed the pattern generated by the absorbance at 280 nm, accumulating the most on the two peaks (**Fig. 4.3B**).

To characterize NRG1A, samples of the two peaks were taken for negative staining. The negative samples were then irradiated and visualized on a Hitachi H-7650 transmission electron microscope. In the 17 ml fraction, no clear particles could be identified, probably because of the limitations of transmission electron microscopy in observing small-sized particles. In the 13 ml fraction, large particles are scattered throughout the pictures, most of which are ~20 nm in size (**Fig. 4.3C**). However, we were not able to classify these particles as homogeneous oligomers according to their shape. One reason might be the lack of interaction partners or ligands that could stabilize NRG1A.

The nucleotide acid binding domain is a typical feature of plant NLRs. Exchange of ADP for ATP is one of the critical steps in the activation of ZAR1 (Wang et al., 2019b). Alignment of activated ZAR1 and the NRG1A model shows that a high similarity exists around the ATP binding pocket (**Figure 4.1B**). The hypothesis here is that ATP binding could activate NRG1A leading to formation of a stable oligomer under conditions of recombinant protein expression. To test this hypothesis, 1 mM of ATP was added to the purification steps. However, analysis of the gel filtration chromatography and SDS-PAGE-gel implies that addition of ATP is insufficient to induce oligomerization of NRG1A. Altogether, we conclude that NRG1A is not self-activating *in vitro*.

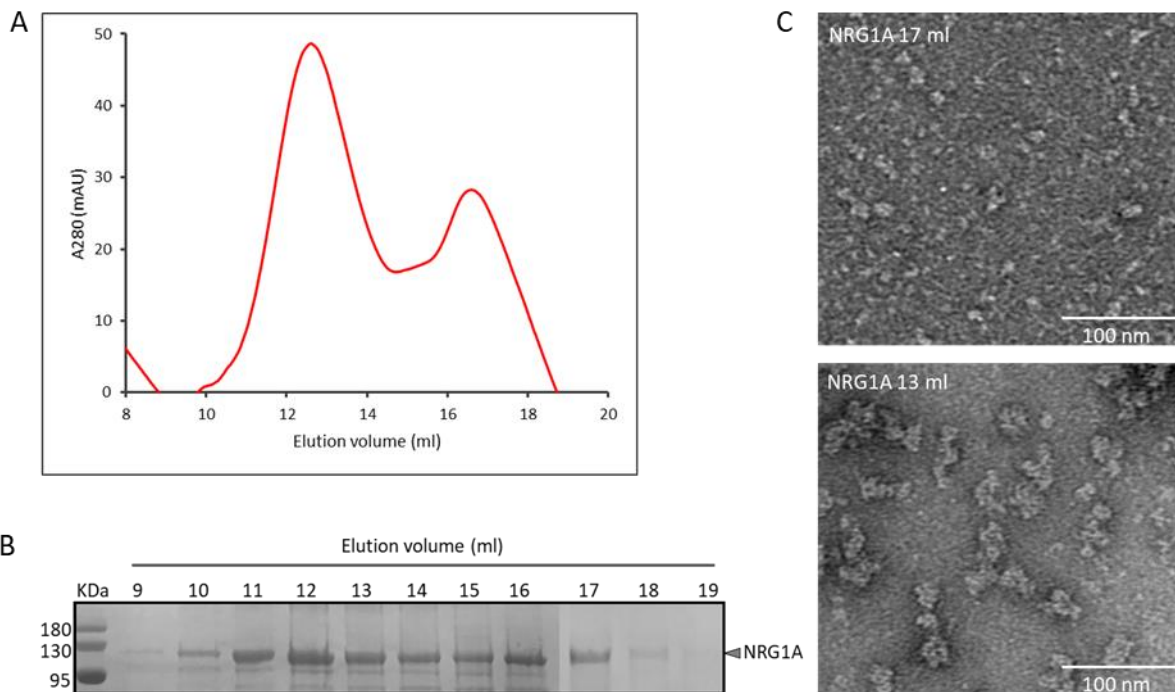


**Figure 4.3 Expression and characterization of NRG1A in insect cells.** (A) Gel filtration of NRG1A using size exclusion chromatography. Red solid line indicates NRG1A absorbance at 280 nm from 8 ml to 20 ml elution volume. Black dash indicates the peak elution volume of protein markers of different sizes. (B) Proteins from different fractions were separated by SDS-PAGE and detected by Coomassie brilliant blue staining. (C) Negative staining of protein samples at 17 ml and 13 ml elution volumes were then irradiated and visualized on a Hitachi H-7650 transmission electron microscope.

#### 4.2.5 Expression, purification, and characterization of ADR1\_L1 in insect cells

The ADR1\_L1 protein sample was prepared in the same way as that of NRG1A. However, unlike NRG1A, it was difficult to obtain highly pure ADR1\_L1 using the His affinity tag. To reduce the amount of unspecific protein contamination, ADR1\_L1 was additionally fused with a twin-strep tag at the C-terminus so that two-step affinity purification could be applied to increase the purity of ADR1\_L1. Both the 6×His tag and the twin-Strep tag are very small and therefore do not significantly add additional mass to the target protein. After sequential elution from Ni Sepharose 6 Fast Flow resin and Strep-Tactin Superflow high capacity resin (Strep affinity resin), proteins were concentrated and loaded for gel filtration using Superose 6 Increase 10/300 GL glass columns for gel filtration. ADR1\_L1-N-Sumo-6×His-C-Strep showed a unique peak at an elution volume of around 14 ml, which indicates a ~500 kDa size particle (Fig. 4.4A). SDS-PAGE gel loaded with proteins from different elution volumes confirmed the ADR1\_L1 peak and showed a highly pure target band in each well (Fig. 4.4B). Thus, protein samples from the 14 ml fraction were prepared

for negative staining. However, certain homogeneity could not be identified in the collected pictures using a transmission electron microscope (**Fig. 4.4C**). As with NRG1A, ADR1\_L1 obtained *in vitro* might simply represent aggregates. Very likely, some critical factors are essential to trigger the activation of helper-NLRs *in vitro*.

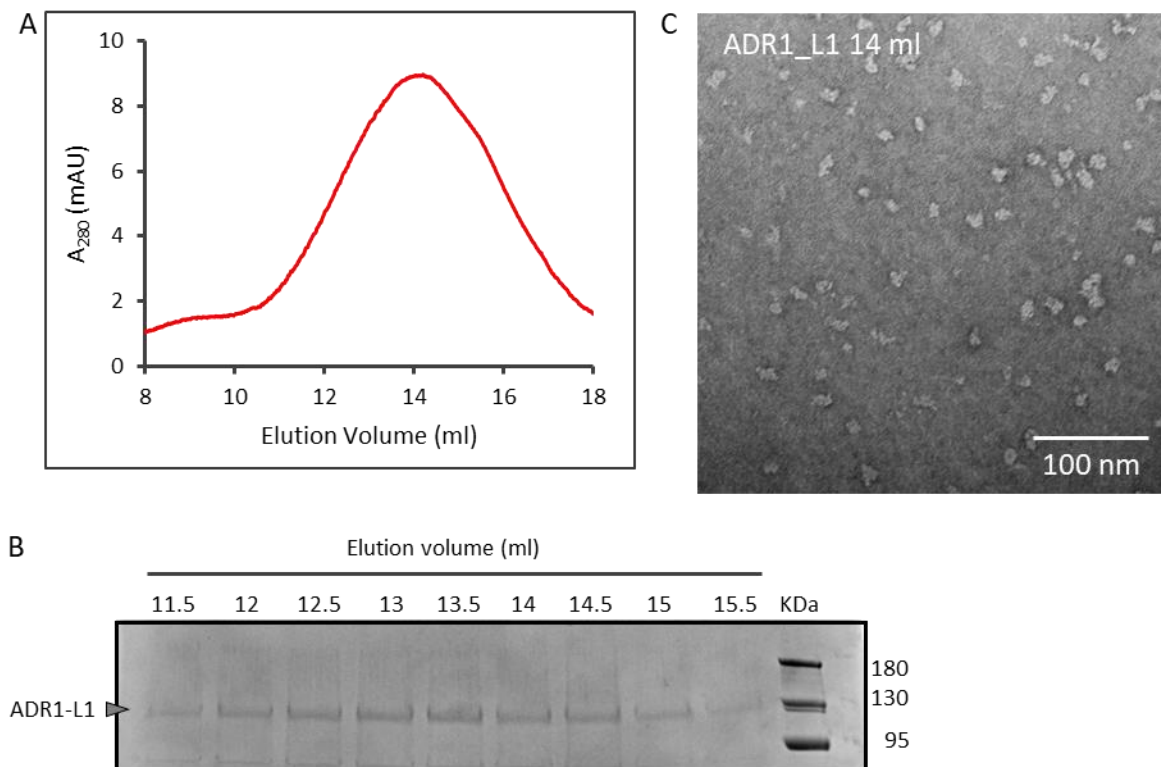


**Figure 4.4 Expression and characterization of ADR1\_L1 in insect cells.** (A) Gel filtration of ADR1\_L1 using size exclusion chromatography. Red solid line indicates the ADR1\_L1 absorbance at 280 nm from 8 ml to 20 ml elution volumes. Black dash indicates the peak elution volume of protein markers of different sizes. (B) Proteins from different fractions were separated by SDS-PAGE and detected by Coomassie brilliant blue staining. (C) Negative staining of protein samples at 14 ml elution volume was then irradiated and visualized on a Hitachi H-7650 transmission electron microscope.

## 4.3 Expression and purification of EDS1 family heterodimers

### 4.3.1 Expression and purification of EDS1-PAD4 in insect cells

Wagner et al. has solved the structure of EDS1-SAG101 heterodimer by expressing recombinant EDS1 and SAG101 in *E. coli* (Wagner et al., 2013). However, the expression and purification of PAD4 in *E. coli* was not successful. In Arabidopsis, scientists observed a significantly reduced amount of PAD4 when the EDS1-PAD4 interaction was disrupted in leaves (Rietz et al., 2011).

This indicates that, compared to SAG101, levels of PAD4 are highly sensitive to perturbation in both recombinant systems and the native environment.

To test whether accumulation of soluble PAD4 could be achieved in a eukaryotic expression system, PAD4 was cloned into the Bac-to-Bac baculovirus expression system and expression levels were tested. As shown in **Figure 4.5A**, unlike EDS1, neither SAG101 or PAD4 can be purified in significant amounts when expressed alone in insect cells. However, when PAD4 and SAG101 were co-expressed with EDS1, respectively, significant amounts of PAD4 and SAG101 can be purified together with EDS1 (**Fig. 4.5A**). This strongly implies that significant amounts of soluble PAD4 can only be retrieved when the interacting partner EDS1 is available to stabilize it. Milligrams of EDS1-PAD4 were purified by scale-up culture of co-expression in insect cells. EDS1-N-Sumo-6×His and PAD4-C-Strep were pulled down by each other using two-step AC purification. This indicates that EDS1 and PAD4 bind tightly to each other and form a stable complex *in vitro*.

To prepare recombinant protein samples of EDS1 and PAD4 complex, N-terminally Sumo-6×His-tagged EDS1 with C-terminally Strep-tagged PAD4 were co-expressed in insect cells. The two-step affinity purification method greatly increases the purity of the recovered EDS1-PAD4 complex. Approximately 6 mg of pure EDS1-PAD4 heterodimer were purified from 2 L of insect cell culture. After purification, the N-Sumo-6×His tag from PAD4 and C-Strep from EDS1 were cleaved using PreScission Protease. Gel filtration showed that EDS1 and PAD4 complex peaks at 66 ml elution volume using HiLoad 26/600 Superdex 200 pg column (Cytiva), which indicates the size of the complex is ~150 kDa (**Fig. 4.5B**). The EDS1-SAG101 heterodimer (~140 kDa) was used here as a control, which peaks at the same place on the column as the EDS1 and PAD4 complex (**Fig. 4.5B**). Comparison of SDS-PAGE gels of these two protein samples confirmed the peak at the same elution volume (**Fig. 4.5C**). Given that PAD4 and SAG101 have similar molecular sizes (~63 kDa), this strongly suggests that EDS1 and PAD4 associate as a heterodimer. Negative staining of elution samples at 66 ml for the EDS1-SAG101 heterodimer and EDS1-PAD4 heterodimer confirmed that these two heterodimers are similar in size (**Fig. 4.5D**).

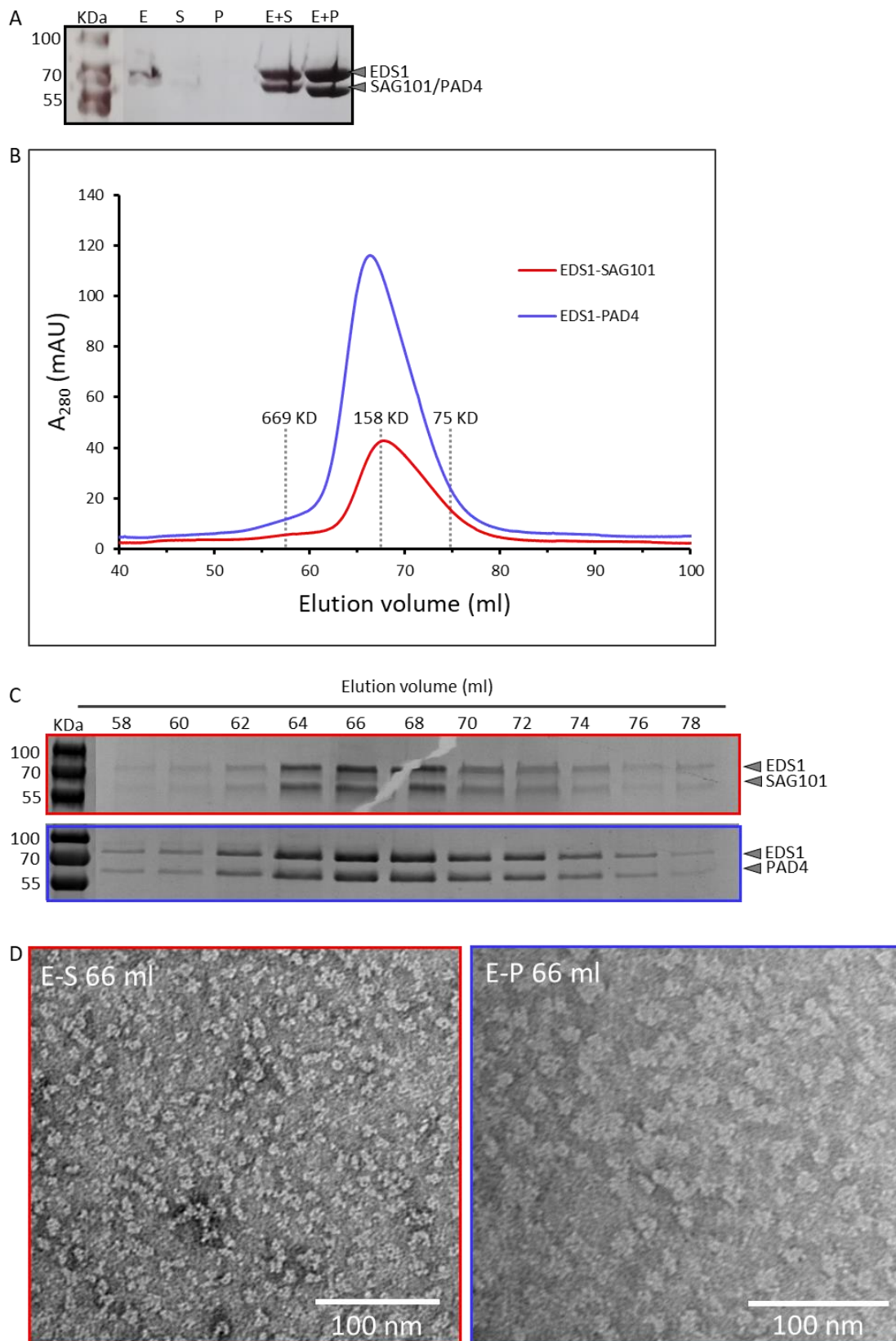


**Figure 4.5 Expression and purification of EDS1 family heterodimers in insect cells.** (A) Comparison of expression levels of EDS1, SAG101, PAD4, EDS1 co-expressed with SAG101, and EDS1 co-expressed with PAD4. Proteins were separated on an SDS-PAGE gel and detected by Coomassie brilliant blue staining. (B) Gel filtration of EDS1-SAG101 and EDS1-PAD4 using size exclusion chromatography. (C) SDS-PAGE gel indicates the EDS1-SAG101 heterodimer and EDS1-PAD4 heterodimer peaks in the same elution volume. Proteins were separated by SDS-PAGE and detected by Coomassie brilliant blue staining. (D) Negative staining of 66 ml samples of EDS1-SAG101 heterodimer and EDS1-PAD4 heterodimer. Negative staining samples were irradiated and visualized on a Hitachi H-7650 transmission electron microscope.

### 4.3.2 Crystallization of the EDS1-PAD4 heterodimer

Although the model of the EDS1-PAD4 heterodimer has a high similarity to the EDS1-SAG101 heterodimer, an empirically determined EDS1-PAD4 heterodimer structure is still required because of the marked differences in function (Lapin et al., 2019; Sun et al., 2021). Thus, to obtain the structure of the EDS1-PAD4 heterodimer, I performed crystallization using different crystallization screening kits. These included JBScreen classic kits (10 kits, each kit has 24 conditions), JBScreen basic kits (6 kits, each kit has 24 conditions), JBScreen PEG/Salt (4 kits, each kit has 24 conditions), JBScreen PACT++ (4 kits, each kit has 24 conditions), Hampton research PEG/Ion (48 conditions), Hampton research PEG/Ion 2 (48 conditions). These kits are designed for preliminary screening of biomolecules for crystallization. They cover a wide range of pH values, anions and cations as well as a variety of salts and precipitants. I expected that EDS1-PAD4 protein crystals could be obtained through continuous experimentation and optimization.

In general, the protein crystallization process consists of four phases: (1) sample in the drop is undersaturated; (2) evaporation of the solvents concentrates the protein sample, and gradually the protein sample becomes supersaturated; (3) supersaturation of protein sample, which either becomes precipitate or enters into a nucleation zone; (4) protein in the nucleation zone starts to grow crystals with the nucleus as the center. The change in protein sample concentration is critical for crystal growth and is generally set in the range of 5 mg/ml to 25 mg/ml.

Highly homogenous EDS1-PAD4 heterodimer was first screened in a buffer containing 100 mM NaCl, 10 mM Tris pH8.0 at a concentration of 10 mg/ml. However, precipitates emerged in more than 70% of the hanging drops. This indicated that the concentration of protein sample was too high. Thus, I reduced the EDS1-PAD4 protein concentration to 8 mg/ml and then to 6 mg/ml, which eventually gave a good ratio of clear drops to precipitate drops.



I also included temperature as one of the variables because it strongly influences the solubility of protein. Thus, the screening was performed both at 18°C and at 4°C.

To prevent the proteins aggregating and denaturing, 2 mM dithiothreitol (DTT) was added to the purification buffer as a reducing agent.

However, despite a variety of different conditions and extensive optimization, EDS1-PAD4 protein samples did not develop crystals under the conditions tested. The structure of EDS1-PAD4 will be discussed in the discussion section.

#### **4.4 Pull-down assay analyzing the interaction of helper-NLRs and EDS1 family heterodimers *in vitro***

Recent studies have proposed that, both in *Arabidopsis* and in *N. benthamiana*, the EDS1-SAG101 heterodimer co-functions with NRG1s, and EDS1-PAD4 heterodimer with ADR1s (Gantner et al., 2019; Lapin et al., 2019). This exclusivity defines two distinct immune pathways downstream of TNL activation. To investigate whether E-S heterodimers interact with NRG1A and E-P heterodimers interact with ADR1\_L1 *in vitro*, these two helper-NLRs were fused with N-terminal GST tags to differentiate them from the tags that are attached to EDS1 family members.

In this experiment, NRG1A was co-expressed with EDS1 and SAG101 in insect cells. NRG1A was used as bait. After cell lysis and centrifugation, the supernatant was allowed to flow through Glutathione Sepharose 4B GST affinity resin (GS4B) to check whether EDS1 and SAG101 could be pulled down by NRG1A-N-GST. Unfortunately, on the SDS-PAGE-gel, I did not detect EDS1 and SAG101 captured along with NRG1A (**Fig. 4.6A**). Instead, in the flow-through, large amounts of EDS1 and SAG101 were visible, which were captured later on using Strep affinity resin (**Fig. 4.6A**). This indicates that expression of the EDS1-SAG101 heterodimer was not the reason why NRG1A could not capture EDS1 and SAG101. As controls, EDS1-SAG101 and NRG1A were also expressed alone in insect cells, and after purification samples were applied as input to SDS-PAGE-gels (**Fig. 4.6A**). The interaction assay for ADR1\_L1 and EDS1-PAD4 heterodimers was performed in the same way. Nevertheless, binding of E-S to NRG1A and binding of E-P to ADR1\_L1 were not detected on GST affinity resin (**Fig. 4.6B**). This indicated that neither of the two helper-NLRs directly interact with EDS1 family members *in vitro*.

Using immunoprecipitation and mass spectrometry, Sun et al. found that upon effector recognition, the EDS1-SAG101 heterodimer can be pulled down by NRG1A, and the EDS1-PAD4 heterodimer can be pulled down by ADR1\_L1 (Sun et al., 2021). The association of EDS1 family members and helper-NLRs is totally dependent on the activation of TNL receptors but not cell surface receptors (Sun et al., 2021). As the NADase enzymatic activity of TNLs is important for cell death and resistance dependent on EDS1 family members and helper-NLRs (Horsefield et al., 2019; Wan et al., 2019; Duxbury et al., 2020), we realized that the structure of EDS1-SAG101 heterodimer solved by Wagner et al. might be the inactive form. This implies that the EDS1-SAG101 heterodimer and EDS1-PAD4 heterodimer that were purified from insect cells are likely to be inactive forms as well. Thus, we assumed that some critical factors transmitted from upstream TNL activation can trigger the activation of EDS1 heterodimers by invoking conformational changes. The active EDS1 family heterodimers can thus activate helper-NLRs by direct interaction.

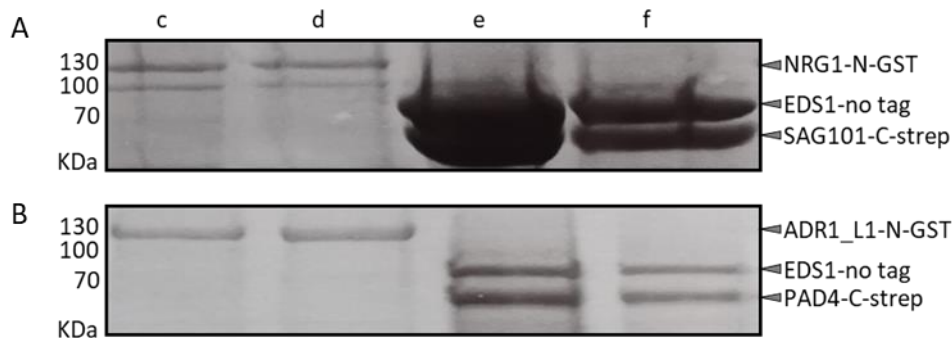


**Figure 4.6 Helper-NLRs do not interact with EDS1 heterodimers *in vitro*.** (A) Pull down assay of NRG1A and EDS1-SAG101 heterodimer. (B) Pull down assay of ADR1\_L1 and EDS1-PAD4 heterodimer. c well refers NRG1A or ADR1\_L1 expressed alone and then eluted from GS4B resin. d well refers NRG1A and ADR1\_L1 were co-expressed with EDS1-SAG101 or EDS1-PAD4, respectively, and then eluted from GS4B resin. e well refers the flow-throughs of GS4B resin from co-expression of helper-NLRs alone were applied to Strep-Tactin XT High Capacity Strep affinity resin (STHC). c well refers the flow-throughs of GS4B resin from co-expression of helper-NLRs and EDS1 family heterodimers were applied to STHC resin, respectively. GS4B-bound and STHC-bound proteins were eluted, separated by SDS-PAGE and detected by Coomassie brilliant blue staining.

## 4.5 Can EDS1-chi2 escape the control of upstream signals?

### 4.5.1 Auto-immune PAD4-SAG101 chimera

To investigate the activation mechanism of helper-NLRs further, I introduced a chimera combining the sequences of PAD4 and SAG101 constructed by Lapin et al. (Lapin et al., 2019). Chi2 is

engineered to contain N-terminal PAD4 amino acids (1–198) and C-terminal SAG101 amino acids (289–537). The alignment of the EDS1-SAG101 heterodimer to the chi2 model (using I-TASSER) showed that the C-terminus of chi2 with the amino acid sequence from SAG101 is conformationally shifted (**Fig. 4.7A**). In Arabidopsis, data show that stable over-expression of chi2 in the background of *pad4 sag101* mutation causes an auto-immune phenotype (unpublished Data from Haitao Cui et. al.). This phenotype strongly resembles those of some auto-immune NLRs (Wu et al., 2019). Intriguingly, transient expression of chi2 in *N. benthamiana* in the background of *eds1 pad4 sag101a sag101b (epss)* with AtEDS1 and AtNRG1A triggers cell death only under the condition that the effector XopQ is recognized by the Roq1 receptor (Lapin et al., 2019). This indicates that, in Arabidopsis, chi2 activates an immune response independent of upstream signal transmission. Nevertheless, in *N. benthamiana*, chi2 is functionally exchangeable with SAG101 in the reconstitution system. Given this information, we developed two main questions: (1) does chi2 interact with EDS1 and form a heterodimer *in vitro*? (2) can EDS1-chi2 interact with NRG1A or ADR1\_L1?

#### **4.5.2 Expression and purification of chi2**

To explore its biochemical function, chi2 was cloned into the Bac-to-Bac baculovirus expression system. As with SAG101 and PAD4, significant amounts of chi2 could be purified from insect cells only when chi2 was co-expressed with EDS1. This strongly implies that EDS1 prevents inappropriate folding and insolubility of chi2. To test whether chi2 interacts with EDS1, EDS1-N-Sumo-6×His and chi2-C-Strep were co-expressed in insect cells. During the purification, both EDS1 and chi2 can be pulled down by each other using two-step affinity purification (one step with Ni-NAT resin and a second step with Strep-Tactin Superflow High Capacity resin). This indicated that EDS1 and chi2 bind tightly to each other.

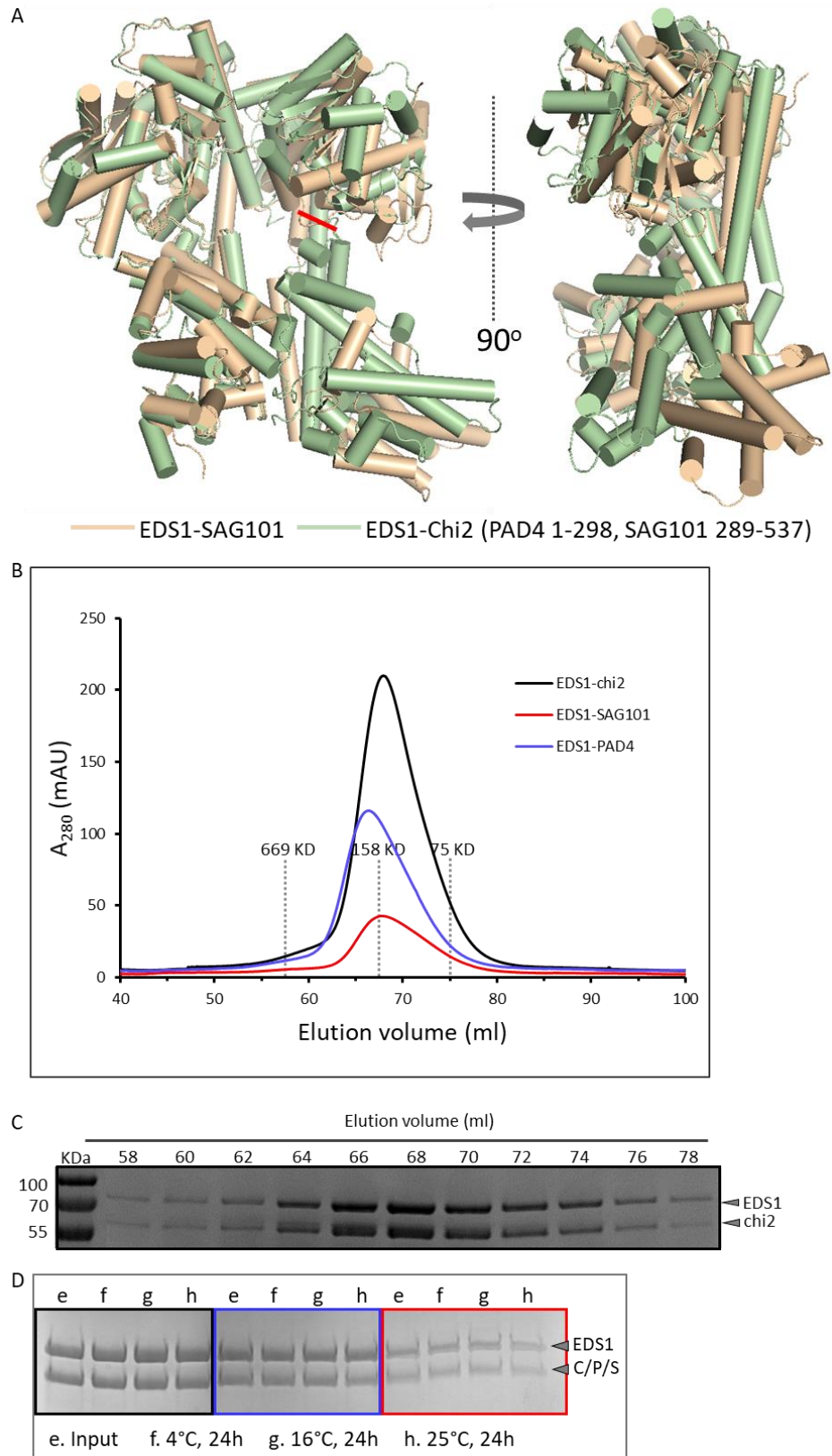


**Figure 4.7 Expression and purification of the EDS1-chi2 heterodimer in insect cells. (A)** Superimposition of EDS1-chi2 model with EDS1-SAG101 heterodimer. The red solid line indicates the

fusion point of PAD4 and SAG101 in chi2. **(B)** Gel filtration of EDS1-SAG101, EDS1-PAD4, and EDS1-chi2 using size exclusion chromatography. Overlap of all three gel filtrations showed the same peaking point. **(C)** Protein samples from different fractions were separated by SDS-PAGE and detected by Coomassie brilliant blue staining. **(D)** Stabilization assay of EDS1-SAG101 heterodimer (red), EDS1-PAD4 heterodimer (blue), and EDS1-chi2 heterodimer (black) at 4°C, 16°C, and 25°C for 24 hours, respectively. Protein samples were separated by SDS-PAGE and detected by Coomassie brilliant blue staining.

The EDS1-chi2 complex was then digested using PreScission Protease to remove the N-Sumo-6×His from chi2 and C-Strep from EDS1. Characterization of EDS1 and chi2 complexes using gel filtration shows that EDS1 and chi2 complexes peak at 66 ml elution volume on the HiLoad 26/600 Superdex 200 pg column (Cytiva) (**Fig. 4.7B**). This indicated that the molecular mass of the EDS1-chi2 complex is ~150 kDa. EDS1-SAG101 and EDS1-PAD4 were taken as heterodimer controls. EDS1 and chi2 complexes peaked at the same elution volume as both EDS1-SAG101 and EDS1-PAD4 heterodimers (**Fig. 4.7B and C**). This strongly suggested that EDS1 and chi2 form a heterodimer *in vitro*.

Wagner et al. tested the stability of the EDS1-SAG101 heterodimer under different temperatures (Wagner et al., 2013). To check whether the EDS1-PAD4 and EDS1-chi2 heterodimers are as stable as the EDS1-SAG101 heterodimer, protein samples were incubated at 4°C, 16°C, and 25°C. After 24 hours, equal amounts of protein were sampled from each treatment for electrophoresis. Consistent with previous data, on the SDS-PAGE-gel, the band intensity of EDS1 and SAG101 at different temperatures did not change compared to the input sample. The band intensity of the EDS1-PAD4 and EDS1-chi2 heterodimers showed the same pattern as the EDS1-SAG101 heterodimer, indicating that the heterodimers did not degrade over time under any of the tested temperatures (**Fig. 4.7D**). This confirmed the strong molecular association of the EDS1-PAD4 heterodimer and EDS1-chi2 heterodimer.

### 4.5.3 Interaction assay of EDS1-chi2 and helper-NLRs

As described in section 4.5.1, replacement of SAG101 with chi2 in the reconstitution system in *N. benthamiana* did not attenuate the cell death response (Lapin et al., 2019). This strongly implied that chi2 has kept the functional domain of SAG101. The auto-immune phenotype observed upon over-expression of chi2 in Arabidopsis implies self-activation of chi2. We formulated the hypothesis that chimeric engineering of PAD4 and SAG101 into chi2 makes a critical conformational change in the E-P domain compared to inactive EDS1-SAG101 heterodimer, and

activation of the EDS1-chi2 heterodimer can influence downstream helper-NLRs by direct interaction.

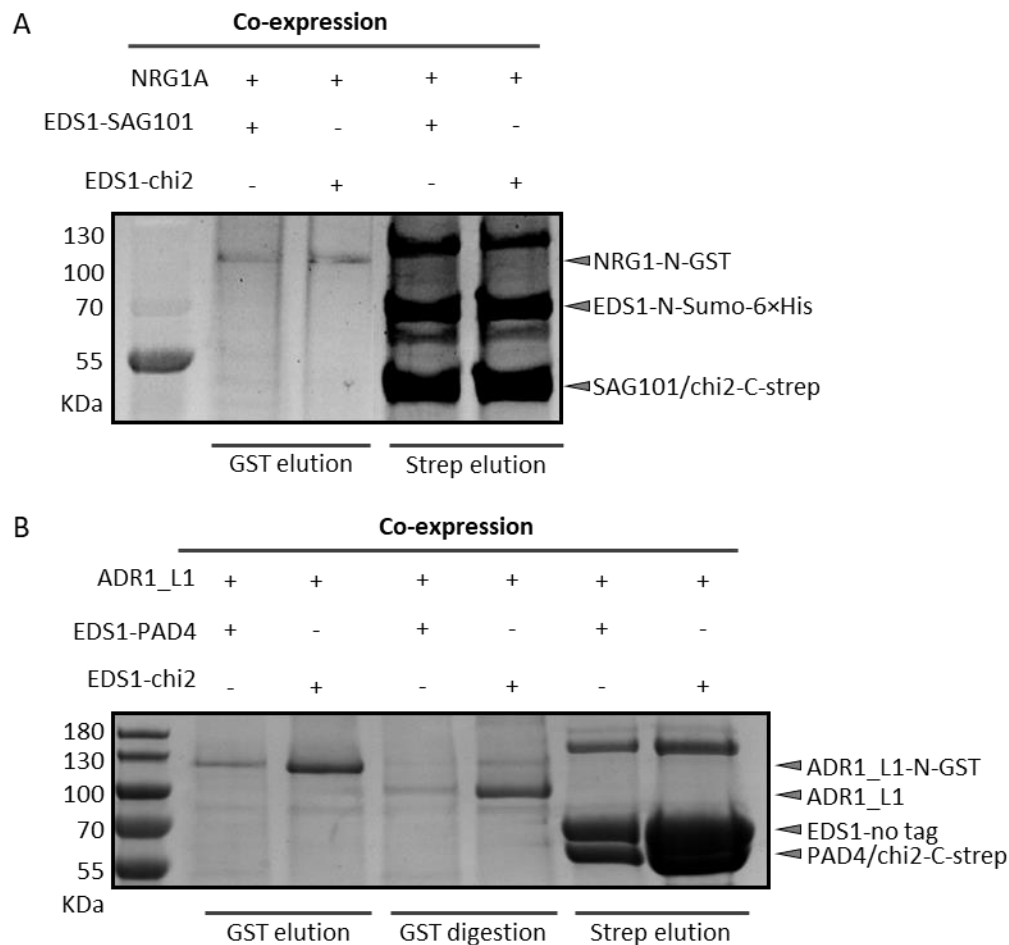


**Figure 4.8 The EDS1-chi2 heterodimer does not interact with helper-NLRs.** (A) EDS1-chi2 does not bind to NRG1A. NRG1A-N-GST was co-expressed with EDS1-N-Sumo-6 $\times$ His and SGA101 or with EDS1 and chi2 in insect cells. NRG1A was then purified using GS4B resin. The flow-throughs of GS4B resin were then applied to STHC resin. GS4B-bound and STHC-bound proteins were eluted, separated by SDS-PAGE and detected by Coomassie brilliant blue staining. (B) EDS1-chi2 does not bind to ADR1\_L1. The experiment was performed as described in (A) except that NRG1A was replaced with ADR1\_L1. In addition, the eluted GS4B-bound proteins were digested using PreScission Protease.

To test this, I co-expressed helper-NLRs and EDS1 heterodimers in insect cells. Co-expression of NRG1A and the EDS1-SAG101 heterodimer, and co-expression of ADR1\_L1 and the EDS1-PAD4 heterodimer were set as controls since previous experiments showed that helper-NLRs and EDS1 heterodimers cannot interact when expressed recombinantly (Fig. 4.6). To perform pull-down assays, helper-NLRs were tagged with N-terminal GST tags, and EDS1 family members were tagged either with polyhistidine, twin-strep, or no tag. The results show that neither NRG1A

nor ADR1\_L1 can pull down the EDS1-chi2 heterodimer. The majority of the EDS1, SAG101, PAD4, and chi2 proteins accumulated in the flow-through from the GST column and were then collected on the Strep-Tactin resin because SAG101, PAD4, and chi2 were fused to the twin-strep tag (**Fig 4.8A and B**). This confirmed that the expression of EDS1 family members was not a problem. ADR1\_L1 was co-purified with some unspecified proteins (additional band in Fig. 4.8B). Thus, to prove that the target bands were ADR1\_L1, I did a protease digestion of the samples eluted from GS4B to check whether the tag could be removed. The results showed that both target bands can be digested into smaller-sized proteins which matched exactly the size of ADR1\_L1 (**Fig. 4.8B**). Altogether, this suggested that the conformational change in the EDS1-chi2 heterodimer did not enable it to stably interact with either NRG1A or ADR1\_L1.

## **4.6 Reconstitution of EDS1 family members and helper-NLR association *in vitro***

Conformational changes might be insufficient for EDS1-chi2 heterodimer self-activation and subsequent triggering of the association with NRG1A or ADR1\_L1. Based on the indispensable role of activated TNLs in triggering the association of helper-NLRs with EDS1 family members (Horsefield et al., 2019; Wan et al., 2019; Duxbury et al., 2020), in a next step I tried to reconstitute the system by co-expressing TIR proteins together with Helper-NLRs and EDS1 family members in insect cells. We hypothesized that activated TIR proteins can induce the interaction of the EDS1-SAG101 heterodimer with NRG1A and the EDS1-PAD4 heterodimer with ADR1\_L1.

### **4.6.1 Co-expression and/or co-purification of TIR proteins with EDS1 heterodimers and helper-NLRs**

To check whether activated TIR proteins could trigger the interaction of EDS1 family members with helper-NLRs, I, together with Wen Song, co-expressed NRG1A-N-GST, EDS1-no tag, SAG101-C-Strep, and RPP1-ATR1/RPP1<sup>TIR</sup> in insect cells.

SGT1 (Suppressor of G2 allele of SKP1) and RAR1 (Required for Mla Resistance 1) are HSP90 co-chaperones. It has been reported that both SGT1 and RAR1 are important for NLR stabilization (Kadota et al., 2010). Thus, SGT1 and RAR1 were always co-expressed with RPP1 as described in (Ma et al., 2020). Consistent with previous results, co-expression of NRG1A and the EDS1-

SAG101 heterodimer could not induce the interaction (**Fig. 4.9A**). However, when NRG1A, EDS1, SAG101, RPP1, and ATP1 were co-expressed, both EDS1 (no tag) and SAG101 (C-terminal strep tag) were pulled down together with NRG1A on the GST column (**Fig. 4.9A**). Interestingly, co-expression of RPP1<sup>TIR</sup> with NRG1A, EDS1, and SAG101 did not trigger the interaction of the EDS1-SAG101 heterodimer with NRG1A, although the NAD<sup>+</sup> catalytic activity of RPP1<sup>TIR</sup> is comparable with that of the RPP1 resistosome.

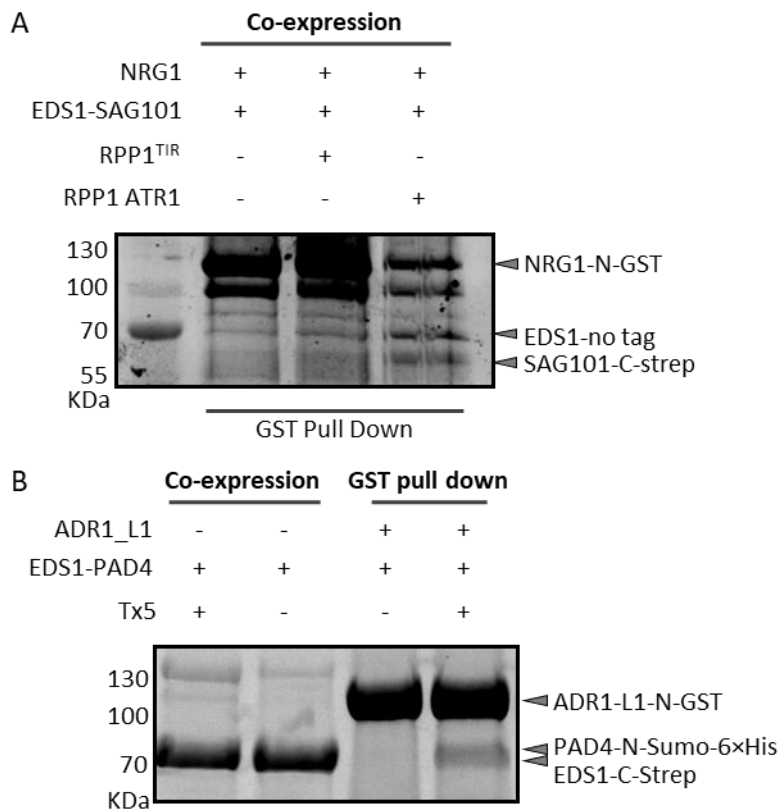


**Figure 4.9 TIR NADase products induce interaction of EDS1 heterodimers with helper-NLRs in insect cells.** (A) RPP1-ATR1 induces EDS1-SAG101 interaction with NRG1A in insect cells. NRG1A-N-GST was co-expressed with EDS1-no tag, SAG101-C-Strep, or with EDS1-no tag, SAG101-C-Strep, RPP1-C-Strep and ATR1-10xHis, or with EDS1-no tag, SAG101-C-Strep, RPP1<sup>TIR</sup>-N-Sumo-6xHis in insect cells. NRG1A was then purified using GS4B resin. GS4B-bound proteins were eluted, separated by SDS-PAGE, and detected by Coomassie brilliant blue staining. (B) Tx5-N-Sumo-6xHis induces the interaction of EDS1-PAD4 with ADR1\_L1. EDS1 and PAD4 were co-expressed either alone or with Tx5. EDS1-PAD4 was then purified using STHC resin. Purified EDS1-PAD4 was incubated with ADR1\_L1-N-GST on GS4B resin for 16 hours at 4°C. GS4B-bound proteins were eluted, separated by SDS-PAGE, and detected by Coomassie brilliant blue staining. Experiments were performed together with Wen Song.

Tx5 has a TIR domain in the N-terminus that is fused with an unidentified domain in the C-terminus. High concentrations of Tx5 (50~100  $\mu$ M) can efficiently catalyze NAD<sup>+</sup> and produce NAM,



cADPR, and ADPR as main products and other unidentified small molecules (unpublished data from Hanna Bernardy and Wen Song). The product profile of Tx5 is very similar to that of the RPP1 resistosome and thus was considered as one possible source of the small molecules. To simplify the expression system, Wen and I co-expressed Tx5 instead of RPP1 resistosome with EDS1 and PAD4 and then mixed the pre-triggered EDS1-PAD4 heterodimer with ADR1\_L1. In this experiment, PAD4 was fused with an N-Sumo-6×His tag, EDS1 with a C-terminal Strep tag, and ADR1\_L1 with an N-terminal GST tag. EDS1-PAD4 that was co-expressed with Tx5 but not the E-P heterodimer expressed alone was pulled down on the GS4B resin by ADR1\_L1 (**Fig. 4.9B**). This indicates that certain compounds in the co-expression culture pre-activated the E-P heterodimer and triggered the interaction with ADR1\_L1. Together with the association of NRG1A with the E-S heterodimer under the tested conditions, we conclude that NADase products of TNLs or TIR proteins could trigger the direct interaction of NRG1A with the EDS1-SAG101 heterodimer and ADR1\_L1 with the EDS1-PAD4 heterodimer.

#### **4.6.2 Role of TIR products in inducing the interaction of NRG1A and the EDS1-SAG101 heterodimer**

Using  $\text{NAD}^+$  as a substrate, the RPP1 resistosome produces various small molecules (Ma et al., 2020). Previous research has shown that these small molecules are critical for the activation of the downstream EDS1-SAG101-NRG1A module, which is, in turn, essential for TNL immune outputs (Horsefield et al., 2019; Wan et al., 2019; Duxbury et al., 2020; Ma et al., 2020).

The inactive E-S heterodimer forms a cavity in the EP structural domain, and the surface of this cavity is enriched with positively charged amino acids, thus creating a positively charged electroactive surface (Wagner et al., 2013) (**Fig 4.10A**). Given that the products of TNLs mostly carry phosphate chains (negatively charged), we propose that EDS1 family heterodimers can capture small molecules produced by activated TNLs, which leads to a conformational change and thus an activated state that then induces direct binding of helper-NLRs and EDS1 family members.

To test whether small molecules can trigger the interaction of NRG1A with the E-S heterodimer, and ADR1\_L1 with the E-P heterodimer, pull-down assays were performed using NRG1A and ADR1\_L1 as baits.

The preparation of RPP1 resistosome NADase products comprises the following steps: (1) Purification and concentration of RPP1-ATR1 resistosome; (2) Incubation of proteins with  $Mg^{2+}$  (final concentration 10 mM), ATP (final concentration 0.1 mM), and  $NAD^+$  (final concentration 0.1 Mm) at 25 °C, ~16 hours; (3) Boiling of samples at 95 °C, 10 mins to denature proteins; (4) Loading 10  $\mu$ l samples on HPLC to check the consumption of  $NAD^+$ , and storing products from step 3 only if the  $NAD^+$  is fully catalyzed.

NRG1A-N-GST, E-S heterodimer (EDS1-no tag, SAG101-C-Strep), ADR1\_L1-N-GST, and EDS1-PAD4 heterodimer (EDS1-no tag, PAD4-C-Strep) were purified. Then, Wen and I incubated NRG1A-N-GST, E-S heterodimer, and RPP1 NADase products altogether on GS4F resin for 16 hours at 4°C. As a control, we incubated NRG1A-N-GST and E-S heterodimer together with buffer instead of RPP1 NADase products on GS4F resin. In the meantime, we also performed the assay in the same way to test whether RPP1 NADase products could promote the interaction of ADR1\_L1 with the E-P heterodimer. As shown in **Figure 4.10B**, both EDS1 and SAG101 bound GS4F resin together with NRG1A when the proteins were incubated with RPP1 NADase, indicating a specific and direct interaction of NRG1A and EDS1-SAG101. However, in the control sample, in which RPP1 NADase products was replaced with buffer, EDS1 and SAG101 band intensities were much weaker compared to samples with RPP1 NADase products (**Fig. 4.10B**). The same pattern was shown in the pull-down assay using ADR1\_L1 as bait, in which the EDS1-PAD4 heterodimer was pulled down by mixing with RPP1 NADase products but not buffer (**Fig. 4.10C**). Altogether, we concluded that RPP1 resistosome NADase products could trigger the direct interaction of NRG1A with the EDS1-SAG101 heterodimer and ADR1\_L1 with the EDS1-PAD4 heterodimer.

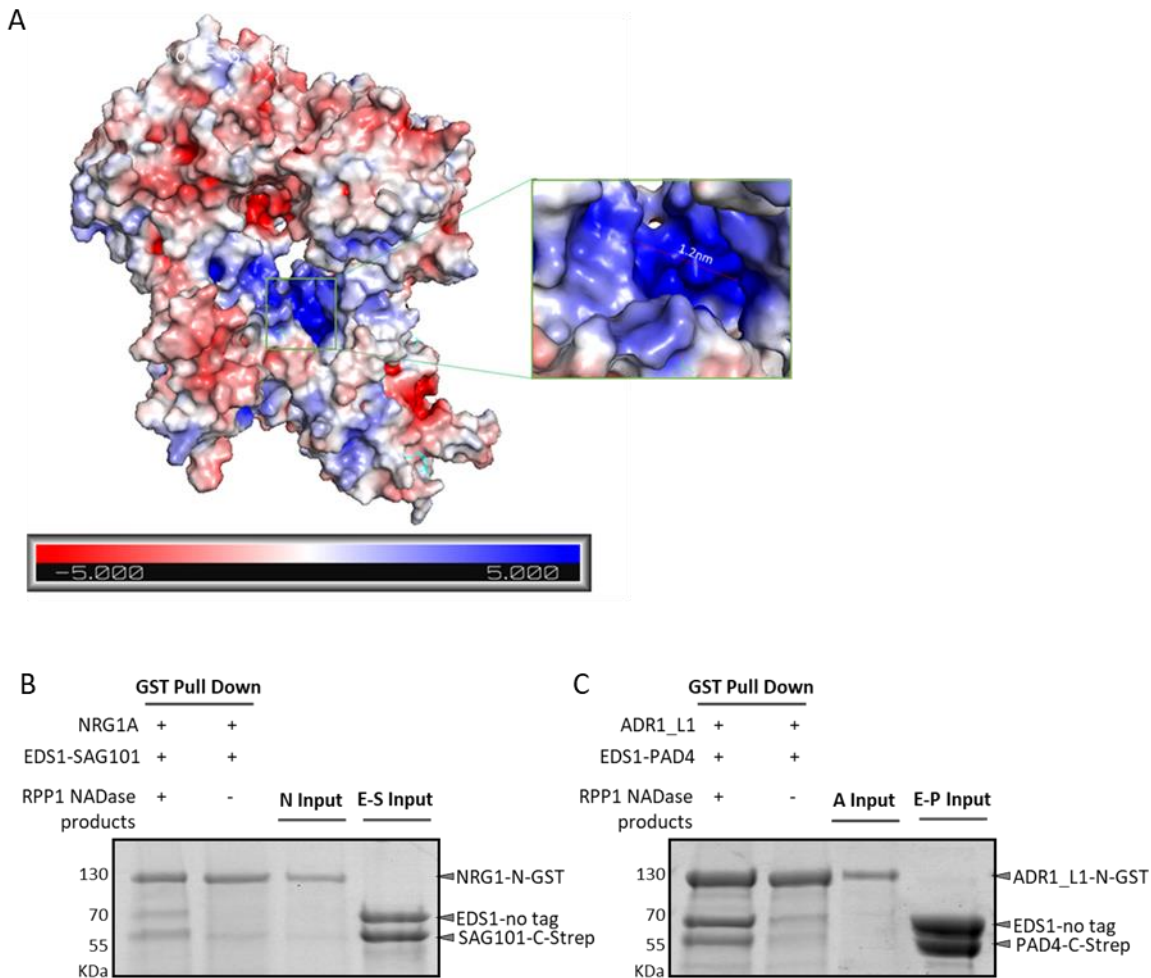


**Figure 4.10 RPP1 resistosome NADase products trigger the interaction of helper-NLRs with EDS1 family members.** (A) Surface electroactivity analysis of EDS1-SAG101 heterodimer structure. Green open frame shows the positively-charged cavity. (B) NADase products induce the interaction of NRG1 with the EDS1-SAG101 heterodimer. After incubation on the GS4F resin, proteins were eluted, separated by SDS-PAGE and detected by Coomassie brilliant blue staining. (C) The experiment was performed the same way as described in (B). Experiments were performed together with Wen Song.

## 4.7 TIR NADase products mediate SAG101 cleavage *in vitro*

High concentrations of RPP1<sup>TIR</sup> (50~100  $\mu$ M) can efficiently catalyze NAD<sup>+</sup>, producing NAM, cADPR, and ADPR as main products and other unidentified small molecules. The product profile of RPP1<sup>TIR</sup> is very similar to that of the RPP1 resistosome and thus was considered as a replacement for the RPP1 resistosome in this study.

The interaction assay yielded a surprising result when I was performing the experiments together with Wen: mixing E-S heterodimer with RPP1<sup>TIR</sup> NADase products caused cleavage of SAG101.

This cleavage happened immediately once the E-S heterodimer was mixed with the products. After incubation for 6 hours at 4°C, SAG101 is almost 100% percent cleaved (**Fig. 4.11A**). As shown in **Figure 4.11A**, instead of the full-length band of SAG101 on the SDS-PAGE-gel, a new band appears at about 55 kDa. This suggests that the small molecules might trigger the cleavage of SAG101 *in vitro*.

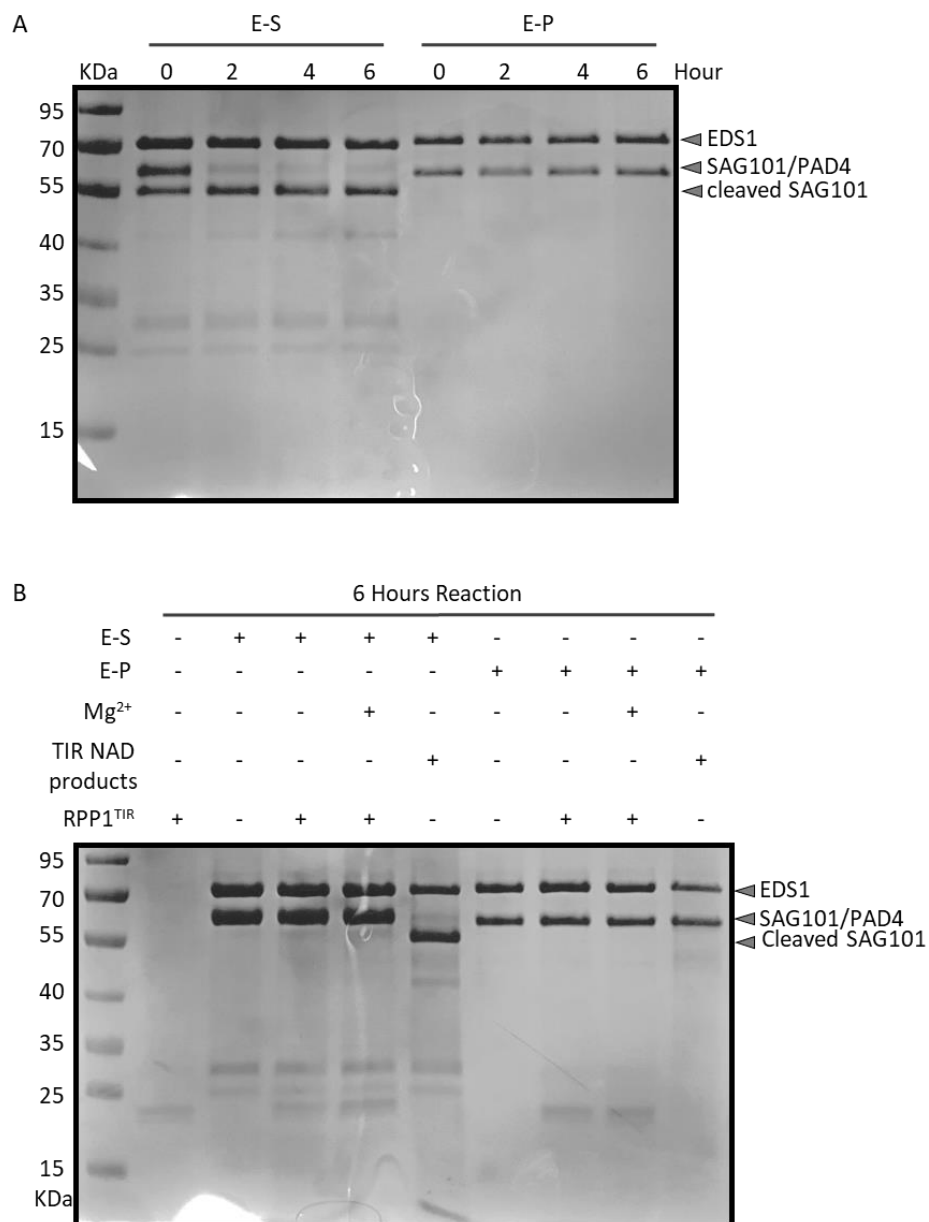


**Figure 4.11 TIR NAD products trigger the cleavage of SAG101.** (A) Rapid cleavage of SAG101. The cleavage time-course of the EDS1-SAG101 heterodimer and EDS1-PAD4 heterodimer. EDS1-SAG101 and EDS1-PAD4 were incubated together with RPP1<sup>TIR</sup> products for 0 hours, 2 hours, 4 hours, and 6 hours, respectively. (B) EDS1-SAG101 and EDS1-PAD4 were incubated with RPP1<sup>TIR</sup>, Mg<sup>2+</sup>, and RPP1<sup>TIR</sup> NADase products, respectively. RPP1<sup>TIR</sup> protein and all the samples from different treatments were

separated by SDS-PAGE and detected by Coomassie brilliant blue staining. Experiments were performed together with Wen Song.

To investigate whether this is exclusively dependent on the TIR protein NADase products or other components in the system, like  $Mg^{+}$  and TIR protein, we tested the cleavage of SAG101 upon incubation with  $Mg^{+}$  and TIR protein, respectively. The results showed that only the small molecules could trigger the cleavage of SAG101 (**Fig. 4.11B**).

The E-S and E-P heterodimers exhibit high similarity both at the sequence and structural levels. Although they have distinct biological functions, both are essential components downstream of TNLs and very likely function as receptors for the TIR NADase small molecule products. To test whether the E-P heterodimer is also sensitive to these products, E-S heterodimer and E-P heterodimer were mixed with the products and incubated under the same conditions. Interestingly, irrespective of the length of the reaction, PAD4 was cleaved in the same way as SAG101 (**Fig. 4.11**). This indicated that another possible distinct biochemical feature of EDS1-SAG101 heterodimer from EDS1-PAD4 heterodimer.

To test whether the 55 kDa SAG101 cleavage product still associates with EDS1, I compared the gel filtration profiles of samples with products and without products. The same amounts of EDS1-SAG101 heterodimer were prepared, one mixed with buffer and the other portion mixed with the products. After incubation for 6 hours, both samples were applied to the gel filtration, respectively. The overlap of the peaks in both graphics indicates that EDS1 still interacts with the cleaved scaffold of SAG101 (**Fig. 4.12**).

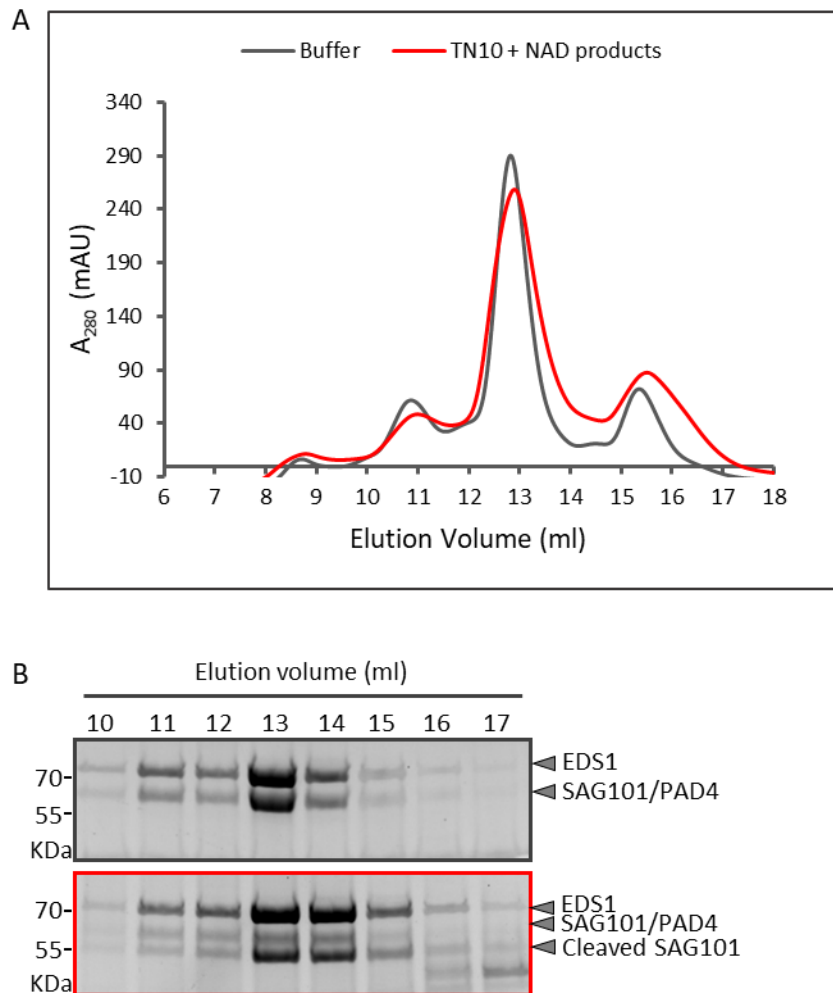


**Figure 4.12 Truncated SAG101 still interacts with EDS1 and forms a heterodimer.** (A) EDS1-SAG101 was incubated either with RPP1<sup>TIR</sup> products or with buffer. The mixtures were analyzed using gel filtration. The black solid line refers to EDS1-SAG101 mixed with buffer. The red solid line refers to EDS1-SAG101 mixed with RPP1<sup>TIR</sup> NADase products. (B) Proteins from different fractions were separated by SDS-PAGE and detected by Coomassie brilliant blue staining. The black open frame refers to EDS1-SAG101 mixed with buffer. The red open frame refers to EDS1-SAG101 mixed with RPP1<sup>TIR</sup> NADase products. Experiments were performed together with Wen Song.

## 5 Discussion

One of the main goals of the experiments described in this thesis was to uncover the mechanism of how EDS1 family members link sensor TNLs and helper-NLRs. Overall, the results showed trends that could be helpful for learning about the mechanism of TNL-mediated association and activation of EDS1 family members and helper-NLRs. The interactions of the EDS1-SAG101 heterodimer with NRG1A and the EDS1-PAD4 heterodimer with ADR1\_L1 were tested under different conditions, including using engineered PAD4-SAG101 chimera. These results both negate and support some of the hypotheses that were formulated at the outset of the study. It was predicted that recombinant expression of helper-NLRs could trigger both NRG1A and ADR1\_L1 self-activation, or that co-expression of EDS1 family members with helper-NLRs could favor these interactions, but these hypotheses were not supported by my data. The data rather suggested that the activated TNLs or TIR proteins are essential for the interaction of the EDS1-SAG101 complex with NRG1A and the EDS1-PAD4 complex with ADR1\_L1.

### 5.1 Protein interaction studies *in vitro*

For many years plant scientists have studied the mechanism of how EDS1 family members bridge upstream effector perception and downstream helper-NLRs. Because of the complexity of this pathway and the gaps in our knowledge, progress in understanding this mechanism has been extremely slow. In 2018, Qi et al. showed that upon ROQ1 activation, EDS1 associates with NRG1 to protect tobacco against *Xanthomonas euvesicatoria* and *Xanthomonas gardneri* (Qi et al., 2018). However, the interaction of EDS1 with NRG1 was not demonstrated *in vitro*. What's more, the interaction of NRG1s with the EDS1-SAG101 complex was not reported until recently in *Arabidopsis* (Sun et al., 2021; Wu et al., 2021).

At the outset of these experiments (2018–2019), it was not known whether if in *Arabidopsis* upon activation, the EDS1-SAG101 heterodimer would self-associate into a higher-order complex. We also had very limited knowledge about direct interaction of the EDS1 heterodimers with helper-NLRs or indirect interactions through transmission of the signal to helper-NLRs.

The application of biochemical tools and techniques in this field has certainly accelerated the pace of research. I successfully expressed and purified AtNRG1A, AtADR1\_L1, and AtPAD4 for the

first time, which facilitated studies of the interactions between helper-NLRs and EDS1 family members *in vitro* (**Fig. 4.3, Fig. 4.4, and Fig. 4.5**). Before I successfully co-expressed the EDS1 family members with helper-NLRs, I mixed the purified proteins together and attempted to observe the particle shape using transmission electron microscopy with negative staining. However, due to the limitations of the method, the poor homogeneity of the protein samples, and the subjectivity of the observer, I was unable to make a solid conclusion.

Subsequently, I co-expressed NRG1A with EDS1-SAG101 heterodimers and ADR1\_L1 with EDS1-PAD4 heterodimers to investigate their biochemical interaction. Pull-down tests showed no interaction between NLRs and EDS1 family members in the absence of other components (**Fig. 4.6**). Consistent with this observation, in 2021, Sun et al. demonstrated that the association of NRG1A with EDS1-SAG101 and ADR1\_L1 with EDS1-PAD4 in Arabidopsis is entirely dependent on upstream activation signals. Without effector perception by TNLs, EDS1 family members do not interact with NLRs (Sun et al., 2021). This led us to conclude that in unchallenged plants, the EDS1 family heterodimers are in an inactive, resting state.

## **5.2 Studying the interaction of EDS1 heterodimers and helper-NLRs using a reconstitution system**

The association of EDS1 family members and helper-NLRs in plants requires activation of TNLs. Sun et al. used recombinant transient expression in *N. benthamiana* and detected co-precipitation of AtEDS1 and AtSAG101 with AtNRG1A after effector XopQ recognition. This suggests a possible association of EDS1-SAG101 and NRG1A (Sun et al., 2021). Similarly, ADR1\_L1 could pull down significant amount of EDS1 and PAD4 only in RBA1-pretreated leaves. Without RBA1 pretreatment or with NADase mutant RBA1<sup>E86A</sup> pretreatment, the amount of EDS1 and PAD4 pulled down by ADR1\_L1 is very low. This suggests that RAB1 strongly promotes the interaction of ADR1\_L1 and EDS1-PAD4 complexes (Wu et al., 2021). This prompted us to establish an efficient recombination system in insect cells to explore whether such interactions could be triggered *in vitro*. We hypothesized that the interaction could be facilitated by co-expression, and therefore, together with my colleague Wen Song, we co-expressed all the necessary protein components in insect cells to bring them into physical proximity. The results show that co-expression of the EDS1-SAG101-NRG1A module with RPP1 and effector ATR1 triggers NRG1A



to pull down EDS1 and SAG101 (**Fig. 4.9**). In the EDS1-PAD4-ADR1\_L1 module, ADR1\_L1 can pull down EDS1 and PAD4 when EDS1 and PAD4 are co-expressed with the TIR protein Tx5 (**Fig. 4.9**). In addition, incubation of EDS1 family heterodimers and helper-NLRs with RPP1 NADase products confirmed the interaction of ADR1\_L1 with EDS1-PAD4 and NRG1A with EDS1-SAG101 (**Fig. 4.10**). These results strongly support the hypothesis that the NADase products of TNLs or TIR proteins are critical for activating EDS1 family members and triggering their interactions with helper-NLRs. The success of *in vitro* recombination combined with the *in vivo* data from Sun et al. and Wu et al. represent exciting advances in understanding the mechanisms of activation of EDS1 family members and helper-NLRs.

There are also some limitations to our study: (1) when using RPP1<sup>TIR</sup> as the trigger, EDS1 and SAG101 do not significantly interact with NRG1A compared to the use of full-length RPP1 with effector as trigger. One explanation is that RPP1<sup>TIR</sup> might not be as active in producing sufficient numbers of small molecules as the RPP1 resistosome in insect cells. (2) The reliability of these data is impacted by the sticky character of EDS1 protein. EDS1 may adhere non-specifically to the resin, which causes confusion and false-positive result. This problem has been improved by preparing freshly purified EDS1 heterodimers. (3) We did not investigate whether mutation of the conserved glutamic acid of RPP1 abolishes the interaction. (4) We could not solve the structure of activated EDS1 family heterodimers.

Consistent with our data, Huang et al. and Jia et al. confirmed the interaction of EDS1 family members and helper-NLRs using multiple techniques. For instance, co-expression of RPP1, ATR1, EDS1, PAD4, and ADR1\_L1 in insect cells clearly indicated the interaction of ADR1\_L1 with EDS1 and PAD4. To support their theory, Huang et al. also co-expressed RPS4<sup>TIR</sup> with EDS1 family members and helper-NLRs. The results demonstrated that both activated TNLs and TIR proteins trigger the interaction of NRG1A with EDS1 and SAG101 as well as ADR1\_L1 with EDS1 and PAD4. As expected, mutation of the catalytic residues responsible for NADase activity in RPP1 and RPS4<sup>TIR</sup> abolished the interaction. Furthermore, Huang et al. co-expressed EDS1, PAD4, RPP1, and ATR1, and then purified the compounds from the EDS1-PAD4 complex and demonstrated that the specific compounds could induce the interaction of ADR1\_L1 and the EDS1-PAD4 heterodimer (Huang et al., 2022; Jia et al., 2022). These innovative approaches identified a critical link between activated TNLs/TIR structural domains and EDS1 family members.

Combined with our data, we suggest that EDS1 family members capture compounds derived from activated TNLs/TIR domains, which consequently triggers their interaction with helper-NLRs.

### **5.3 Structural comparison of inactive and active EDS1 family heterodimers**

Despite efforts aimed at determining the structure of the EDS1 and PAD4 complex, we could not solve the structures of either inactive or active EDS1-PAD4 complexes, partially because of the lack of appropriate facilities.

Huang et al. solved the structure of the EDS1-PAD4 heterodimer using cryo-EM and also the crystal structure of the EDS1-PAD4 complex; both were purified from the insect cell culture co-expressing with/without RPP1 and ATR1. Their results showed that the active EDS1 and PAD4 complex remains as a heterodimer.

Compared to the inactive form, the active EDS1-PAD4 heterodimer shows a distinct conformational change in the EP structural domain, which creates a cavity that perfectly accommodates a small molecule. This molecule engages in strong, multi-site interactions with EDS1 and PAD4 by hydrogen bonding and polar interactions with the cavity surface residues (Huang et al., 2022). It appears that the interaction force pulls the EP domain of PAD4 towards the center of the pocket and thus shrinks the pocket size. Interestingly, apart from the EP domain of PAD4, the other parts of the heterodimer are not significantly affected on the structural level by ligand binding (**Fig. 5.1**). The conformational change in the EP domain of the active EDS1-PAD4 heterodimer supports the idea that the EP domain might provide the platform for the interaction with ADR1s.

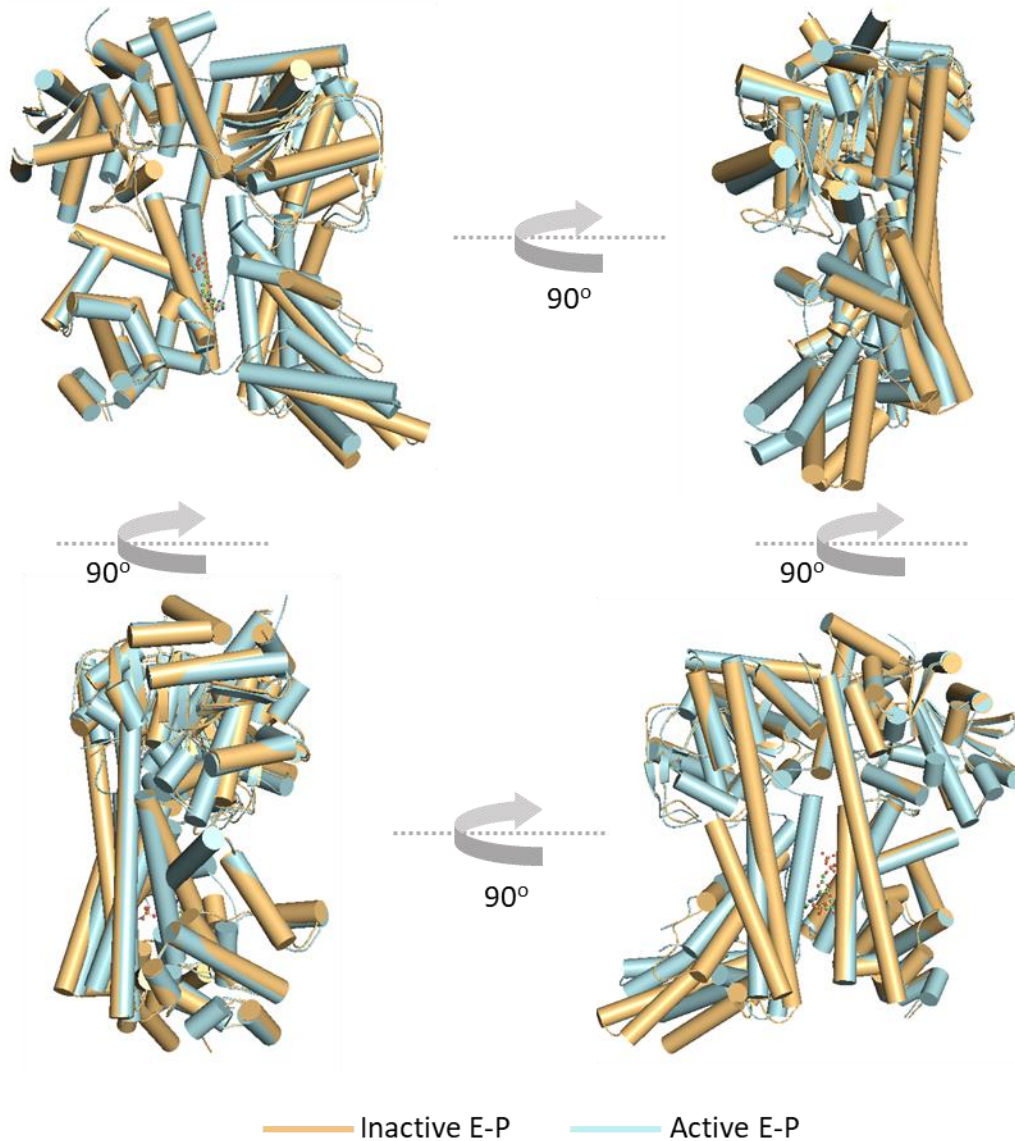


**Figure 5.1 Structural superimposition of inactive EDS1-PAD4 heterodimer and active EDS1-PAD4 heterodimer.**

PAD4<sup>R314</sup> and PAD4<sup>K380</sup> are two conserved amino acids located on the surface of the EP domain cavity. Data from both Huang et al. and Dongus et al. found that mutation of either PAD4<sup>R314</sup> or PAD4<sup>K380</sup> to alanine completely abrogated resistance. Further inspection showed that the PAD4<sup>R314A</sup> does not interfere with the formation of the EDS1 family heterodimers *in vivo* and *in vitro*. However, association of the EDS1 and PAD4 complex with ADR1\_L1 is compromised in these two mutants (Dongus et al., 2022; Huang et al., 2022). Thus, these authors concluded that PAD4<sup>R314</sup> and PAD4<sup>K380</sup> do not directly line the interaction surface of the EDS1-PAD4 heterodimer but are critical for signaling in the TNL-mediated resistance pathway. Analysis of the active EDS1-

PAD4 heterodimer structure demonstrated that the side chains of these two amino acids form hydrogen bonds with the small molecule, thus playing an important role in maintaining ligand binding.

Using the same approach, Jia et al. deciphered the crystal structure of the EDS1-SAG101 heterodimer with ligand binding. Superimposition of the inactive EDS1-SAG101 heterodimer (solved by Wagner et al. 2013) and active EDS1-SAG101 heterodimer shows that ligand binding of the EDS1-SAG101 complex caused the rearrangement the EP domain of SAG101. However, the structure of EDS1 and the lipase-like domain of SAG101 are highly similar to that of the inactive EDS1-SAG101 heterodimer (**Fig. 5.2**).

SAG101<sup>M304</sup> and SAG101<sup>R373</sup> are conserved amino acids that correspond to PAD4<sup>R314</sup> and PAD4<sup>K380</sup>, respectively. Giving the importance of PAD4<sup>R314</sup> and PAD4<sup>K380</sup> for resistance, Dongus et al. analyzed the function of SAG101<sup>M304</sup> and SAG101<sup>R373</sup>, which are located on the cavity surface of SAG101. They found that both SAG101<sup>M304</sup> and SAG101<sup>R373</sup> are essential for the ETI response in Arabidopsis. These data are highly consistent with the data reported by Huang et al. and Jia et al. and confirm the strong interaction of ligands with EDS1 family heterodimers.

Comparison of the two activated states of the heterodimers shows that the interactions of the two ligands with EDS1 do not exclusively involve the same amino acids on the surface of the two EP cavities. This implies that the ligand binding activation mechanism is specific to the two different EDS1 heterodimers. This again demonstrates the specificity of the cavity surface residues in the two EDS1 family heterodimers and the unique functions of these two heterodimers (Dongus et al., 2022; Huang et al., 2022; Jia et al., 2022).

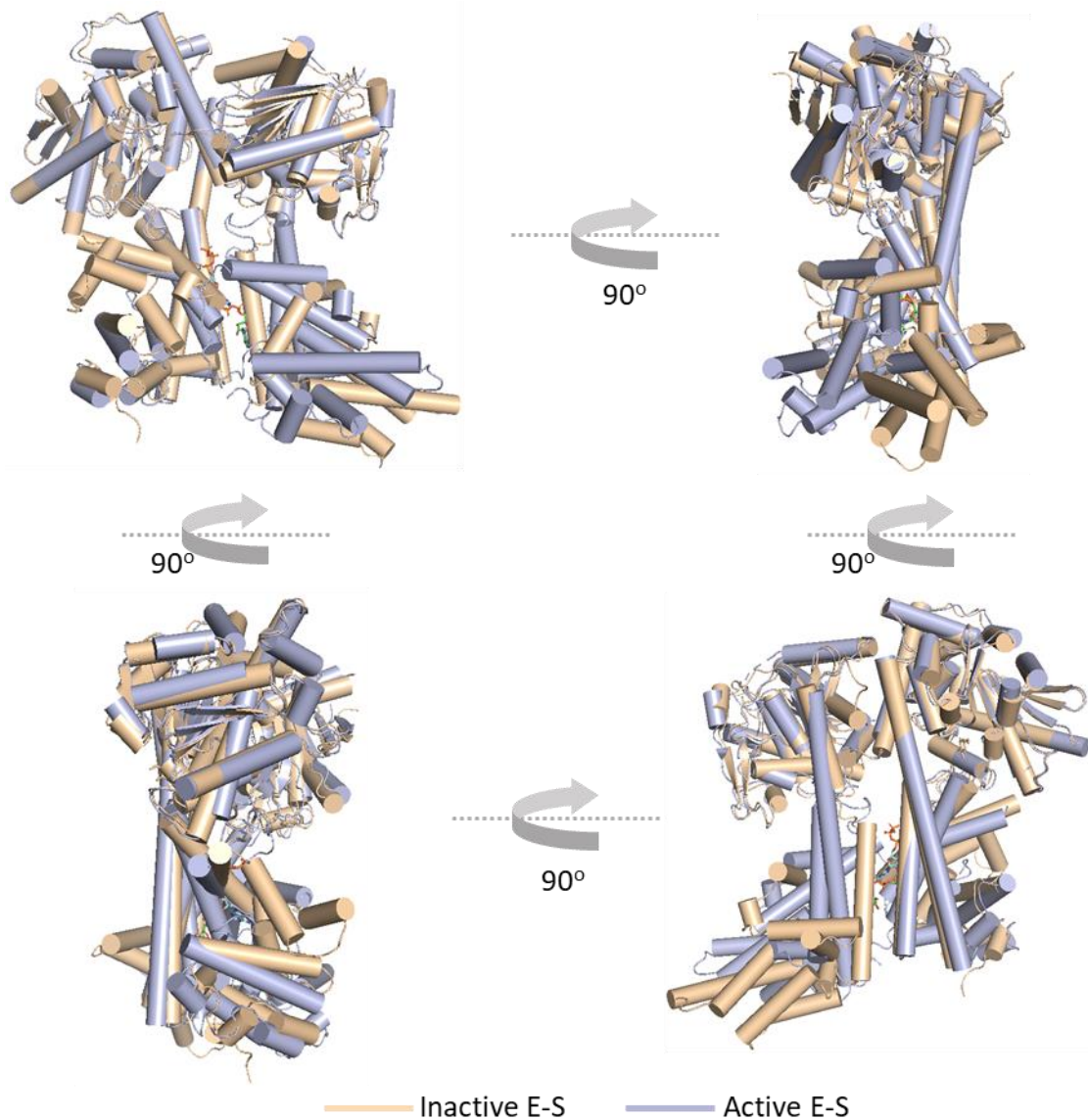


**Figure 5.2 Structural superimposition of inactive EDS1-SAG101 heterodimer and active EDS1-SAG101 heterodimer.**

## **5.4 Why does auto-immune EDS1-chi2 not robustly interact with NRG1A?**

The profound conformational changes in the EP domain upon ligand binding and the triggered interactions between EDS1 family members and helper-NLRs imply that the specific interactions of NRG1A with the EDS1-SAG101 complex and ADR1\_L1 with the EDS1-PAD4 complex, respectively, are most likely to be mainly mediated by the EP structural domain. Therefore, If EDS1-chi2 interacts with helper-NLRs, it is most likely with NRG1A because chi2 has the EP

structural domain of SAG101.

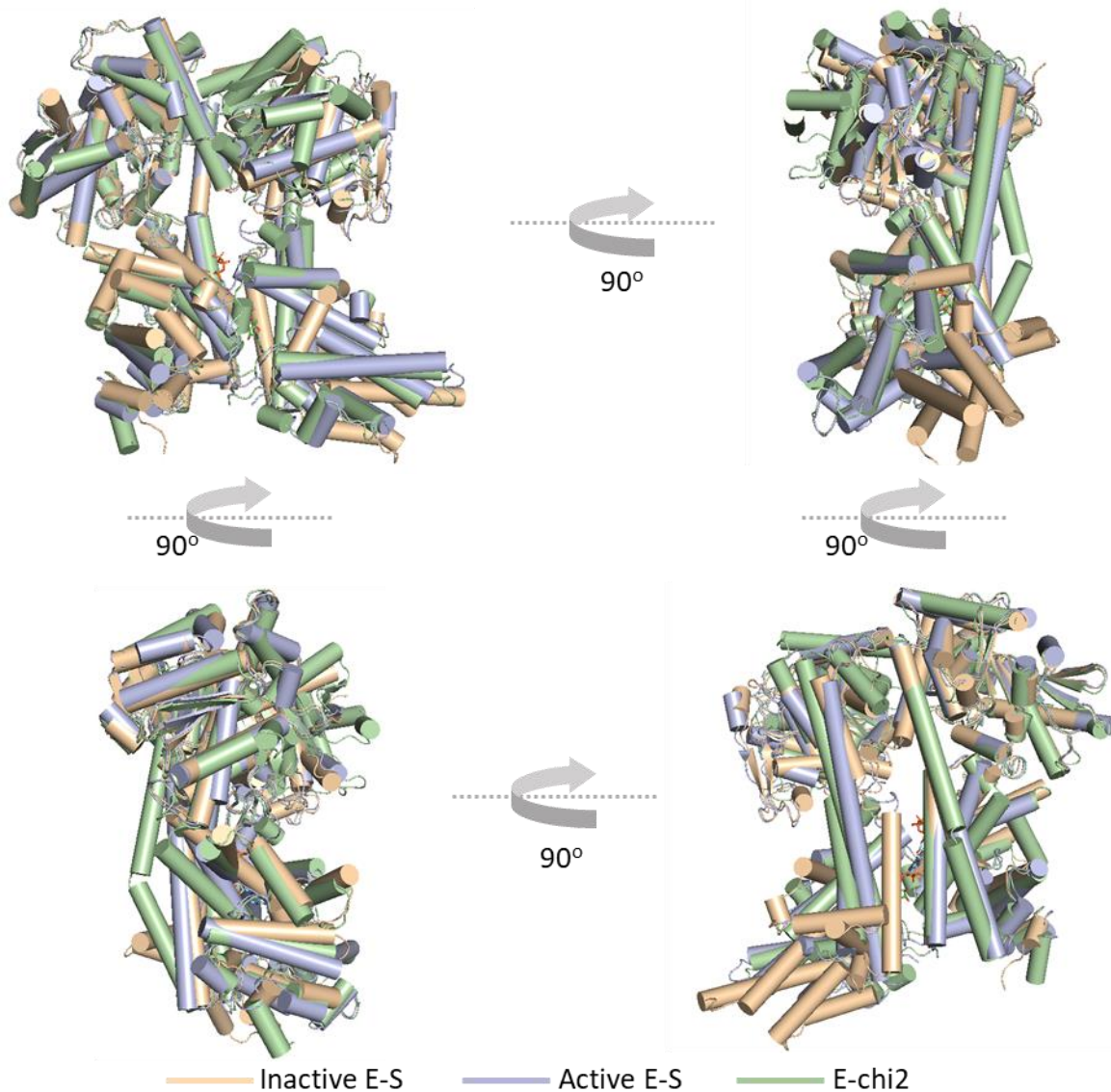


**Figure 5.3 Structural superimposition of the inactive EDS1-SAG101 heterodimer, active EDS1-SAG101 heterodimer, and EDS1-chi2 heterodimer model.**

Huang et al. (2022) suggested that the interaction of EDS1-PAD4 with ADR1\_L1 does not involve direct interaction with the small molecule in the EP domain cavity. Therefore, it is very likely that conformational changes in the active form of the EDS1-SAG101 heterodimer promote the interaction. We speculate that the conformational change in the active form of the EDS1-SAG101 heterodimer is the direct trigger for inducing the interaction.



Superimposition of the EDS1-chi2 model with active and inactive E-S heterodimers indicates a close match of chi2 with active SAG101 (**Fig. 5.3**). The structural arrangement of the chi2 model closely mimics the structure of active SAG101, especially in the E-P domain. Instead of binding to the small molecule, which is the driving force for rearrangement of the cavity of the active EDS1-SAG101 heterodimer, the engineered  $\alpha$ -helix in chi2 (containing the fusion point of PAD4 and SAG101) pulls the EP domain of chi2 and maintains the heterodimeric structure. Thus, the autoimmune phenotype in Arabidopsis is not surprising given the high similarity of chi2 and SAG101 on the structural level. However, this active EDS1-chi2 heterodimer is not able to maintain a long-lasting and stable interaction with NRG1A *in vitro* (**Fig 4.8**). One explanation is that the structural model of the EDS1-chi2 heterodimer might be different from the experimentally determined structure, and thus not be a faithful representation of the active form. Besides, instability of the EDS1-chi2 heterodimer, especially around the cavity, might prevent successful interaction of the EDS1-chi2 heterodimer and NRG1A. *In planta*, residual protein interaction might be sufficient to cause the phenotype. In addition, it is also possible that chi2 may interfere with another EDS1 family-related pathway, which is linked to the autoimmune phenotype *in vivo*.

While we did not succeed in obtaining the structure of the EDS1-chi2 heterodimer, it will definitely be worthwhile to continue to investigate the mechanism of autoimmunity induced by overexpression of chi2 in Arabidopsis, which may shed light on plant protection.

## **5.5 Small molecule binding promotes the interaction of EDS1 family heterodimers with helper-NLRs**

Despite intense efforts, we did not succeed in identifying specific TNLs or TIR-catalyzed products that activate EDS1 family members. There are some major obstacles to unraveling these mechanisms: (1) The co-expression of all proteins is a big challenge because it's difficult to ensure the high expression of every component. RPP1 and helper-NLRs are large NLR proteins and expressing them in sufficient amounts was a constant challenge. (2) Due to the lack of a reference compound, the identification of EDS1 family heterodimers ligands is difficult.

The groundbreaking work of Huang et al. and Jia et al. shows that a novel small molecule, 2'-(5'-phosphoribosyl)-5'-adenosine diphosphate (pRib-ADP), binds specifically to the conserved cavity

in the E-P domain of EDS1 and PAD4. Liquid chromatography-high resolution mass spectrometry (LC-HRMS) confirmed the binding of pRib-ADP and identified 2'-(5''-phosphoribosyl)-5'-adenosine monophosphate (pRib-AMP) in the active EDS1-PAD4 complex. Huang et al. (2022) demonstrated that both pRib-ADP and pRib-AMP, as ligands of the EDS1-PAD4 heterodimer, are capable of triggering the interaction of EDS1-PAD4 and ADR1\_L1; however, these two small molecules could only induce weak association of NRG1A with the EDS1-SAG101 complex. Note that co-expression of RPP1, ATR1, EDS1, SAG101, and NRG1A strongly activates the interaction of NRG1A with the EDS1-SAG101 complex (Huang et al., 2022; Jia et al., 2022). This suggests that there are other TIR products that may specifically prompt the interaction of EDS1 and SAG101 with NRG1A. I could only observe that the products of RPP1 NADase activity trigger a weak interaction of EDS1-SAG101 with NRG1A, strengthening the hypothesis that the activation of the EDS1-SAG101 complex may be explained by other mechanisms.

Further investigation by Jia et al. demonstrated that ADP-ribosylated adenosine triphosphate (ADPr-ATP) is the ligand of active EDS1-SAG101 heterodimer and that it induces the interaction of the EDS1-SAG101 heterodimer and NRG1A *in vitro*. Unlike pRib-ADP and pRib-AMP, ADPr-ATP is synthesized by TIR-catalyzed transfer of ADPR from NAD<sup>+</sup> to ATP. Thus, pRib-ADP and pRib-AMP are synthesized likely through the breakdown of ADPr-ATP between phosphate-phosphate bonds. A related product, di-ADPR could induce the interaction of EDS1-SAG101 with NRG1A, but not that of EDS1-PAD4 with ADR1\_L1, demonstrating the distinct activation mechanism of these two branches (Huang et al., 2022; Jia et al., 2022).

## 5.6 Function of helper-NLRs

The Cryo-EM structure of inactive, intermediate, and activated ZAR1 shows the conformational change of this protein upon effector perception and its assembly into an active pentamer termed the 'resistosome' (Wang et al., 2019a; Wang et al., 2019b). The ZAR1 CC domain (ZAR1<sup>CC</sup>) contains four  $\alpha$ -helix barrels. Upon activation,  $\alpha 1$  helix is released and invades the exterior of the ZAR1 resistosome. It was demonstrated that  $\alpha 1$  helix is associated with the plasma membrane and contributes to Ca<sup>2+</sup> influx, thereby inducing cell death and resistance to *Xanthomonas campestris* (Wang et al., 2019a; Wang et al., 2019b) (Bi et al., 2021).



In fungi and mammals, MLKLs contain a HeLo domain, which consists of four helical bundles, and form pores in the membrane to trigger cell death (Daskalov et al., 2016; Quarato et al., 2016). On the sequence and structure level, CC<sub>R</sub> is very similar to the HeLo domain. Recently, Arabidopsis MLKLs were identified and it was demonstrated that their HeLo domains are similar to those of MLKLs in animals. It was shown that AtMLKL plays a role in TNL-mediated resistance and induces cell death but is not required for the immune response (Mahdi et al., 2020).

The crystal structure of NRG1<sup>CCR</sup> was solved by Jacob et al. (2021) and shows a high degree of similarity to the Arabidopsis MLKL HeLo domain, and to some extent, also to the CC domain of ZAR1. Superimposition of ZAR1<sup>CC</sup> and NRG1<sup>CCR</sup> is reminiscent of the ZAR1 and NRG1A model, pointing out the  $\alpha$ 1 helix of NRG1A consisting of 16 amino acids more compare to ZAR1 (Jacob et al., 2021). A longer  $\alpha$ 1 helix in NRG1A might indicate a distinctive function compare to ZAR1 in Arabidopsis. Data suggested that the  $\alpha$ 1 helix of NRG1A is associated with the plasma membrane (PM) and forms an ion channel which is permeable to Ca<sup>2+</sup>. Both mutations of the negatively charged residues and deletions of the NRG1A  $\alpha$ 1 helix abrogate cell death upon activation (Jacob et al., 2021). Furthermore, Saile et al. demonstrated that ADR1s interacts with PM phospholipids and interference with this the interaction abolishes the PM localization of ADR1s and also ADR1s-mediated immune responses (Saile et al., 2021). In conclusion, this strongly suggests that activated NRG1s and ADR1s bind to the cell membrane and consequently cause cell death and resistance.

## 5.7 The biological relevance of SAG101 cleavage *in planta*

Although the cleavage of SAG101 *in vitro* after TIR NADase activation is clearly demonstrated in the experiments described in this thesis, the function of cleavage in Arabidopsis remains to be determined. Furthermore, we do not know whether NRGs could prevent SAG101 cleavage *in vitro* and *in vivo*. Recently, it was reported that the N-terminal truncated NRG1C antagonizes the immune response mediated by NRG1A and NRG1B, likely by interfering with EDS1 and SAG101 (Wu et al., 2022). It is plausible that SAG101 cleavage might also act as a negative feedback to ETI, allowing plants to limit the extent of cell death. However, this would need to be tested in plants.

## 5.8 Outlook

Exciting structural insights into the active forms of EDS1 family heterodimers and the inducible interactions of EDS1 family members with helper-NLRs have elucidated the mechanism of how EDS1 family members bridge the gap between activation of TNLs by pathogen effectors and activation of helper-NLRs. Oligomerization of NLRs, the structure of EDS1-SAG101-NRG1s and EDS1-PAD4-ADR1s and how these two groups of NLRs function in Arabidopsis will further improve our understanding of the TNL-mediated immune response. The structure of the helper-NLR resistosome will help us to understand the mechanism of interaction between helper-NLRs and EDS1 family members and also the specific functions executed by the different structures. The EDS1-PAD4-ADR1s module has also been reported to be involved in the PTI response (Pruitt et al., 2021; Tian et al., 2021), so it would be interesting to explore how this branch mediates both the PTI and ETI pathways upon activation.

## 6 References

- Bi, G.Z., Su, M., Li, N., Liang, Y., Dang, S., Xu, J.C., Hu, M.J., Wang, J.Z., Zou, M.X., Deng, Y.A., Li, Q.Y., Huang, S.J., Li, J.J., Chai, J.J., He, K.M., Chen, Y.H., and Zhou, J.M. (2021). The ZAR1 resistosome is a calcium-permeable channel triggering plant immune signaling. *Cell* **184**, 3528-+.
- Daskalov, A., Habenstein, B., Sabate, R., Berbon, M., Martinez, D., Chaignepain, S., Coulary-Salin, B., Hofmann, K., Loquet, A., and Saupe, S.J. (2016). Identification of a novel cell death-inducing domain reveals that fungal amyloid-controlled programmed cell death is related to necroptosis. *P Natl Acad Sci USA* **113**, 2720-2725.
- Dongus, J.A., Bhandari, D.D., Penner, E., Lapin, D., Stolze, S.C., Harzen, A., Patel, M., Archer, L., Dijkgraaf, L., Shah, J.T., Nakagami, H., and Parker, J.E. (2022). Cavity surface residues of PAD4 and SAG101 contribute to EDS1 dimer signaling specificity in plant immunity. *Plant J* **110**, 1415-1432.
- Huang, S.J., Jia, A.L., Song, W., Hessler, G., Meng, Y.G., Sun, Y., Xu, L.N., Laessle, H., Jirschitzka, J., Ma, S.C., Xiao, Y., Yu, D.L., Hou, J., Liu, R.Q., Sun, H.H., Liu, X.H., Han, Z.F., Chang, J.B., Parker, J.E., and Chai, J.J. (2022). Identification and receptor mechanism of TIR-catalyzed small molecules in plant immunity. *Science* **377**, 487-+.
- Jacob, P., Kim, N.H., Wu, F.H., El Kasmr, F., Chi, Y., Walton, W.G., Furzer, O.J., Lietzan, A.D., Sunil, S., Kempthorn, K., Redinbo, M.R., Pei, Z.M., Wan, L., and Dangl, J.L. (2021). Plant "helper" immune receptors are Ca<sup>2+</sup>-permeable nonselective cation channels. *Science* **373**, 420-+.
- Jia, A.L., Huang, S.J., Song, W., Wang, J.L., Meng, Y.G., Sun, Y., Xu, L.N., Laessle, H., Jirschitzka, J., Hou, J., Zhang, T.T., Yu, W.Q., Hessler, G., Li, E.T., Ma, S.C., Yu, D.L., Gebauer, J., Baumann, U., Liu, X.H., Han, Z.F., Chang, J.B., Parker, J.E., and Chai, J.J. (2022). TIR-catalyzed ADP-ribosylation reactions produce signaling molecules for plant immunity. *Science* **377**, 488-+.
- Mahdi, L.K., Huang, M., Zhang, X., Nakano, R.T., Kopp, L.B., Saur, I.M.L., Jacob, F., Kovacova, V., Lapin, D., Parker, J.E., Murphy, J.M., Hofmann, K., Schulze-Lefert, P., Chai, J., and Maekawa, T. (2020). Discovery of a Family of Mixed Lineage Kinase Domain-like Proteins in Plants and Their Role in Innate Immune Signaling. *Cell Host Microbe* **28**, 813-824 e816.
- Pruitt, R.N., Locci, F., Wanke, F., Zhang, L.S., Saile, S.C., Joe, A., Karelina, D., Hua, C.L., Frohlich, K., Wan, W.L., Hu, M.J., Rao, S.F., Stolze, S.C., Harzen, A., Gust, A.A., Harter, K., Joosten, M.H.A.J., Thomma, B.P.H.J., Zhou, J.M., Dangl, J.L., Weigel, D., Nakagami, H., Oecking, C., El Kasmr, F., Parker, J.E., and Nurnberger, T. (2021). The EDS1-PAD4-ADR1 node mediates Arabidopsis pattern-triggered immunity. *Nature* **598**, 495-+.
- Qi, T., Seong, K., Thomazella, D.P.T., Kim, J.R., Pham, J., Seo, E., Cho, M.J., Schultink, A., and Staskawicz, B.J. (2018). NRG1 functions downstream of EDS1 to regulate TIR-NLR-mediated plant immunity in *Nicotiana benthamiana*. *P Natl Acad Sci USA* **115**, E10979-E10987.
- Quarato, G., Guy, C.S., Grace, C.R., Llambi, F., Nourse, A., Rodriguez, D.A., Wakefield, R., Frase, S., Moldoveanu, T., and Green, D.R. (2016). Sequential Engagement of Distinct MLKL Phosphatidylinositol-Binding Sites Executes Necroptosis. *Mol Cell* **61**, 589-601.
- Saile, S.C., Ackermann, F.M., Sunil, S., Keicher, J., Bayless, A., Bonardi, V., Wan, L., Doumane, M., Stobbe, E., Jaillais, Y., Caillaud, M.C., Dangl, J.L., Nishimura, M.T., Oecking, C., and El Kasmr, F. (2021). Arabidopsis ADR1 helper NLR immune receptors localize and function at the plasma membrane in a phospholipid dependent manner. *New Phytol* **232**, 2440-2456.
- Tian, H.N., Wu, Z.S., Chen, S.Y., Ao, K.V., Huang, W.J., Yaghmaiean, H., Sun, T.J., Xu, F., Zhang, Y.N., Wang, S.C., Li, X., and Zhang, Y.L. (2021). Activation of TIR signalling boosts pattern-triggered immunity. *Nature* **598**, 500-+.

- Wu, Z.S., Tian, L., Liu, X.R., Huang, W.J., Zhang, Y.L., and Li, X.** (2022). The N-terminally truncated helper NLR NRG1C antagonizes immunity mediated by its full-length neighbors NRG1A and NRG1B. *Plant Cell* **34**, 1621-1640.
- Aarts, N., Metz, M., Holub, E., Staskawicz, B.J., Daniels, M.J., and Parker, J.E.** (1998). Different requirements for EDS1 and NDR1 by disease resistance genes define at least two R gene-mediated signaling pathways in Arabidopsis. *Proc Natl Acad Sci U S A* **95**, 10306-10311.
- Bernoux, M., Ve, T., Williams, S., Warren, C., Hatters, D., Valkov, E., Zhang, X.X., Ellis, J.G., Kobe, B., and Dodds, P.N.** (2011). Structural and Functional Analysis of a Plant Resistance Protein TIR Domain Reveals Interfaces for Self-Association, Signaling, and Autoregulation. *Cell Host Microbe* **9**, 200-211.
- Bhandari, D.D., Lapin, D., Kracher, B., von Born, P., Bautor, J., Niefind, K., and Parker, J.E.** (2019). An EDS1 heterodimer signalling surface enforces timely reprogramming of immunity genes in Arabidopsis. *Nat Commun* **10**.
- Bi, G.Z., Su, M., Li, N., Liang, Y., Dang, S., Xu, J.C., Hu, M.J., Wang, J.Z., Zou, M.X., Deng, Y.A., Li, Q.Y., Huang, S.J., Li, J.J., Chai, J.J., He, K.M., Chen, Y.H., and Zhou, J.M.** (2021). The ZAR1 resistosome is a calcium-permeable channel triggering plant immune signaling. *Cell* **184**, 3528-+.
- Bonardi, V., Tang, S.J., Stallmann, A., Roberts, M., Cherkis, K., and Dangl, J.L.** (2011). Expanded functions for a family of plant intracellular immune receptors beyond specific recognition of pathogen effectors. *P Natl Acad Sci USA* **108**, 16463-16468.
- Burdett, H., Hu, X., Rank, M.X., Maruta, N., and Kobe, B.** (2021). Self-association configures the NAD<sup>+</sup> - binding site of plant NLR TIR domains.
- Castel, B., Ngou, P.M., Cevik, V., Redkar, A., Kim, D.S., Yang, Y., Ding, P.T., and Jones, J.D.G.** (2019). Diverse NLR immune receptors activate defence via the RPW8-NLR NRG1. *New Phytol* **222**, 966-980.
- Cesari, S., Kanzaki, H., Fujiwara, T., Bernoux, M., Chalvon, V., Kawano, Y., Shimamoto, K., Dodds, P., Terauchi, R., and Kroj, T.** (2014). The NB-LRR proteins RGA4 and RGA5 interact functionally and physically to confer disease resistance. *Embo J* **33**, 1941-1959.
- Cui, H.T., Gobbato, E., Kracher, B., Qiu, J.D., Bautor, J., and Parker, J.E.** (2017). A core function of EDS1 with PAD4 is to protect the salicylic acid defense sector in Arabidopsis immunity. *New Phytol* **213**, 1802-1817.
- Daskalov, A., Habenstein, B., Sabate, R., Berbon, M., Martinez, D., Chaignepain, S., Coulary-Salin, B., Hofmann, K., Loquet, A., and Saupe, S.J.** (2016). Identification of a novel cell death-inducing domain reveals that fungal amyloid-controlled programmed cell death is related to necroptosis. *P Natl Acad Sci USA* **113**, 2720-2725.
- Dodds, P.N., Lawrence, G.J., Catanzariti, A.M., Teh, T., Wang, C.I.A., Ayliffe, M.A., Kobe, B., and Ellis, J.G.** (2006). Direct protein interaction underlies gene-for-gene specificity and coevolution of the flax resistance genes and flax rust avirulence genes. *P Natl Acad Sci USA* **103**, 8888-8893.
- Dongus, J.A., Bhandari, D.D., Penner, E., Lapin, D., Stolze, S.C., Harzen, A., Patel, M., Archer, L., Dijkgraaf, L., Shah, J.T., Nakagami, H., and Parker, J.E.** (2022). Cavity surface residues of PAD4 and SAG101 contribute to EDS1 dimer signaling specificity in plant immunity. *Plant J* **110**, 1415-1432.
- Dou, D.L., and Zhou, J.M.** (2012). Phytopathogen Effectors Subverting Host Immunity: Different Foes, Similar Battleground. *Cell Host Microbe* **12**, 484-495.
- Duxbury, Z., Wang, S.S., MacKenzie, C.I., Tenthorey, J.L., Zhang, X.X., Huh, S.U., Hu, L.X., Hill, L., Ngou, P.N., Ding, P.T., Chen, J., Ma, Y., Guo, H.L., Castel, B., Moschou, P.N., Bernoux, M., Dodds, P.N., Vance, R.E., and Jones, J.D.G.** (2020). Induced proximity of a TIR signaling domain on a plant-mammalian NLR chimera activates defense in plants. *P Natl Acad Sci USA* **117**, 18832-18839.

- Essuman, K., Summers, D.W., Sasaki, Y., Mao, X.R., Yim, A.K.Y., DiAntonio, A., and Milbrandt, J.** (2018). TIR Domain Proteins Are an Ancient Family of NAD(+)-Consuming Enzymes. *Curr Biol* **28**, 421-+.
- Feys, B.J., Moisan, L.J., Newman, M.A., and Parker, J.E.** (2001). Direct interaction between the Arabidopsis disease resistance signaling proteins, EDS1 and PAD4. *Embo J* **20**, 5400-5411.
- Feys, B.J., Wiermer, M., Bhat, R.A., Moisan, L.J., Medina-Escobar, N., Neu, C., Cabral, A., and Parker, J.E.** (2005). Arabidopsis SENESCENCE-ASSOCIATED GENE101 stabilizes and signals within an ENHANCED DISEASE SUSCEPTIBILITY1 complex in plant innate immunity. *Plant Cell* **17**, 2601-2613.
- Flor, H.H.** (1971). Current Status of Gene-for-Gene Concept. *Annu Rev Phytopathol* **9**, 275-+.
- Gantner, J., Ordon, J., Kretschmer, C., Guerois, R., and Stuttmann, J.** (2019). An EDS1-SAG101 Complex Is Essential for TNL-Mediated Immunity in *Nicotiana benthamiana*. *Plant Cell* **31**, 2456-2474.
- Guzman, L.M., Belin, D., Carson, M.J., and Beckwith, J.** (1995). Tight Regulation, Modulation, and High-Level Expression by Vectors Containing the Arabinose P-Bad Promoter. *J Bacteriol* **177**, 4121-4130.
- Horsefield, S., Burdett, H., Zhang, X.X., Manik, M.K., Shi, Y., Chen, J., Qi, T.C., Gilley, J., Lai, J.S., Rank, M.X., Casey, L.W., Gu, W.X., Ericsson, D.J., Foley, G., Hughes, R.O., Bosanac, T., von Itzstein, M., Rathjen, J.P., Nanson, J.D., Boden, M., Dry, I.B., Williams, S.J., Staskawicz, B.J., Coleman, M.P., Ve, T., Dodds, P.N., and Kobe, B.** (2019). NAD(+) cleavage activity by animal and plant TIR domains in cell death pathways. *Science* **365**, 793-+.
- Huang, S.J., Jia, A.L., Song, W., Hessler, G., Meng, Y.G., Sun, Y., Xu, L.N., Laessle, H., Jirschitzka, J., Ma, S.C., Xiao, Y., Yu, D.L., Hou, J., Liu, R.Q., Sun, H.H., Liu, X.H., Han, Z.F., Chang, J.B., Parker, J.E., and Chai, J.J.** (2022). Identification and receptor mechanism of TIR-catalyzed small molecules in plant immunity. *Science* **377**, 487-+.
- Jacob, P., Kim, N.H., Wu, F.H., El Kasmr, F., Chi, Y., Walton, W.G., Furzer, O.J., Lietzan, A.D., Sunil, S., Kempthorn, K., Redinbo, M.R., Pei, Z.M., Wan, L., and Dangl, J.L.** (2021). Plant "helper" immune receptors are Ca<sup>2+</sup>-permeable nonselective cation channels. *Science* **373**, 420-+.
- Jia, A.L., Huang, S.J., Song, W., Wang, J.L., Meng, Y.G., Sun, Y., Xu, L.N., Laessle, H., Jirschitzka, J., Hou, J., Zhang, T.T., Yu, W.Q., Hessler, G., Li, E.T., Ma, S.C., Yu, D.L., Gebauer, J., Baumann, U., Liu, X.H., Han, Z.F., Chang, J.B., Parker, J.E., and Chai, J.J.** (2022). TIR-catalyzed ADP-ribosylation reactions produce signaling molecules for plant immunity. *Science* **377**, 488-+.
- Jirage, D., Tootle, T.L., Reuber, T.L., Frost, L.N., Feys, B.J., Parker, J.E., Ausubel, F.M., and Glazebrook, J.** (1999). Arabidopsis thaliana PAD4 encodes a lipase-like gene that is important for salicylic acid signaling. *Proc Natl Acad Sci U S A* **96**, 13583-13588.
- Jones, J.D.G., and Dangl, J.L.** (2006). The plant immune system. *Nature* **444**, 323-329.
- Jones, J.D.G., Vance, R.E., and Dangl, J.L.** (2016). Intracellular innate immune surveillance devices in plants and animals. *Science* **354**.
- Kadota, Y., Shirasu, K., and Guerois, R.** (2010). NLR sensors meet at the SGT1-HSP90 crossroad. *Trends Biochem Sci* **35**, 199-207.
- Keen, N.T.** (1990). Gene-for-Gene Complementarity in Plant-Pathogen Interactions. *Annu Rev Genet* **24**, 447-463.
- Lapin, D., Kovacova, V., Sun, X.H., Dongus, J.A., Bhandari, D., von Born, P., Bautor, J., Guarneri, N., Rzemieniewski, J., Stuttmann, J., Beyer, A., and Parker, J.E.** (2019). A Coevolved EDS1-SAG101-NRG1 Module Mediates Cell Death Signaling by TIR-Domain Immune Receptors. *Plant Cell* **31**, 2430-2455.
- Le Roux, C., Huet, G., Jauneau, A., Camborde, L., Tremousaygue, D., Kraut, A., Zhou, B.B., Levaillant, M., Adachi, H., Yoshioka, H., Raffaele, S., Berthome, R., Coute, Y., Parker, J.E., and Deslandes, L.** (2015). A Receptor Pair with an Integrated Decoy Converts Pathogen Disabling of Transcription Factors to Immunity. *Cell* **161**, 1074-1088.

- Lee, C.C., Wood, M.D., Ng, K., Andersen, C.B., Liu, Y., Luginbuhl, P., Spraggon, G., and Katagiri, F. (2004). Crystal structure of the type III effector AvrB from *Pseudomonas syringae*. *Structure* **12**, 487-494.
- Lu, X.L., Kracher, B., Saur, I.M.L., Bauer, S., Ellwood, S.R., Wise, R., Yaeno, T., Maekawa, T., and Schulze-Lefert, P. (2016). Allelic barley MLA immune receptors recognize sequence-unrelated avirulence effectors of the powdery mildew pathogen. *P Natl Acad Sci USA* **113**, E6486-E6495.
- Ma, S., Lapin, D., Liu, L., Sun, Y., Song, W., Zhang, X., Logemann, E., Yu, D., Wang, J., Jirschitzka, J., Han, Z., Schulze-Lefert, P., Parker, J.E., and Chai, J. (2020). Direct pathogen-induced assembly of an NLR immune receptor complex to form a holoenzyme. *Science* **370**.
- Mackey, D., Belkhadir, Y., Alonso, J.M., Ecker, J.R., and Dangl, J.L. (2003). Arabidopsis RIN4 is a target of the type III virulence effector AvrRpt2 and modulates RPS2-mediated resistance. *Cell* **112**, 379-389.
- Mahdi, L.K., Huang, M., Zhang, X., Nakano, R.T., Kopp, L.B., Saur, I.M.L., Jacob, F., Kovacova, V., Lapin, D., Parker, J.E., Murphy, J.M., Hofmann, K., Schulze-Lefert, P., Chai, J., and Maekawa, T. (2020). Discovery of a Family of Mixed Lineage Kinase Domain-like Proteins in Plants and Their Role in Innate Immune Signaling. *Cell Host Microbe* **28**, 813-824 e816.
- Martin, R., Qi, T.C., Zhang, H.B., Liu, F.R., King, M., Toth, C., Nogales, E., and Staskawicz, B.J. (2020). Structure of the activated ROQ1 resistosome directly recognizing the pathogen effector XopQ. *Science* **370**, 1185-+.
- Mestre, P., and Baulcombe, D.C. (2006). Elicitor-mediated oligomerization of the tobacco N disease resistance protein. *Plant Cell* **18**, 491-501.
- Nandety, R.S., Caplan, J.L., Cavanaugh, K., Perroud, B., Wroblewski, T., Michelmore, R.W., and Meyers, B.C. (2013). The Role of TIR-NBS and TIR-X Proteins in Plant Basal Defense Responses. *Plant Physiol* **162**, 1459-1472.
- Ofir, G., Herbst, E., Baroz, M., Cohen, D., Millman, A., Doron, S., Tal, N., Malheiro, D.B.A., Malitsky, S., Amitai, G., and Sorek, R. (2021). Antiviral activity of bacterial TIR domains via immune signalling molecules. *Nature* **600**, 116-+.
- Parker, J.E., Holub, E.B., Frost, L.N., Falk, A., Gunn, N.D., and Daniels, M.J. (1996). Characterization of eds1, a mutation in Arabidopsis suppressing resistance to *Peronospora parasitica* specified by several different RPP genes. *Plant Cell* **8**, 2033-2046.
- Peart, J.R., Mestre, P., Lu, R., Malcuit, I., and Baulcombe, D.C. (2005). NRG1, a CC-NB-LRR protein, together with N, a TIR-NB-LRR protein, mediates resistance against tobacco mosaic virus. *Curr Biol* **15**, 968-973.
- Pruitt, R.N., Locci, F., Wanke, F., Zhang, L.S., Saile, S.C., Joe, A., Karelina, D., Hua, C.L., Frohlich, K., Wan, W.L., Hu, M.J., Rao, S.F., Stolze, S.C., Harzen, A., Gust, A.A., Harter, K., Joosten, M.H.A.J., Thomma, B.P.H.J., Zhou, J.M., Dangl, J.L., Weigel, D., Nakagami, H., Oecking, C., El Kasmi, F., Parker, J.E., and Nurnberger, T. (2021). The EDS1-PAD4-ADR1 node mediates Arabidopsis pattern-triggered immunity. *Nature* **598**, 495-+.
- Qi, T., Seong, K., Thomazella, D.P.T., Kim, J.R., Pham, J., Seo, E., Cho, M.J., Schultink, A., and Staskawicz, B.J. (2018). NRG1 functions downstream of EDS1 to regulate TIR-NLR-mediated plant immunity in *Nicotiana benthamiana*. *P Natl Acad Sci USA* **115**, E10979-E10987.
- Quarato, G., Guy, C.S., Grace, C.R., Llambi, F., Nourse, A., Rodriguez, D.A., Wakefield, R., Frase, S., Moldoveanu, T., and Green, D.R. (2016). Sequential Engagement of Distinct MLKL Phosphatidylinositol-Binding Sites Executes Necroptosis. *Mol Cell* **61**, 589-601.
- Rietz, S., Stamm, A., Malonek, S., Wagner, S., Becker, D., Medina-Escobar, N., Vlot, A.C., Feys, B.J., Niefind, K., and Parker, J.E. (2011). Different roles of Enhanced Disease Susceptibility1 (EDS1) bound to and dissociated from Phytoalexin Deficient4 (PAD4) in Arabidopsis immunity. *New Phytol* **191**, 107-119.

- Saile, S.C., Jacob, P., Castel, B., Jubic, L.M., Salas-Gonzales, I., Backer, M., Jones, J.D.G., Dangl, J.L., and El Kasmí, F. (2020). Two unequally redundant "helper" immune receptor families mediate Arabidopsis thaliana intracellular "sensor" immune receptor functions. *Plos Biol* **18**.
- Saile, S.C., Ackermann, F.M., Sunil, S., Keicher, J., Bayless, A., Bonardi, V., Wan, L., Doumane, M., Stobbe, E., Jaillais, Y., Caillaud, M.C., Dangl, J.L., Nishimura, M.T., Oecking, C., and El Kasmí, F. (2021). Arabidopsis ADR1 helper NLR immune receptors localize and function at the plasma membrane in a phospholipid dependent manner. *New Phytol* **232**, 2440-2456.
- Sun, X.H., Lapin, D., Feehan, J.M., Stolze, S.C., Kramer, K., Dongus, J.A., Rzemieniewski, J., Blanvillain-Baufume, S., Harzen, A., Bautor, J., Derbyshire, P., Menke, F.L.H., Finkemeier, I., Nakagami, H., Jones, J.D.G., and Parker, J.E. (2021). Pathogen effector recognition-dependent association of NRG1 with EDS1 and SAG101 in TNL receptor immunity. *Nat Commun* **12**.
- Swiderski, M.R., Birker, D., and Jones, J.D.G. (2009). The TIR Domain of TIR-NB-LRR Resistance Proteins Is a Signaling Domain Involved in Cell Death Induction. *Mol Plant Microbe In* **22**, 157-165.
- Teper, D., Salomon, D., Sunitha, S., Kim, J.G., Mudgett, M.B., and Sessa, G. (2014). Xanthomonas euvesicatoria typell effector XopQ interacts with tomato and pepper 14-3-3 isoforms to suppress effector-triggered immunity. *Plant J* **77**, 297-309.
- Tian, H.N., Wu, Z.S., Chen, S.Y., Ao, K.V., Huang, W.J., Yaghmaiean, H., Sun, T.J., Xu, F., Zhang, Y.N., Wang, S.C., Li, X., and Zhang, Y.L. (2021). Activation of TIR signalling boosts pattern-triggered immunity. *Nature* **598**, 500-+.
- Vagenende, V., Yap, M.G.S., and Trout, B.L. (2009). Mechanisms of Protein Stabilization and Prevention of Protein Aggregation by Glycerol. *Biochemistry-U.S.* **48**, 11084-11096.
- Voss, M., Toelzer, C., Bhandari, D.D., Parker, J.E., and Niefind, K. (2019). Arabidopsis immunity regulator EDS1 in a PAD4/SAG101-unbound form is a monomer with an inherently inactive conformation. *J Struct Biol* **208**.
- Wagner, S., Stuttmann, J., Rietz, S., Guerois, R., Brunstein, E., Bautor, J., Niefind, K., and Parker, J.E. (2013). Structural Basis for Signaling by Exclusive EDS1 Heteromeric Complexes with SAG101 or PAD4 in Plant Innate Immunity. *Cell Host Microbe* **14**, 619-630.
- Wan, L., Essuman, K., Anderson, R.G., Sasaki, Y., Monteiro, F., Chung, E.H., Nishimura, E.O., DiAntonio, A., Milbrandt, J., Dangl, J.L., and Nishimura, M.T. (2019). TIR domains of plant immune receptors are NAD(+)-cleaving enzymes that promote cell death. *Science* **365**, 799-+.
- Wang, G.X., Roux, B., Feng, F., Guy, E., Li, L., Li, N.N., Zhang, X.J., Lautier, M., Jardinaud, M.F., Chabannes, M., Arlat, M., Chen, S., He, C.Z., Noel, L.D., and Zhou, J.M. (2015). The Decoy Substrate of a Pathogen Effector and a Pseudokinase Specify Pathogen-Induced Modified-Self Recognition and Immunity in Plants. *Cell Host Microbe* **18**, 285-295.
- Wang, J.Z., Hu, M.J., Wang, J., Qi, J.F., Han, Z.F., Wang, G.X., Qi, Y.J., Wang, H.W., Zhou, J.M., and Chai, J.J. (2019a). Reconstitution and structure of a plant NLR resistosome conferring immunity. *Science* **364**, 44-+.
- Wang, J.Z., Wang, J., Hu, M.J., Wu, S., Qi, J.F., Wang, G.X., Han, Z.F., Qi, Y.J., Gao, N., Wang, H.W., Zhou, J.M., and Chai, J.J. (2019b). Ligand-triggered allosteric ADP release primes a plant NLR complex. *Science* **364**, 43-+.
- Wu, Z.S., Tian, L., Liu, X.R., Zhang, Y.L., and Li, X. (2021). TIR signal promotes interactions between lipase-like proteins and ADR1-L1 receptor and ADR1-L1 oligomerization. *Plant Physiol* **187**, 681-686.
- Wu, Z.S., Tian, L., Liu, X.R., Huang, W.J., Zhang, Y.L., and Li, X. (2022). The N-terminally truncated helper NLR NRG1C antagonizes immunity mediated by its full-length neighbors NRG1A and NRG1B. *Plant Cell* **34**, 1621-1640.
- Wu, Z.S., Li, M., Dong, O.X., Xia, S.T., Liang, W.W., Bao, Y.K., Wasteneys, G., and Li, X. (2019). Differential regulation of TNL-mediated immune signaling by redundant helper CNLs. *New Phytol* **222**, 938-953.

- Xu, F., Zhu, C.P., Cevik, V., Johnson, K., Liu, Y.N., Sohn, K., Jones, J.D., Holub, E.B., and Li, X.** (2015). Autoimmunity conferred by chs3-2D relies on CSA1, its adjacent TNL-encoding neighbour. *Sci Rep-Uk* **5**.
- Yang, J.Y., Yan, R.X., Roy, A., Xu, D., Poisson, J., and Zhang, Y.** (2015). The I-TASSER Suite: protein structure and function prediction. *Nat Methods* **12**, 7-8.
- Zhang, X.X., Bernoux, M., Bentham, A.R., Newman, T.E., Ve, T., Casey, L.W., Raaymakers, T.M., Hu, J., Croll, T.I., Schreiber, K.J., Staskawicz, B.J., Anderson, P.A., Sohn, K.H., Williams, S.J., Dodds, P.N., and Kobe, B.** (2017). Multiple functional self-association interfaces in plant TIR domains. *P Natl Acad Sci USA* **114**, E2046-E2052.
- Zhou, N., Tootle, T.L., Tsui, F., Klessig, D.F., and Glazebrook, J.** (1998). PAD4 functions upstream from salicylic acid to control defense responses in Arabidopsis. *Plant Cell* **10**, 1021-1030.



# LIST OF ABBREVIATIONS

## Amino acids

Ala, A	Alanine
Arg, R	Arginine
Asn, N	Asparagine
Asp, D	Aspartate
Cys, C	Cysteine
Glu, E	Glutamate
Gln, Q	Glutamine
Gly, G	Glycine
His, H	Histidine
Ile, I	Isoleucine
Leu, L	Leucine
Lys, K	Lysine
Met, M	Methionine
Phe, F	Phenylalanine
Pro, P	Proline
Ser, S	Serine
Thr, T	Threonine
Trp, W	Tryptophan
Tyr, Y	Tyrosine
Val, V	Valine

## Chemicals and buffers

ADP	Adenosine diphosphate
ADPR	ADP-Ribose
ATP	Adenosine triphosphate
cADPR	Cyclic ADPR
cAMP	Cyclic AMP

dATP	Deoxyadenosine triphosphate
DTT	Dithiothreitol
EDTA	Ethylenediaminetetraacetic acid
GSH	Glutathione
GST	Glutathione S-transferases
IPTG	Isopropyl $\beta$ -d-1-thiogalactopyranoside
NAD <sup>+</sup>	Nicotinamide adenine dinucleotide
NAM	Nicotinamide
NMN	Nicotinamide mononucleotide
SA	Salicylic acid

### **Biology terms**

AA	Amino acids
ADR1	Activated disease resistance 1
ATR1	Arabidopsis thaliana recognized 1
BIK1	Botrytis-induced kinase 1
bp	Base pair
CC	Coiled-coil
CC <sub>R</sub>	Powdery mildew 8-like coiled-coil
CED-3	Cell death protein 3
CED-4	Cell death protein 4
CED-9	Cell death abnormality gene 9
CNL	NLRs with N-terminal CC domains
C-JID	C-terminal jelly roll and ig-like domain
C-terminal	Carboxy-terminal
DNA	Deoxyribonucleic acid
<i>E. coli</i>	<i>Escherichia coli</i>
DAMP	Danger-associated molecular pattern
EDS1	Enhanced disease susceptibility 1

ETI	Effector-triggered immunity
LRR	Leucine-rich repeat
MAPKs	Mitogen-activated protein kinases
MLKLs	Mixed lineage kinase domain-like
NBD	Nucleotide-binding domain
NLR	Nod-like receptor
NOD	Nucleotide-binding and oligomerization domain
N-terminal	Amino-terminal
NRG1	N requirement gene 1
PAD4	Phytoalexin deficient 4
PAMP	Pathogen-associated molecular pattern
PBL2	PBS1-like protein 2
PM	Plasma membrane
PRRs	Pattern recognition receptors
PTI	Pattern-triggered immunity
RIN4	RPM1-interacting protein 4
RKS1	Resistance related kinase 1
RLCK	Receptor-like cytoplasmic kinases
RNL	Helper NLRs
ROQ1	Recognition of XopQ 1
RPP1	Recognition of Peronospora parasitica 1
RPS4	Resistance to Pseudomonas syringae 4
RPW8	Resistance to Powdery mildew 8
RRS1	Resistance to Ralstonia solanacearum 1
SAG101	Senescence-associated gene 101
SARM1	Sterile alpha and TIR pattern-containing protein 1
TIR	Toll/Interleukin-1 receptor
TMV	Tobacco mosaic virus
TNL	NLRs with N-terminal TIR domains

WHD	Winged-helix domain
XopQ	XANTHOMONAS OUTER PROTEIN Q
ZAR1	HOPZ-ACTIVATED RESISTANCE 1
<b>Others</b>	
Cryo-EM	Cryo-electron microscopy
SDS-PAGE	SDS-polyacrylamide gel electrophoresis
HPLC-MS	High performance liquid chromatography-mass spectrometry

## **ACKNOWLEDGEMENTS**

Sincere thanks to my supervisor, Prof. Dr. Jijie Chai. I still remember the first time I met you. It was at 7:30 am in the cafeteria. I had heard about your excellent publications and distinguished scientific reputation, but never imagined that you could be so humble and hardworking. You didn't talk much, yet what you did say has had a profound impact on me over the past four years. It was with you that I learned the enormous role that perseverance plays in the scientific journey and the importance of rigor and honesty in science.

Another big thank you goes to my co-supervisor, Prof. Dr. Jane Parker. I cannot overestimate how much you have influenced me by emphasizing the importance of logic in science and in writing scientific articles, and also your patience when explaining things to me. Thank you so much for guiding me on this journey.

I'm eternally grateful for my colleagues, every group member in AG Chai and AG Parker. I truly appreciate everyone's efforts and commitment to our great atmosphere. I am deeply impressed by the merits you all have achieved and am inspired to improve myself in my life. Thank you for helping me in the lab and for the wonderful time we spent together.

I would also like to thank my TAC member, Dr. Takaki Maekawa. Thank you very much for your effort and suggestions during my PhD training.

A big thank you to all the established platforms and the people in the administration of the MPIPZ and the University of Cologne, the PSL department and the MPIPZ Graduate Office. Especially to Neysan Donnelly, who guided me through the Journal Club and showed me how to review papers and write scientific papers. I would also like to thank Stephan Wagner for his generous help and support over the past four years.

Last but not least, I would like to thank my family members and friends. Being negative only makes a difficult journey more difficult. Thank you for providing me with a positive and wonderful environment and for your constant support and love.

# ERKLÄRUNG ZUR DISSERTATION

gemäß der Promotionsordnung vom 12. März 2020

**Diese Erklärung muss in der Dissertation enthalten sein.**

**(This version must be included in the doctoral thesis)**

„Hiermit versichere ich an Eides statt, dass ich die vorliegende Dissertation selbstständig und ohne die Benutzung anderer als der angegebenen Hilfsmittel und Literatur angefertigt habe. Alle Stellen, die wörtlich oder sinngemäß aus veröffentlichten und nicht veröffentlichten Werken dem Wortlaut oder dem Sinn nach entnommen wurden, sind als solche kenntlich gemacht. Ich versichere an Eides statt, dass diese Dissertation noch keiner anderen Fakultät oder Universität zur Prüfung vorgelegen hat; dass sie - abgesehen von unten angegebenen Teilpublikationen und eingebundenen Artikeln und Manuskripten - noch nicht veröffentlicht worden ist sowie, dass ich eine Veröffentlichung der Dissertation vor Abschluss der Promotion nicht ohne Genehmigung des Promotionsausschusses vornehmen werde. Die Bestimmungen dieser Ordnung sind mir bekannt. Darüber hinaus erkläre ich hiermit, dass ich die Ordnung zur Sicherung guter wissenschaftlicher Praxis und zum Umgang mit wissenschaftlichem Fehlverhalten der Universität zu Köln gelesen und sie bei der Durchführung der Dissertation zugrundeliegenden Arbeiten und der schriftlich verfassten Dissertation beachtet habe und verpflichte mich hiermit, die dort genannten Vorgaben bei allen wissenschaftlichen Tätigkeiten zu beachten und umzusetzen. Ich versichere, dass die eingereichte elektronische Fassung der eingereichten Druckfassung vollständig entspricht.“

Teilpublikationen:

Teilpublikationen liegen nicht vor.

Datum, Name und Unterschrift

02/11/2022 Huanhuan Sun



# CURRICULUM VITAE

## Personal information

Name: Huanhuan Sun

Address: Ostring 27, Pulheim 50259, Germany

Mobile: (+49)1776662108

E-mail: [hsun@mpipz.mpg.de](mailto:hsun@mpipz.mpg.de)

Researchgate: [https://www.researchgate.net/profile/Huanhuan\\_Sun](https://www.researchgate.net/profile/Huanhuan_Sun)

---

**Self-evaluation:** I see myself as self-disciplined and ambitious, full of fantasy but with focus on real life. I am stubborn but also persistent, believing that perseverance and hardworking creates success. I am looking for a meaningful, fulfilled, healthy, positive and colorful life.

**Motivation:** I am looking forward to do the next step in my career, training myself as a scientist, explore new research areas, meeting new people and expanding my horizon.

## Work Experience

2016.08 - 2017.08      **Research Associate** at the Kunming Institute of Botany, CAS

Research on: Regulation of scopoletin synthesis in *N. attenuata*

## Education

2018.09 – present      Doctor candidate in MPIPZ

2013.09 - 2016.07      **M.S:** Biochemistry and Molecular Biology at the Kunming Institute of Botany,  
Chinese Academy of Sciences

**Thesis:** The regulation of phytoalexin scopoletin by phytohormones Jasmonic acid and Ethylene

2009.09 – 2013.07      **B.S:** Biotechnology at the Henan University of Urban Construction,  
Pingdingshan, China

### Technical skills

During the last nine years in the laboratory, I have acquired a profound knowledge in basic molecular biology techniques like RNA/DNA and protein extraction, cloning, qRT-PCR and protein activity studies. I am also familiar with analyzing big datasets from RNA-sequencing, with fluorescence microscopy and with routine work on our HPLC-MS/MS system. During my PhD study, I mastered the standard techniques of molecular biology and biochemistry and I am also proficient in more advanced methods, including recombinant protein expression and purification, protein structure analysis, protein crystallization, optimization, and data processing.

### Language skills

**Chinese**          Mother Language

**English**          Fluent

**German**          C1

### Publications

- 1) Shijia Huang, Aolin Jia<sup>1</sup>, Wen Song, Giuliana Hessler, Yonggang Meng, Yue Sun, Lina Xu, Henriette Laessle, Jan Jirschitzka, Shoucai Ma, Yu Xiao, Dongli Yu, Jiao Hou, Ruiqi Liu, **Huanhuan Sun**, Xiaohui Liu, Zhifu Han<sup>1</sup>, Junbiao Chang, Jane E. Parker, and Jijie Chai, Identification and receptor mechanism of TIR-catalyzed small molecules in plant immunity. Biorxiv, submitted to Science.
- 2) Na Song, Lan Ma, Weiguang Wang, **Huanhuan Sun**, Lei Wang, Ian T. Baldwin, and Jinsong Wu, An ERF2-like transcription factor regulates production of the defense sesquiterpene capsidiol upon *Alternaria alternata* infection. Journal of Experimental Botany 2019.
- 3) Christian Hettenhausen, Juan Li, Huifu Zhuang, **Huanhuan Sun**, Yuxing Xu, Jinfeng Qi, Jingxiong Zhang, Yunting Lei, Yan Qin, Guiling Sun, Lei Wang, Ian T. Baldwin, and Jianqiang Wu, Stem parasitic plant *Cuscuta australis* (dodder) transfers herbivory-induced signals among plants. Proc Natl Acad Sci USA 2017.



- 4) **Sun, H.**; Song, N.; Ma, L.; Li, J.; Ma, L.; Wu, J.; Wu, J., Ethylene signalling is essential for the resistance of *Nicotiana attenuata* against *Alternaria alternata* and phytoalexin scopoletin biosynthesis. *Plant Pathology* 2016, 66, 277-284.
- 5) **Sun, H.**; Wang, L.; Zhang, B.; Ma, J.; Hettenhausen, C.; Cao, G.; Sun, G.; Wu, J.; Wu, J., Scopoletin is a phytoalexin against *Alternaria alternata* in wild tobacco dependent on jasmonate signalling. *Journal of Experimental Botany* 2014, 65, 4305-15.
- 6) **Sun, H.**; Hu, X.; Ma, J.; Hettenhausen, C.; Wang, L.; Sun, G.; Wu, J.; Wu, J., Requirement of ABA signalling-mediated stomatal closure for resistance of wild tobacco to *Alternaria alternata*. *Plant Pathology* 2014, 63, 1070-1077.

Ocotober 16, 2022

Huanhuan Sun

